Solar-Terrestrial Centre of Excellence

Annual Report 2012

Belgian Science Policy Office belspo

Royal Observatory of Belgium

RMI

BIRA-IASB

.be

STCE

Solar-**T**errestrial **C**entre of **E**xcellence

http://stce.be/

Ringlaan 3

B-1180 Brussels

Tel.: +32 2 373 0211

Fax: + 32 2 374 9822

Front-page: **Some 2012 highlights in Olympics colors.** *The blue image shows the biggest sunspot group of 2012 on 11 July. It was also the first CaII K image taken by USET's new CaII K telescope. The "black" image features a very long filament on the Sun in H-alpha (USET; 4 August), while the red image shows the eruption of the same filament on 31 August as imaged by SOHO's coronagraph (LASCO/C2). The yellow image displays the Venus transit on 6 June as viewed by PROBA2/SWAP, and the green image depicts 2012's strongest solar flare as seen by SOHO's EIT telescope on 7 March.*

Table of Contents

Preface

Dear reader,

The Solar-Terrestrial Centre of Excellence is proud to present highlights of its activities during the year 2012 in the current report. When writing this text, we have continued in the direction that we took last year, i.e. to create a report that does not give all of the details, nor even refers to all of the ongoing efforts, but that is instead restricted to the true highlights of the year. That we – nonetheless – have ample things to write about is clear from the following pages, and this of course reflects the continuing high level of activity within the STCE, a fact that is equally transparent from the long list publications and presentations prepared by staff working within the STCE remit.

This year's story again starts to unfold by looking at what's been happening on the Sun and what were the implications in terms of near-Earth space weather. Thereafter, we have organized the topics in a thematic focus on outreach, research, instrumentation and applications. Lest you forget that scientists like to have fun also every once in a while, a sprinkle of the Olympic year's spirit has been added at the end of each of these chapters.

Enjoy the lecture of this report! Please do not hesitate to contact us if you would like to get more information about any of the particular topics or about any of the STCE activities. We are also open to all forms of collaborations and do not easily shy away from the wildest of ideas.

Kind regards
Ronald Van der Linden
General Coordinator of the Solar-Terrestrial Centre of Excellence
Director General of the Royal Observatory of Belgium

Structure of the STCE

The Solar-Terrestrial Centre of Excellence is a project of scientific collaboration that focuses on the Sun, through interplanetary space, up to the Earth and its atmosphere.

The solid base of the STCE is the expertise that exists in the 3 Federal Scientific Institutes of the Brussels Space Pole: the Royal Observatory of Belgium, the Royal Meteorological Institute and the Belgian Institute for Space Aeronomy. The STCE supports fundamental solar, terrestrial and atmospheric physics research, is involved in earth-based observations and space missions, offers a broad variety of services (mainly linked to space weather and space climate) and operates a fully established space weather application center. The scientists act at different levels within the frame of local, national and international collaborations of scientific and industrial partners.

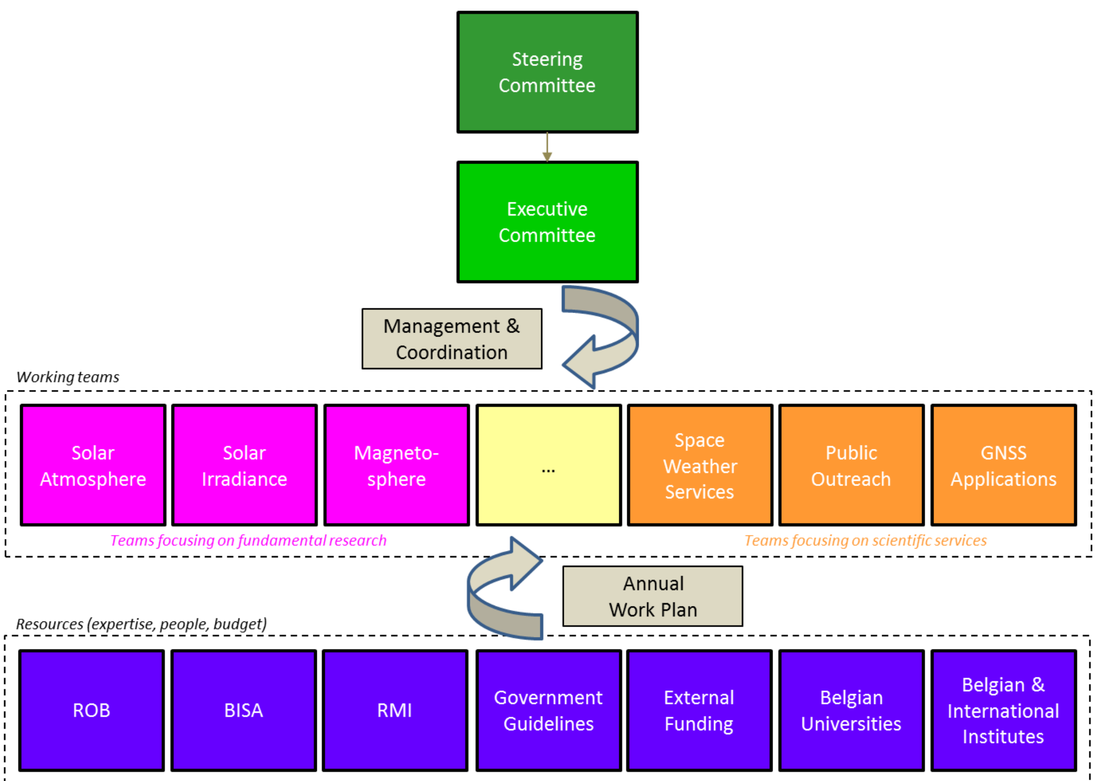

Figure 1: The STCE management structure

The STCE's strengths are based on sharing know-how, manpower, and infrastructure.

In order to optimize the coordination between the various working groups and institutions, as well as the available resources such as ICT, personnel and budget, a management structure for the STCE was put into place, consisting of a steering committee and an executive committee.

The ***steering committee*** takes all the final decisions on critical matters with regard to the STCE. It assures the integration of the STCE into the 3 institutions and the execution of the strategic plans. It is composed of:

- BELSPO Director General "Research Programs and Applications”

  (Position currently to be filled)

- Director General of each of the 3 institutions at the Space Pole

  Dr. Ronald Van der Linden (ROB)
  Dr. Daniel Gellens (RMI)
  Dr. Martine De Mazière (BISA)

The ***executive committee*** assures the global coordination between the working groups and the correct use of the budgetary means for the various projects. It also identifies new opportunities and is the advisory body to the Steering Committee. It is composed of:

- STCE Coordinator

  Dr. Ronald Van der Linden

- Representatives of the research teams in the 3 institutes

  Dr. David Berghmans (ROB)
  Dr. Carine Bruyninx (ROB)
  Dr. Johan De Keyser (BISA)
  Dr. Michel Kruglanski (BISA)
  Dr. Stanimir Stankov (RMI)
  Dr. Steven Dewitte (RMI)

A promotional movie giving a flavor of the STCE’s tasks, interactions and various research programs can be found via the STCE website (in English, and subtitled in French and Dutch).

Figure 2: An international team of researchers attending a Solar Orbiter seminar. As seminars require lots of energy, scientists have developed an outspoken preference for pies and sweets, homemade or not!

Monitoring Space Weather: Solar-Terrestrial Highlights in 2012

In 2012, the official annual sunspot number (SSN) as determined by the SIDC (Solar Influences Data analysis Center), was 57.7. This is slightly higher than the average from the previous year, but lower than the activity recorded during the last months of 2011. As a result, the smoothed monthly SSN has gradually been decreasing.

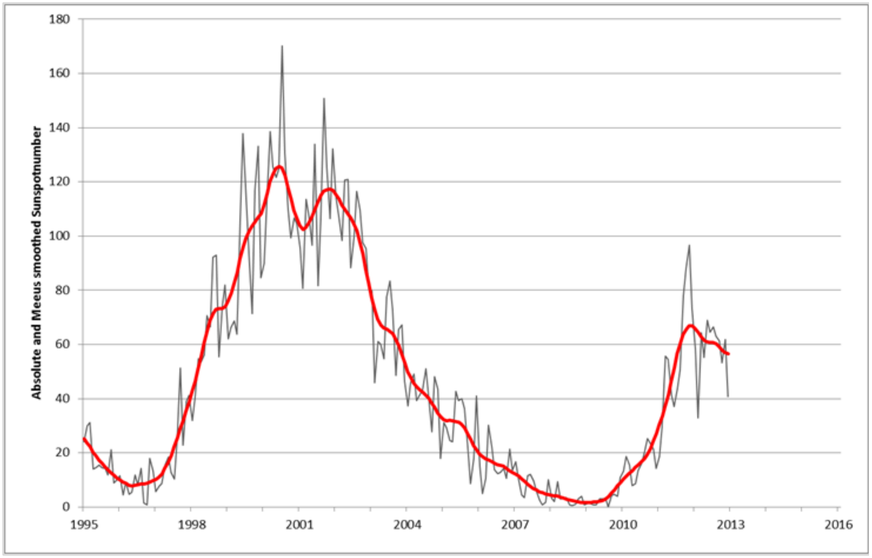

Figure 3: The evolution of the monthly and monthly smoothed SSN since 1995. The low sunspot activity of the current solar cycle compared to the previous one is obvious.

Hemispheric activity evolved oppositely. The southern solar hemisphere reached a maximum during the summer months, while the activity in the northern hemisphere started again to rise during the second half of the year. From May till November, the Sun's outlook alternated between an active hemisphere with relatively many sunspots, and a hemispheric "face" that was pretty much void of these dark blemishes. These periodic ups-and-downs could clearly be seen not only in the daily sunspot numbers, but also in the radio flux, as well as in the extreme ultraviolet (EUV) and x-ray background flux (as measured by resp. PROBA2/LYRA and GOES).

Figure 4: Belgian and Dutch solar amateurs observing the Sun during their annual gathering late 2012, and wondering where the sunspots have gone. Talk of the day was whether SC24 maximum had already passed or not. The solar observations of amateur astronomers constitute a significant contribution to the compilation of the final sunspot number by the SIDC.

Despite the declining SSN, the maximum of solar cycle 24 (SC24) is still expected to happen in the second half of 2013 or even in 2014. Indeed, if the 2011 high would be the real maximum, it would turn out to be an extraordinarily early maximum for such a weak cycle. Moreover, weak solar cycles are also known to show several ups-and-downs during the period of maximum activity. Finally, the magnetic reversals at the solar poles are still not completed. In fact, for the southern hemisphere it still has to begin. As these reversals occur during or near the true solar cycle maximum, it is yet another indication that the SC24 maximum still has to happen. For these reasons, the SC24 maximum is expected to occur a little bit later and to be a little bit lower than the original prediction by the international SC24 Prediction Panel, but still within the uncertainty margins.

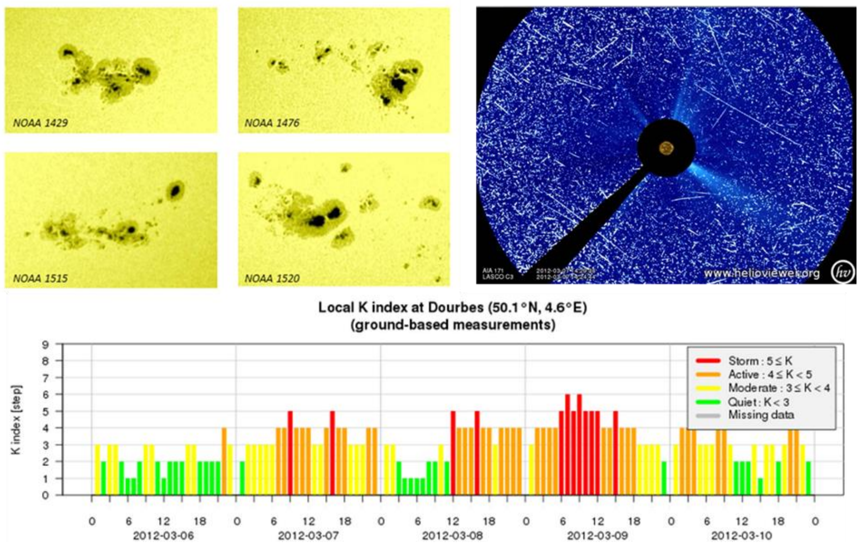

Figure 5: Top left: The four largest sunspot groups in 2012, as imaged by the Solar Dynamics Observatory (SDO). Top right: The effects of the X5 proton flare from NOAA 1429 on the camera of SOHO's coronagraph are readily visible. Bottom: Dourbes recorded geomagnetic storming levels after strong X-class flares from NOAA 1429 on 5 and 7 March. The associated CMEs dumped a large amount of energy into the Earth's atmosphere and also increased substantially the number of electrons in the radiation belts, increasing the risk on malfunctions for Earth orbiting satellites.

Though sunspot numbers were relatively low, 2012 saw several large groups transiting the solar disk. NOAA 1429 (March), 1476 (May), 1515 and 1520 (July) all attained areas about 6 to 8 times larger than Earth's surface, and they added to the number of strong flares. NOAA 1429 produced the 2nd largest flare so far (X5 on 7 March), which was accompanied by the strongest proton storm so far. It was only the second strong solar radiation storm for SC24, following a similar event early 2012 (23-24 January, NOAA 1402). In both cases, some airlines rerouted trans-polar flights because of communication problems, and some of the data received from spacecraft such as ACE were temporarily unusable. Also the Curiosity spacecraft, en route to Mars for a successful 6 August landing, recorded the proton events. As Curiosity keeps on making measurements of these energetic particles from the Martian surface, it continues to provide very valuable data for future (manned) Mars explorations.

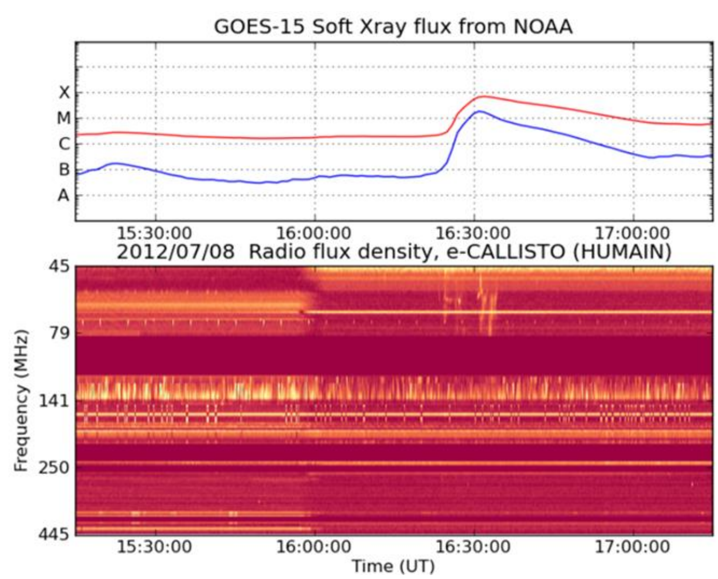

Figure 6: A weak type III radio burst followed by a type II burst recorded by the Humain Solar Observatory following an M6-flare from NOAA 1515. Type III bursts are caused by very fast electrons travelling through the hot solar corona and away from the Sun, while type II bursts usually are excited by magnetohydrodynamic (MHD) shockwaves associated with a CME traveling through the corona.

NOAA 1515 was visible on the Sun from 27 June till 9 July 2012. It displayed significant sunspot dynamics, with sunspots continually whirling, splitting and crashing into each other. Hence, it is no surprise that during its transit, this active region produced 30 M-flares (medium class) and also 1 X-flare (eXtreme class; on 6 July). Such a high number of strong flares are a rare "tour-de-force", only performed by the most active sunspot regions.

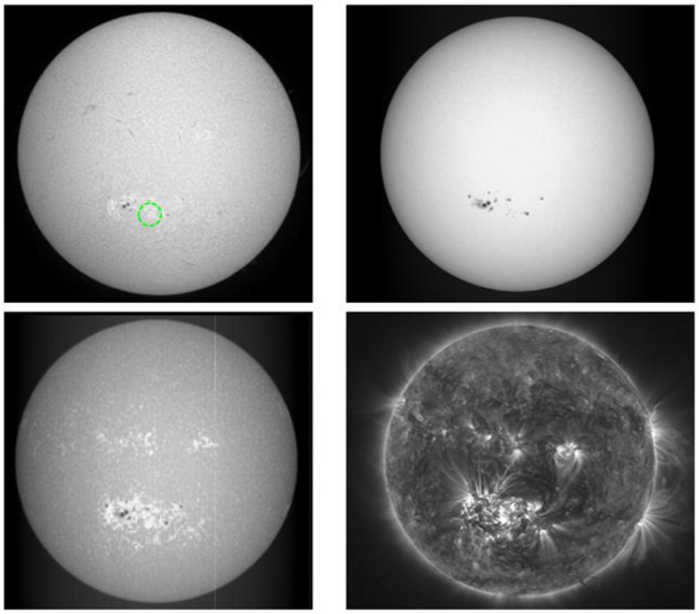

Figure 8: NOAA 1520 as photographed by the telescopes of the Uccle Solar Equatorial Table (USET) and by the PROBA2/SWAP instrument on 11 July. The green circle on the pre-flare H-alpha image (08:15UT; top left) indicates the position of a small flare visible in USET's Ca II K and SWAP's EUV-image just 15 minutes later (resp. bottom left and right).

NOAA 1520 was the largest sunspot group during 2012 and the second largest so far this solar cycle. This super group was magnetically not so complex and produced only a handful of strong flares. However, while it was rounding the west limb, it produced an M7-flare on 19 July which was accompanied by graceful round post-flare coronal loops. On 23 July, well on the Sun's backside, it produced another strong flare accompanied by a proton storm that was even registered on Earth. The speed of the related coronal mass ejection (CME) turned out to be one of the fastest ever recorded, arriving at STEREO-A only 19 hours after the eruption, a so-called "fast transit event".

The last 5 months of 2012 saw a decline in solar activity, with decreasing sunspot numbers and no medium flares at all in December. The last X-class flare was produced on 23 October by NOAA 1598. The period was mainly characterized by many filament and prominence eruptions, with the most spectacular one occurring on 31 August near the south-east solar limb.

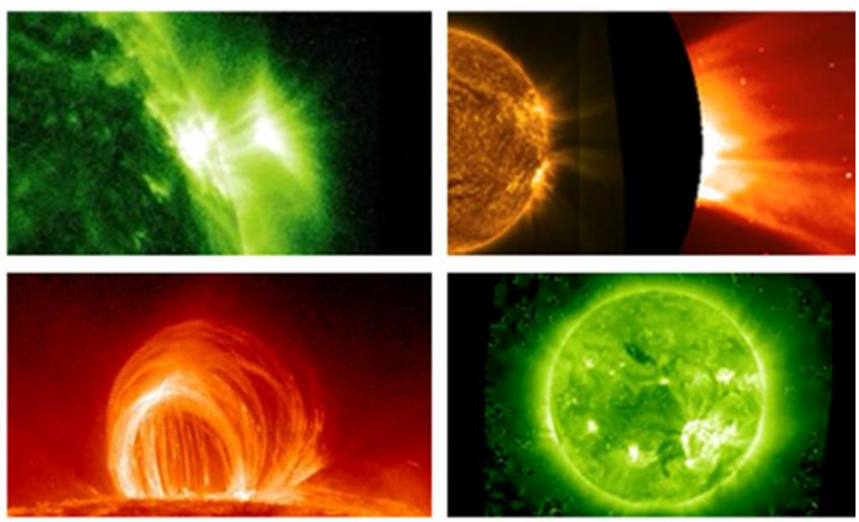

Figure 7: Some fabulous solar flares and eruptions were produced during 2012. Supra-arcade downflows on 13 March (NOAA 1429, top left), a double trans-equatorial CME on 8 July (NOAA 1515, top right), gracious coronal loops on 19 July (bottom left), and a backside proton flare responsible for a transient coronal hole and one of the fastest CMEs ever recorded (23 July). The last two events were both courtesy of NOAA 1520.

So far in this solar cycle, there has not been any extreme geomagnetic storm (Kp=9). Auroral displays have been confined to the higher geomagnetic latitudes. Days with major to severe storming occurred on 9 March and 15 July 2012. The month of March was geomagnetically the most disturbed so far as a result from very active flaring periods. Interestingly, no geomagnetic storms occurred during the last 2 months of 2012. Coronal holes added occasionally to the geomagnetic unrest, especially during the first half of the year. In particular one coronal hole survived 9 (nine!) solar rotations, sparking geomagnetic storms during the first 3 transits.

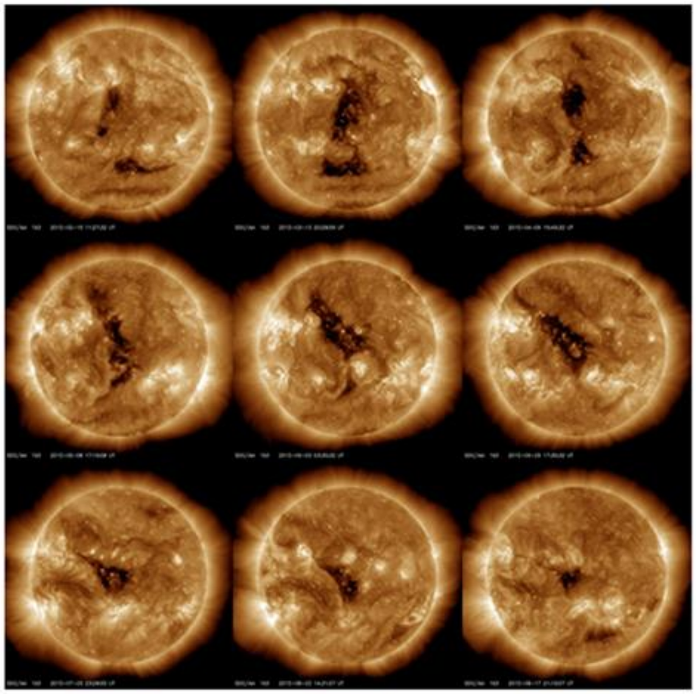

Figure 10: A trans-equatorial coronal hole survived for 9 solar rotations during the February-September 2012 timeframe. Notice the gradual change in shape and size. Only during the first 3 transits (top row), geomagnetic storming was recorded.

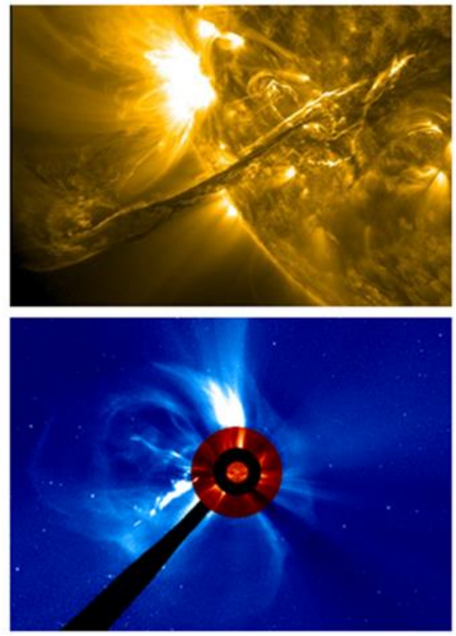

Figure 9: View on the spectacular 31 August filament eruption by SDO (top) and SOHO's coronagraphs (bottom). Even though most of the ejected material was directed away from Earth, a glancing blow sparked a minor geomagnetic storm on 3 September.

In conclusion, despite the currently declining trend in solar activity, solar maximum is still expected for late 2013 or in 2014. Episodes of strong flaring activity can be anticipated, with severe geomagnetic impacts if the associated CMEs are Earth directed. This scenario remains valid even in the first few years of the declining phase of the solar cycle. Thus, Earth and its technology remain vulnerable to space weather effects for years to come.

The 9th European Space Weather Week

International conference with worldwide fame

Space weather describes the conditions in space that affect Earth and its technological systems. It has an impact on a large variety of domains and even on our daily life. Providing observers a view of the beautiful aurorae, it constitutes a threat for aircraft crew and passengers because of radiation. It hampers telecommunication and navigation. Space weather is also a concern for e.g. power companies, who fear a disastrous breakdown of their networks. The STCE understands the necessity of communication about space weather and recognizes at the same time the challenge to do so in thoughtful serenity.

Our knowledge is strengthened through national and international collaborations. The STCE puts a strong effort in building solid scientific foundations. One of the building stones of this scientific basis of space weather is the European Space Weather Week (ESWW), an annual international scientific conference. The worldwide science community benefits from this effort.

With respect to content, the ESWW is interesting for scientists, policy makers, space weather end users, and developers of services. It offers a program for theoreticians and more practical oriented business. Since quite early in its existence, the STCE has been the local organizer of this event. The STCE makes the ESWW run smoothly and regularly introduces new concepts. It is no wonder that this varied and innovative program draws every year more participants: 319 in 2012!

Figure 11: The ninth edition of the European Space Weather Week focused on the space weather landscape in Europe, the innovations and challenges, solar variability and its effect on climate, modeling, spacecraft operations, space weather in the solar system and the final results of a European collaborative project about space weather services and products. This image shows PROBA2 orbiting Earth watching the Sun, the driver of space weather.

One of the innovations in the 2012 edition of the ESWW was the educative program on the first day of the week. The Battle of the Solar Titans was introduced with a dynamic live quiz called “Higher Lower”. Here, participants had to indicate with their arms if they think the true answer is higher (left arm) or lower (right arm) than the proposed answer. An example: “PROBA2 is a micro-satellite launched on 2 November 2009, with onboard the EUV imager SWAP. Does it picture the Sun in a wavelength higher or lower than 170nm?” If you had been a participant and you had put your right arm in the air (the answer is indeed lower since SWAP captures the wavelength of 17.1nm), you would still be in the running for the title “Solar Titan of Monday”. The audience truly enjoyed this simple and amusing quiz with its immediate feedback. The actual “Battle of the Solar Titans” was played online and ran for the entire week. Most of the questions were provided by the participants.

Figure 12: The European Space Weather Week started off with some educative space weather fun. The ninth edition offered “Space Weather Shopping” where participants could meet people involved in a specific area of space weather.

Of course, the quiz was preceded by brain-filling sessions: “Meet and Greet” and “Scientists in the Sofa”.

The “Meet and Greet”, also called “Space Weather Shopping”, introduced the participants to a broad variety of space weather topics. They hopped from one information point to another: Solar Orbiter satellite, Sailing on Sunshine, PROBA2, Comets, the public observatory MIRA, and Imaging the Sun and planets. In sessions lasting 5 to 10 minutes, specialists explained the basics in easy wording and with plenty of demo material.

Since scientists are humans, we put 3 scientists in a sofa and asked them about their passion for space weather. Marilena Mierla's passion is about coronal mass ejections (CMEs). She turns data, provided by a fleet of satellites such as SDO and PROBA2, inside out. Marilena aims for a 3D vision of these massive plasma clouds and wants to know how they interact with the surrounding solar wind that fills the space in the heliosphere, the magnetic bubble that contains our solar system. She finds it especially interesting to see how practical measurements and theoretical science combine. In the end, the result is also useful for real space weather operations like forecasting. Dan Seaton, a PROBA2 scientist at the STCE, stated that “the open discussion format was a great opportunity for me as a scientist to learn about the space weather community's needs, interests, and concerns. And I hope it was an equally good opportunity for data and forecast users to see what goes into the science that stands behind space weather forecasts.”

Figure 13: Dave Pitchford moderated “Scientists in the Sofa” with Marilena Mierla who studies coronal mass ejections, Dan Seaton who gives all his scientific attention to the EUV imager SWAP onboard PROBA2, and Shaun Bloomfield from Trinity College Dublin who also uses SWAP for his solar flare research.

This year’s keynote speaker was none other than Professor Jocelyn Bell Burnell who discovered the first radio pulsars back in 1967. Pulsars are rapidly rotating remnants of exploded stars, emitting beams of electromagnetic radiation toward the Earth, very similar to a lighthouse. To have this top scientist at the ESWW was quite an honor! She gave a down to earth presentation on how radio astronomers worked in the sixties and seventies: screwdrivers and pliers, topped with brains.

Figure 14: Professor Jocelyn Bell Burnell discovered the radio pulsars. She is seen here in action as our keynote lecturer.

We also introduced the participants of the ESWW9 to Twitter and Facebook. You could read instantaneously what the public thought of a presentation. We can assure you that nobody was offended or hurt: Twitter was used and perceived in a positive way.

Public Outreach

COST: The European Space Weather Wave

In the sixties, scientists and engineers started to realize that the Sun and its daily activity had a non-negligible impact on humanity and in particular on the technological tools we use. "Space Weather" as a concept and a science was born. But it wasn't until the nineties that Space Weather really took off as an important new branch of research.

In 2000, the Regional Warning Centre (RWC) for Western Europe was installed in the offices of the Royal Observatory of Belgium. ROB solar physicists started to monitor the Sun and forecast its activity up to 3 days, 7/7. At about the same time, the space weather community in Europe started to organize itself. The Solar Influences Data analyses Centre (SIDC) and later the STCE (2007) established a strong position on the European and world map. In 2008, the STCE became a partner in a project "Developing Space Weather Products and Services in Europe" (ES0803) under the umbrella of the European Cooperation in Science and Technology (COST). This COST project acts as the glue between space researchers across Europe. It offers the communities in different European countries the basis and tools to organize themselves in an efficient way and to converge to a series of products and services. The STCE took the lead in the work group responsible for the specification of recommended products and services. Since its start in 2008, the members decided to include a focus on outreach and communication activities. This challenge was given in the hands of the communication cell of the STCE in 2010. A communication plan was developed, keeping in mind what the target audience is, identifying clear goals and discussing the tools and ways to communicate.

Figure 15: The Journal of Space Weather and Space Climate was launched late 2010. It collects the science that used to be spread over a variety of journals and offers the possibility to publish valuable but more technical oriented papers, as well as papers describing outreach and communication activities.

Within the COST-frame, starting already under a first action (COST-724), and continued under COST-ES0803, the European Space Weather Portal was developed. This website provides a centralized access point for the space weather community to share their knowledge and their research results and models.

Another big effort was the Journal of Space Weather and Space Climate (SWSC) that was launched in November 2010. This online open access journal collects scientific results in the field of space weather and space climate that used to be spread over a variety of journals and offers the possibility to publish valuable technical information, data and communication material. It offers a forum for the scientist organizing activities for the public. The STCE takes care of the editorial office and verifies if there are no hick-ups in the review process.

The STCE contributed also to a publication about the planeterrella, a planetary aurora simulator developed with CNRS support by Jean Lilensten at the Institut de Planétologie et d'Astrophysique de Grenoble (IPAG). We are actually building one ourselves! This is one of the strengths of such a collaborative project, i.e. a national activity can be lifted to an international level such that a broader community can benefit.

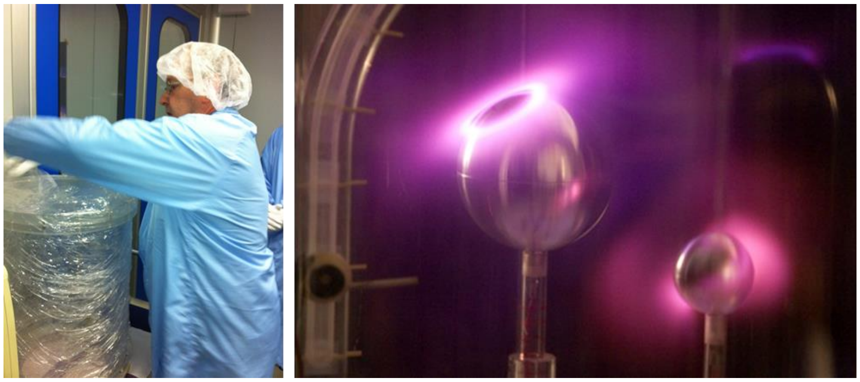

Figure 16: The Norwegian experimental physicist Kristian Birkeland was one of the founding fathers of modern space science. A century ago, he demonstrated with his Terrella experiment the formation of the aurora. Recently, a modernized version of the Terrella has been designed, allowing the visualization of many other phenomena occurring in our space environment. The STCE is now building its own planeterrella. The image depicts the plexiglass case - a protective plastic covers it - in which a very low pressure is created. A cathode then fires electrons to a ball with a magnetic dipole inside.

These are only a few of the many examples that were developed under the umbrella of this project. The COST project ended in 2012, culminating in a dedicated session during the European Space Weather Week where many of its results were presented.

eHEROES go on a space trip

In 2011, a bunch of scientists spread over 15 institutes (in 14 countries) got the idea to work together around space exploration. The STCE was one of those 15. The proposal was approved and the project had its kick-off in March 2012 and got the sounding name eHEROES, short for Environment for Human Exploration and RObotic Experimentation in Space.

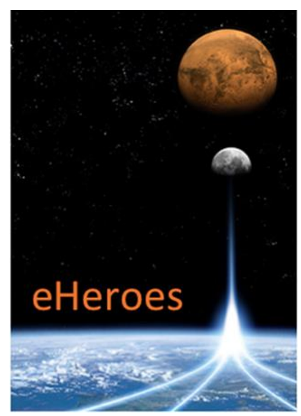

Figure 17: Partners from all over Europe find each other in the project eHEROES. This project includes a study of solar and space events, their evolution and impact, and wants to set up a frame in which space exploration can be performed in the best possible way.

Not that we, the club of 15, wanted to go ourselves into space, but we wanted to exploit the existing data gathered on the numerous European and international space missions. We wanted to learn about the existing models and simulations and finally produce new value-added data products.

By collecting and studying this wealth of information, our knowledge of the space environment could increase dramatically. This definitely helps us to estimate and predict the threats that missions encounter when going outside the protective cocoon that provides the Earth's magnetic field. So, we stay on Earth but do all the science and research necessary to make space exploration as safe as possible. However, these days, space exploration is not only limited to robotic missions but also involves humans. In Belgium for example, space trips are currently sold for the price of 77.777 Euro. This proves that space travels and space tourism are no longer science fiction, but are becoming a reality.

As our society needs to be correctly informed about the dangers and threats that are linked to the Sun and space weather, a full-fledged work package “Dissemination” was included into the eHEROES project. Its main motives are “spread the word”, “make aware”, “instruct” and “educate”. We provide timely information with a daily update on the current space weather. These updates are more frequent in case of an extreme space weather event. The evolution of such events can then be followed in near real-time on the website through presto-messages and news items. The challenge we take now is to produce a space weather broadcast with an easy digestion and with a focused message. 99,99% of the population is not interested in the fact that the solar wind speed is 1062 km/s (which is by the way very high compared to a more normal value of 300 km/s), but many are interested in the chances to see polar light from, for example, Belgium. You can imagine that satellite operators have other interests. For them, it is e.g. crucial to know if the atmosphere will expand due to space weather events.

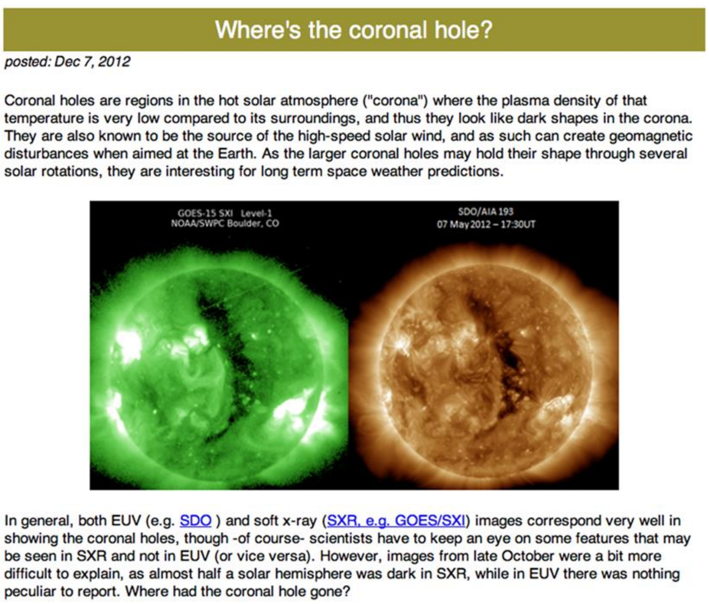
Where's the coronal hole?

posted: Dec 7, 2012

Coronal holes are regions in the hot solar atmosphere ("corona") where the plasma density of that temperature is very low compared to its surroundings, and thus they look like dark shapes in the corona. They are also known to be the source of the high-speed solar wind, and as such can create geomagnetic disturbances when aimed at the Earth. As the larger coronal holes may hold their shape through several solar rotations, they are interesting for long term space weather predictions.

In general, both EUV (e.g. SDO) and soft x-ray (SXR, e.g. GOES/SXI) images correspond very well in showing the coronal holes, though -of course- scientists have to keep an eye on some features that may be seen in SXR and not in EUV (or vice versa). However, images from late October were a bit more difficult to explain, as almost half a solar hemisphere was dark in SXR, while in EUV there was nothing peculiar to report. Where had the coronal hole gone?

Figure 18: The online space weather stories show the violence and beauty of the ongoing solar activity and its impact on us and Earth. These broadcasts give 'Good to know' facts.

On the other hand, we also provide general information, things-to-know about space and space weather. One could consider it a guide to space. On the STCE website, we publish an online story of space interest every week. These stories provide background information on sunspots, flares, violent mass eruptions, satellite observations, and so on.

So, besides producing rocket science, eHEROES and in particular the STCE respond to all sorts of concrete needs, be it general or specific, informative or advisory, regular or near real-time.

Fundamental Research

PROBA2 - Not just observing the Sun!

PROBA2 is the second satellite in the ESA's PROBA series of small-scale satellites that are being used to validate new spacecraft technologies. PROBA2 contains five scientific instruments, two of which are designated to observe the Sun: "The Sun Watcher using Active Pixel Sensors and Image Processing" (SWAP, an EUV imager) which is designed to image the Sun in EUV at temperatures around 1 million degrees Kelvin, and the "Large Yield Radiometer" (LYRA) which measures the intensity of the whole Sun at 4 distinct wave lengths in the ultraviolet range. SWAP takes an image of the Sun every 2 minutes and LYRA makes 12,000 measurements in the same time!

PROBA2 is predominantly used to monitor "space weather". That is, to monitor the Sun for energetic events that may affect the Earth and orbiting satellites. Consequences of space weather are natural phenomena such as the aurora borealis and impacts on man's infrastructure, such as damaging satellites and causing large currents in power stations. We have reported in previous issues and other scientific journals the scientific benefits of PROBA2 for solar and space weather observations, however in this article we aim to look at some of the more unusual celestial observations.

- **Comet Lovejoy – A Sun-grazing Comet**

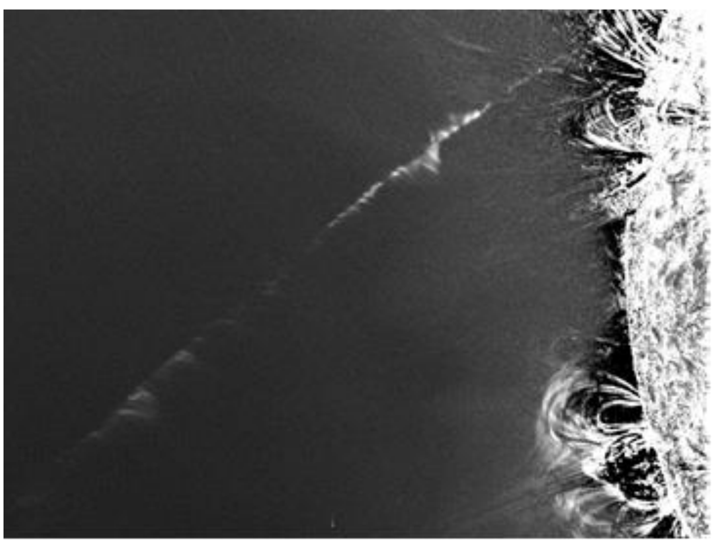

Figure 19: A close up, composite image of the Sun and comet Lovejoy (the striated line) taken with the SWAP EUV imager on PROBA2. This single image is the superposition of several individual images taken with SWAP to show the progression of comet Lovejoy as it travels through the Sun's atmosphere.

Comet C/2011 W3, more commonly known as comet Lovejoy, is a Sun-grazing comet which passed within 140,000 km (1.2 solar radii) of the visible solar surface in December 2011. Comet Lovejoy was observed in the SWAP field of view and can be seen in Figure 19, which is composed of several individual images superimposed on top of each other in order to map out the trail of the comet as it passed through the Sun's atmosphere. Images were taken between 23:41UT on 15 December 2011 and 09:23UT on 16 December 2011. The comet can be seen as a long streak moving from the left of the image to behind the Sun on the right. It appears as a series of striated lines due to its interaction with the Sun's magnetic field.

The Sun is permeated with magnetic fields, which are highlighted by hot plasma trapped on them. These are seen emerging from the solar surface as a series of semicircular (or loopy) structures (close to the Sun on the right of Figure 19). Some magnetic fields cannot be seen as they have no hot material trapped on them, and are therefore invisible. However, when the comet passes through these regions, it interacts with the previously invisible fields and we see substantial changes in the direction and intensity of the comets tail, creating the striated windblown appearance of the comet tail.

- **Venus Transit**

Another important celestial event occurred on 5-6 June 2012, when Venus passed in front of the Sun with respect to the Earth. This event was also captured by SWAP and can be seen in Figure 20, where Venus is the black circle obscuring the EUV light of the Sun. Due to the orbits of Earth and Venus, the alignment of these two planets with the Sun occurs rarely, but in pairs. The first alignment occurred in 2004. Preceding observations were made in 1874 and 1882, and we will have to wait until 2117 and 2125 for our next opportunity to observe a Venus transit in front of the Sun from the Earth.

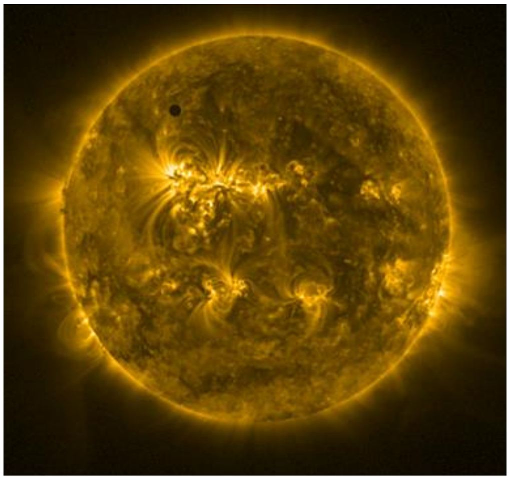

Figure 20: An image of Venus passing in front of the Sun, taken by the PROBA2/SWAP instrument. Venus can be seen as a dark circle in the upper left quadrant of the image.

The transit of Venus was visible from the Earth. However, due to the setting of the Sun and cloudy conditions, it was difficult to observe the transit from several locations on the Earth. PROBA2 was able to make uninterrupted images of the transit from its orbit around the Earth.

- **Solar Eclipse**

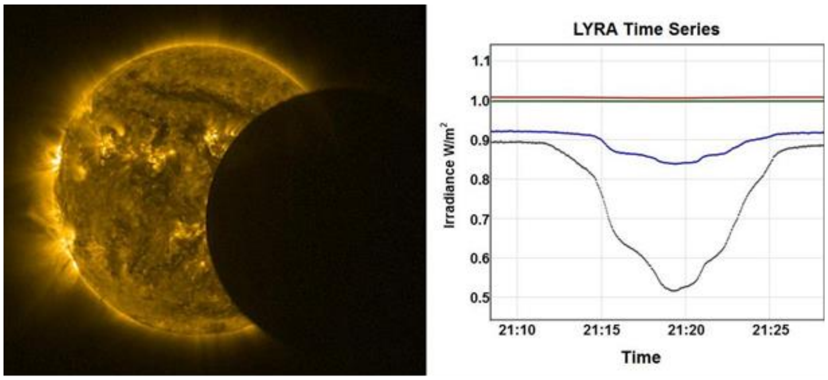

Figure 21: An image of the total solar eclipse taken by SWAP (left) and its corresponding irradiance measured by LYRA (right). The differently colored light curves indicate the different pass bands the eclipse was seen in; Lyman alpha (Red), Herzberg (green); Aluminum (Blue) and Zirconium (Black).

On 20 May 2012, an annular solar eclipse could be observed from some parts of the Earth. An annular eclipse takes place when the Moon passes exactly between the Sun and the Earth, but is not big enough to cover the entire solar disk. PROBA2 orbits at 700 km above the Earth and passed repeatedly through the Moon's shadow taking 4 images of partial eclipses (where only part of the Sun is obscured). Figure 21 shows an image of the eclipse taken by SWAP (left) and the associated solar output (light curves) recorded by LYRA (right). It can be clearly seen how the irradiance of the Sun is diminished by the eclipse. The solar eclipse is not only visually impressive, but gives researchers at the Royal Observatory of Belgium the chance to monitor the health of the SWAP instrument. The places where the Moon occults the Sun should show up as black, and variations from this can be calibrated and corrected in future images.

Merging sunspot catalogs

While digging for clues as to the reason for changes in the relationship between different well-known solar indices, our team discovered that the Sun has changed its behavior during recent years. To understand what is happening, we used a recently compiled catalog, based on several other less detailed catalogs to assess the details. Here we explain how it all works.

- **Sunspots**

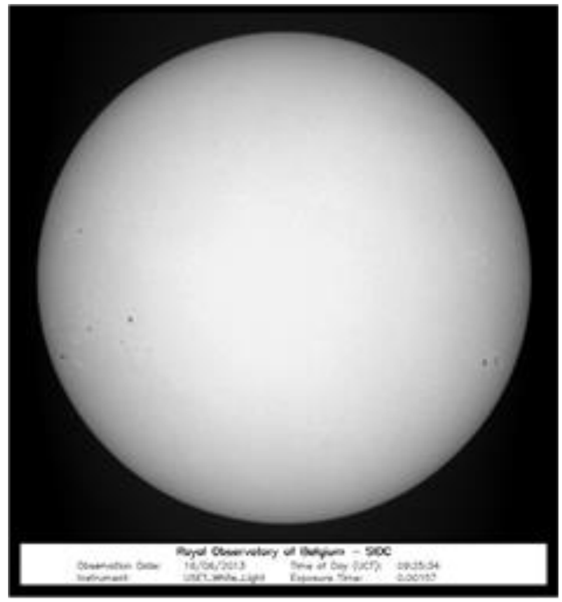

Figure 22: Some small sunspots on the surface of the Sun. Image taken with USET's white light telescope.

Sunspots are areas of the Sun that appear as dark spots compared to their surroundings. This is caused by their intense magnetic field that locally reduces the solar surface temperature. They appear and disappear in a matter of hours to weeks.

Sunspots and groups of sunspots come in different flavors. Over time, different schemes were used to classify them. The most used scheme is called the modified Zurich McIntosh classification. Basically, groups of sunspots are classified by size: A and B groups are the smallest and it goes on through C, D, E, F. The last letter, H, refers to decaying groups that are at the end of their lives.

- **The sunspot number: one aspect of solar variability**

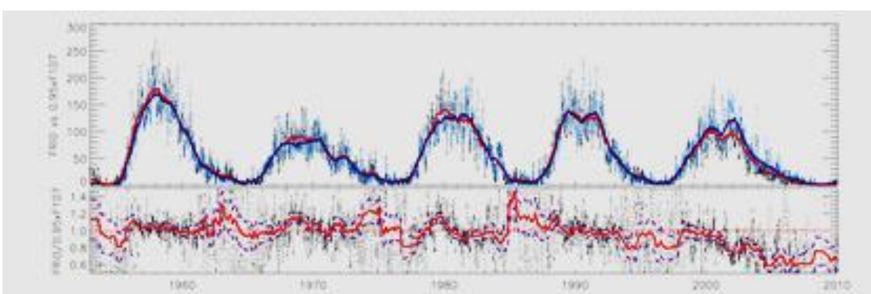

Figure 23: Upper panel: Sunspot Number (red) compared to radio flux (at 10.7 cm, in blue) from the 1950s up to now. Lower panel: Ratio between the two showing recent discrepancies.

The International sunspot number, obtained with a formula combining the number of spots and groups of spots on the Sun's surface every day, has been computed each month by the SIDC since 1981 and exists since 1818. In parallel to this index, a number of other organizations around the world compute their own sunspot indices while various solar measurements are made from other sources (e.g. radio flux). They represent different aspects of the solar variability. For the last 50 years or so, all these quantities have agreed relatively well. However, around 1998-2000, they started to show persisting disagreements. While investigating possible technical or physical causes, the need for more detailed information about the sunspots and sunspot groups led us to look into the information available from sunspot catalogs.

- **Sunspot catalogs**

Various catalogs describing sunspot regions in more or less details are available from different sources over the internet. However, when looking for detailed information about the individual sunspots, information is much sparser. A recent catalog from the Heliophysical Observatory in Debrecen, Hungary (http://fenyi.solarobs.unideb.hu/DPD/index.html) stands out in terms of level of detail: It contains information on the individual sunspots and their relation to a group of spots. On the other hand, it lacks other, more basic information about the morphology of these groups (the different flavors mentioned above).

- **Construction of merged catalogs**

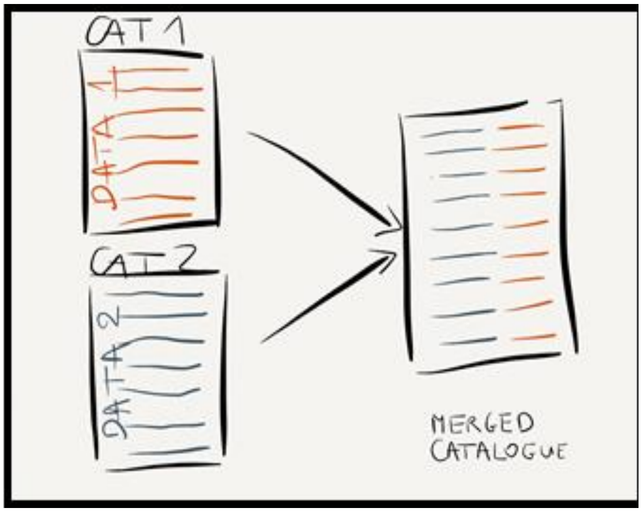

Figure 24: Merging data from different catalogs into one "mother catalog".

We use this very detailed catalog from Debrecen, and complement it with the well-known, but less detailed USAF/NOAA catalog (http://www.ngdc.noaa.gov/) that describes the different flavors of sunspot groups. The results have been published in a specialized scientific journal specialized at the end of 2012 (L. Lefèvre & F. Clette (2012), Survey and Merging of sunspot catalogs, Sol. Phys., DOI: 10.1007/s11207-012-0184-5). This merged catalog enabled to successfully diagnose the recent disagreement between different aspects of solar activity. The discrepancies seem to be caused by a large difference in the number of small sunspots and stems from different sensitivities to the same phenomenon.

Impact of a solar radio burst on the EPN GNSS network

- **Introduction**

The GNSS (Global Navigation Satellite System) research group of the ROB hosts the “Central Bureau” of the EUREF Permanent Network (EPN), a European-wide reference network of GNSS receivers that are used, amongst other things, for the monitoring of the ionospheric conditions. By design, the antennas plugged to the receivers have a wide field of view, in order to catch several satellites at once, and the Sun routinely falls in this field of view. During quiet conditions, the solar emission is too low to be detected by the receivers, but some flares produce intense radio emissions that act as wide band interferences and decrease the efficiency of the receivers.

On 24 September 2011, an M7.1 flare occurred in active region NOAA 1302, accompanied by the strongest radio burst in microwave range since December 2006. STCE solar and GNSS scientists studied this event in more details.

- **The Solar event of 24 September 2011**

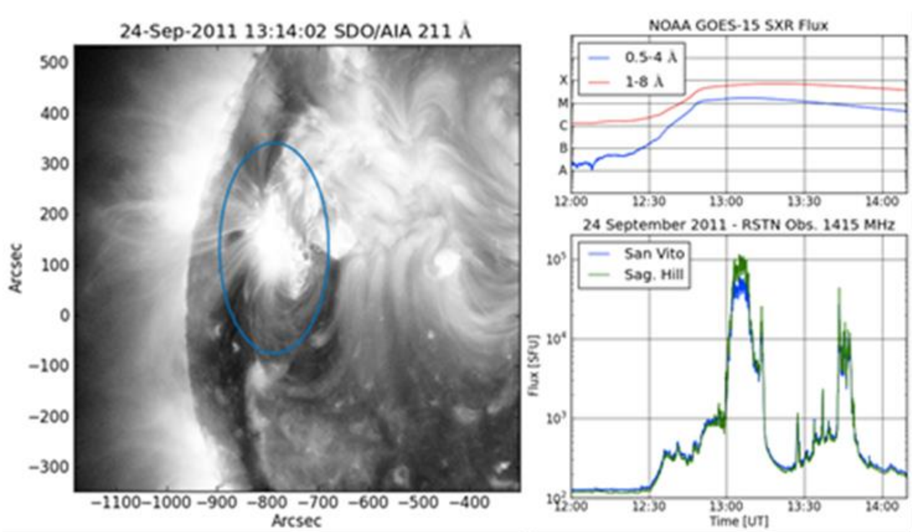

Figure 25: Overview of the solar flare of 24 September 2011. Left: SDO/AIA picture showing the flaring region. Right: Light curves in soft x-ray (top) and at radio wavelengths (bottom).

Figure 25 shows the evolution of the radio flux at 1415 MHz, a frequency which lies in between the two main frequencies used by GPS, i.e. L1 (1575 MHz) and L2 (1228 MHz), as observed by two observatories of the US Air Force Radio Solar Telescope Network. At the peak of the radio burst, the intensity is nearly 3 orders of magnitude above the quiet sun level and reaches nearly 100,000 Solar Flux Units (SFU). According to existing studies, such a flux level occurs less than once per solar cycle.

- **Effects on the EPN network**

The GPS data for each station archived at the observatory contain a “housekeeping” parameter, called the carrier-to-noise ratio (C/N_0), which is an indication of the quality of the received signal. For a given satellite and a given station, this parameter varies during the day depending on the satellite position in the sky. By subtracting two consecutive days, the relative $\Delta C/N_0$ reveals the unusual events such as solar flares. Figure 26 shows a series of maps of the EPN network, where color dots indicate the drop of $\Delta C/N_0$

as the radio burst progresses. Drops down to a factor 100 (20 dB) are observed for some stations, with a strong correlation with the local solar elevation.

The network is made of different hardware (antenna and receivers), and the STCE scientists are looking at the technical parameters that can explain, besides the obvious effect of the solar elevation, the different behaviors observed during the event at different stations.

On the other hand, it is possible, by estimating the noise level of the receivers, to determine the intensity of the solar radio burst at the GPS frequencies.

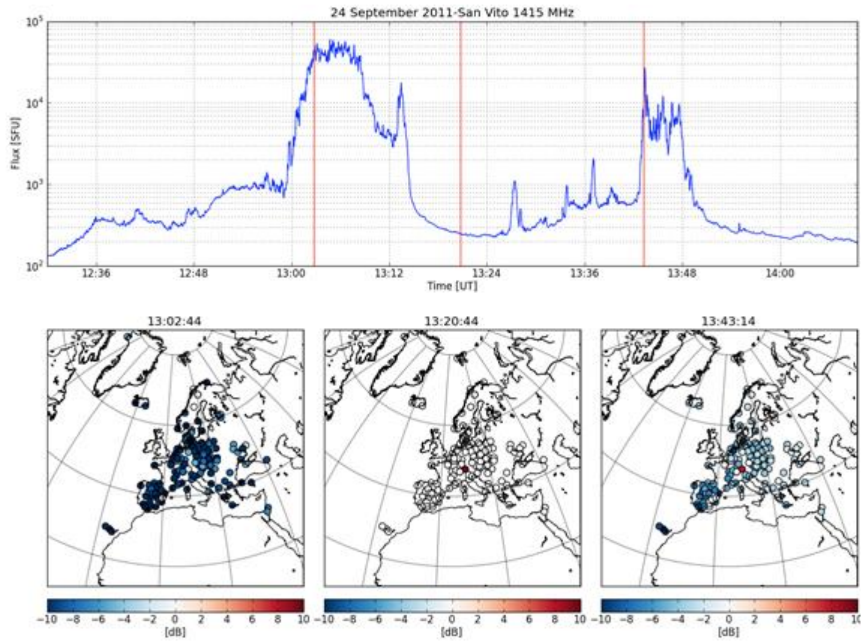

Figure 26: Maps of the relative carrier-to-noise ratio $\Delta C/N_0$ at the L1-frequency during the radio burst, for the timings indicated by the red vertical lines in the top graph.

Coronal Mass Ejections without distinct coronal signatures

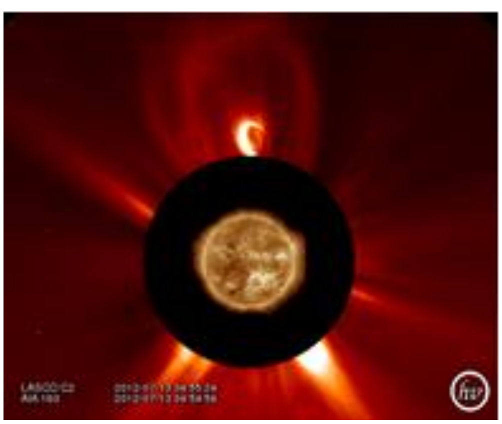

Figure 27: A CME observed on 13 July 2012 with the LASCO coronagraph onboard the SOHO spacecraft.

Throughout the year 2012, there were several periods when the Sun was very active. This can be seen, for example, in the number of solar eruptions compared to previous years. We have different ways of observing these eruptions, as they can involve various phenomena like an impulsive increase in solar radiation, expulsion of solar plasma and the launch of energetic particles into space. All of these manifestations are observed in different ways with different instruments, but each of them tells us that an eruption has taken place on the Sun.

The clouds of plasma ejected from an eruption site travel outwards into space. We monitor them -in white light- with an instrument called a coronagraph. This instrument uses a disk to obscure the Sun and creates an artificial eclipse that allows us to observe the solar corona, the faint, tenuous atmosphere that surrounds the Sun. Whenever a plasma cloud is ejected from the

Sun, it shows up as a bright feature in coronagraph images. We call these features Coronal Mass Ejections (CME, Figure 27).

When a CME occurs, it is important for space weather forecasters to determine from which region on the solar disk this plasma cloud originates. If the eruption happened on the earth-facing side of the Sun, the plasma cloud and the shock that it produces are likely to travel towards Earth, and could spawn different space weather events like disruptions of satellites and communication systems, loss of electrical power, and polar lights.

From the coronagraph images alone, it is not possible to determine the source region of the eruption. Therefore, scientists combine information from different instruments in order to search for signatures in the corona that can indicate where the eruption happened (Figure 28). These signatures include changes in the magnetic configuration of a certain region, solar flares (a sudden increase in the electromagnetic

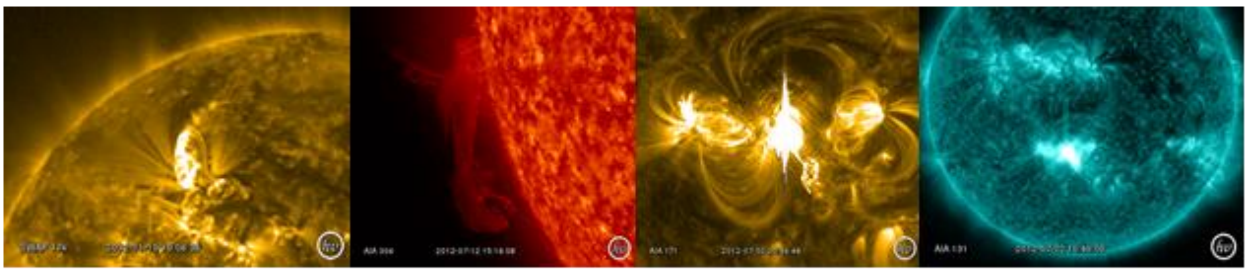

Figure 28: Coronal signatures of solar eruptions: bright post-flare loops (left image), an erupting filament (second image from the left), and a flare observed in two different wavelengths (two images on the right).

radiation we receive from the Sun), the formation of bright post-flare loop arcades, rising filaments (arched, bright, gaseous features extending outwards from the Sun's atmosphere), waves observed in EUV, dimmings (intensity depletions of the solar atmosphere in EUV wavelengths), and brightenings in the solar atmosphere.

However, some CMEs cannot be linked to any of these signatures. In that case, the most likely explanation is that the eruption happened on the far side of the Sun. Luckily, we have the two STEREO (Solar TErrestrial RElations Observatory) spacecraft, which provide us with a side-view of the Sun. They allow us also to identify the eruptions that occur on the backside of the Sun.

Surprisingly, it turns out that there are some CMEs that occur on the earth-facing side of the Sun (as confirmed by STEREO) that cannot be associated with any signatures on the solar disk. These CMEs are sometimes called "stealth CMEs" because they are undetected when they leave the Sun and can only be seen in coronagraph images. These stealth CMEs are problematic for space weather forecasters since their source location, and thus their possible effects, are difficult to identify. We ask the question why these CMEs lack clear signatures at their source regions and what observations of them can tell us about the physics involved.

To identify some stealth CMEs, we take the list of all CMEs detected in July 2012 by CACTus, a software tool that autonomously detects CMEs in the images from LASCO, the coronagraph onboard the SOHO spacecraft. We match this list to different catalogs of solar activity and remove CMEs that can be linked to flares, EUV brightenings or activity on the far side of the Sun. Inspection of solar images in various wavelengths allows us to further filter out the CMEs associated with filament eruptions, EUV waves or dimmings.

We use the resulting list to characterize the general properties of stealth CMEs (Figure 29). We find that these stealth CMEs are generally slow events, with a median velocity between 100 km/s and 500 km/s - although we do find a handful of faster stealth CMEs as well. The angular width of most of the stealth CMEs is below 30 degrees, but again we find an outlier with a much larger width.

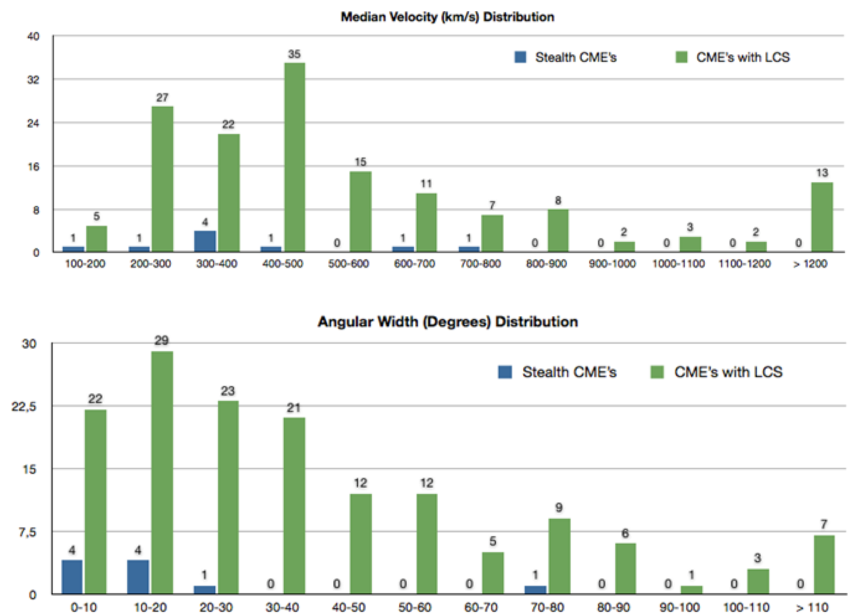

Figure 29: Median velocity (top) and angular width (bottom) distributions of stealth CMEs (blue) and CMEs with local coronal signatures (LCS; green).

The presence or absence of on-disk signatures can be linked to different theoretical models of eruptions to help establish the mechanisms by which the eruption is initiated and driven. We are compiling a list of stealth CMEs that occurred in the year 2012 and will select a few events to study in detail. Modeling these events using analytical and numerical models will give us an indication of which eruption mechanism is at work in triggering these events and help establish whether these CMEs in fact represent a class separate from more prototypical eruptions.

On the nature of prominence emission observed by SDO/AIA

Prominences are bizarre structures in the chromosphere reaching all the way up into the solar corona. They are made of relatively cool (7000 degrees) and dense material suspended in the rarefied, million degrees hot corona (Figure 30). Despite this apparently unstable situation, prominences are common structures and can live for several weeks. Often, their life is ended by an eruption as part of a CME.

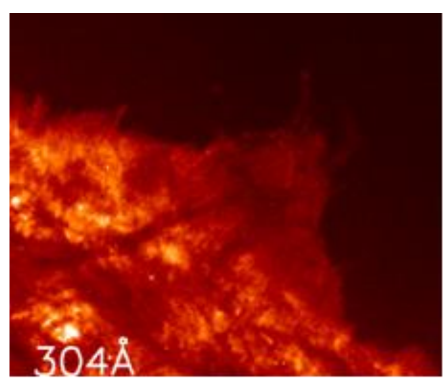

Figure 30: A prominence observed by SDO/AIA which samples the plasma at about 80,000 degrees (304 band).

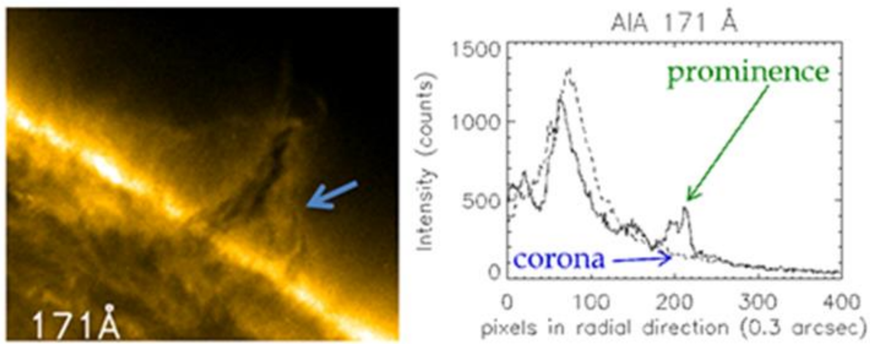

Figure 31: Left: The same prominence as in Figure 30 but seen in the 171 band which samples the plasma at 600,000 degrees. For the first time, this band has shown a faint emission as indicated by the blue arrow. Right: Radial cuts across the prominence (solid line) and outside into the corona (dashed line) are shown. Stronger emission from the prominence above the coronal background is clearly visible.

The physics governing the stability of prominences is still not well understood. This is, amongst other things, because the cool plasma in the prominence core is optically thick. To deduce its properties from observations, a complex physical description is needed, including non-local thermodynamic equilibrium radiative transfer modeling. This core is interfaced to the corona through the prominence-corona transition region (PCTR), a relatively thin layer where the temperature gradient is very steep and the plasma becomes completely rare. This layer contributes to the insulation and pressure balance of the prominence against the corona. As the different properties of these two parts of the prominence require different techniques of investigations, a common picture of the whole core-PCTR is still missing. In particular the PCTR is often ignored or only partially integrated in the modeling. Instead, we concentrate on the understanding of the PCTR properties and aim at linking them to those of the massive and cooler core.

One of the partially known properties of the PCTR is the temperature structure, i.e. the amount of plasma along the temperature gradient. This is important as it allows deriving the total radiative losses of the layer, which feeds the energy balance equation. In the past, it was generally believed that not much emission of the prominence existed above 100,000 degrees. This was deduced from the fact that nothing was seen in prominence images from SOHO/EIT 171 band (sampling plasma at about 600,000 degrees). Other spectroscopic ultraviolet (UV) investigations were not able to disentangle the background-foreground coronal emission from that of prominences.

After the launch of NASA's SDO, things have changed. Its high signal-to-noise (S/N) EUV telescopes have revealed, for the first time, a faint prominence emission in the 171 band, as shown in Figure 31. This has stimulated our curiosity, as the telescope's passband includes, in addition to Fe IX (8 times ionized iron), a smaller contribution from spectral lines emitted at lower temperatures (near 400,000 degrees). So, the question we asked was if this visible emission was coming from the cooler

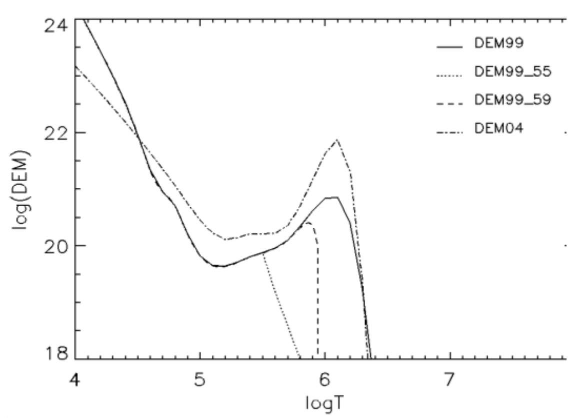

Figure 32: Amount of plasma (indicated as DEM) as a function of the logarithm of the temperature for the four PCTR models.

components falling into the band or from the dominant hotter line Fe IX at 700,000 degrees?

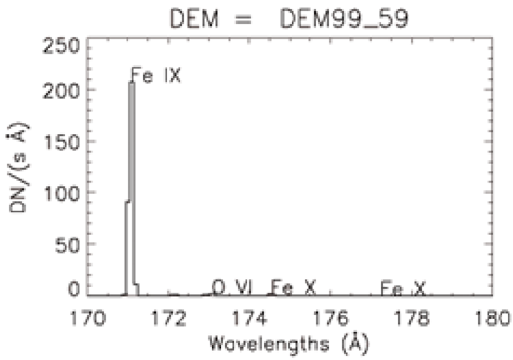

Figure 33: synthetic spectrum obtained using model DEM99_59 within the AIA 171 band. The Fe IX dominates the counts in the band.

To answer this question, we simulated the emission of a prominence measured by AIA (Atmospheric Imaging Assembly), using different thermal models for the PCTR which are shown in Figure 32. From spectroscopic observations, the models DEM99 and DEM04 were derived (DEM: Differential Emission Measure). In addition, we artificially removed the hotter contribution creating the DEM99_59 and DEM99_55 curves. An example of the PCTR emission measured by the AIA 171 band and produced using these models is shown in Figure 33. Our tests show that when there are enough counts above the noise level, the 171 AIA band is always dominated by the emission from the hotter Fe IX ion. As a consequence, we conclude that the PCTR has much more emission above 400,000 degrees than what was previously thought. This very important result implies that, from now on, the core-PCTR model and energy balance equations should include this newly found hot component.

Instrumentation and experiments

Picasso: small satellites for a big project

In the course of 2012, the idea matured to initiate a CubeSat project on the Space Pole. Rather than the traditional idea of using a CubeSat in an educational project or as a technology demonstrator, the idea was to set up a true scientific mission called PICASSO (PICosatellite for Atmospheric and Space Science Observations).

CubeSats are small: Their size is expressed in "units", where each unit represents a 10×10×10 cm^3 cube and can accommodate 1 kg of mass. PICASSO would be a triple CubeSat, 30 cm long. It is planned to fly on the QB50 mission in a quasi-polar orbit at about 500 km altitude, with an orbital lifetime of at least two years. The PICASSO spacecraft will align its long axis with the direction of the Sun, so that its unfolded solar panels receive full sunlight. Science telemetry will be implemented through an S-band link.

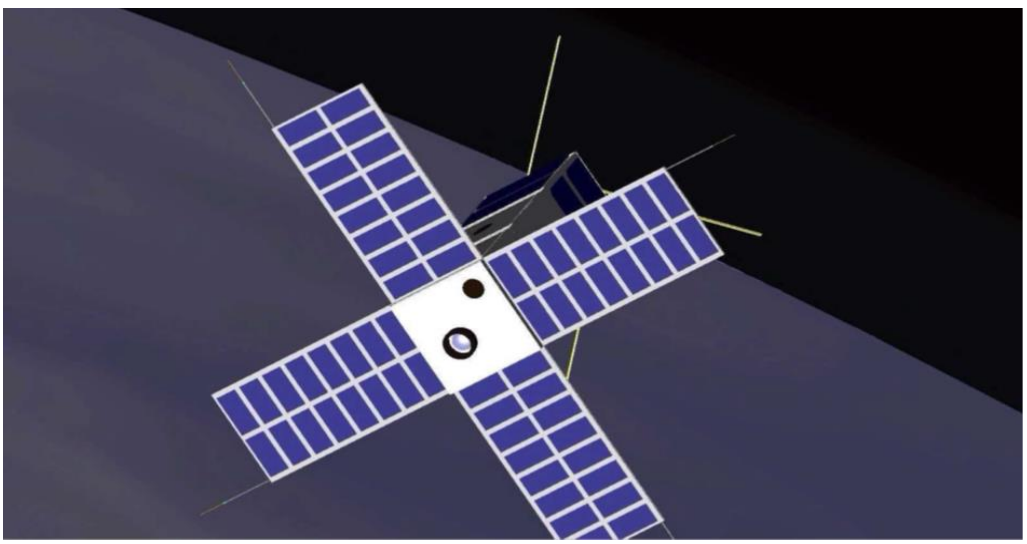

Figure 34: PICASSO has solar panels that unfold so as to receive full sunlight when the spacecraft's long axis points to the Sun. Also visible is the lens of the VISION hyper-spectral camera on the Sun-facing surface. The SLP Langmuir probes are sticking out at the extremities of the solar panels.

There are two reasons to participate in this mission: instrument technology and science. Indeed, a small picosatellite platform poses unique requirements on the size and the capabilities of the instruments. Small instruments require sophisticated measurement technology and instrument design, and such instruments are more likely candidates for any solar-terrestrial science mission. And, if all goes well, PICASSO will return valuable data that are relevant for the study of space weather, the upper atmosphere, and the Earth's radiation budget. The instrument package that will be carried by PICASSO consists of the SLP, the VISION, and the µBOS instruments.

The sweeping Langmuir probe (SLP) is a novel instrument that includes four cylindrical probes, mounted on small booms at the extremities of the deployed solar panels. The instrument sets an electric potential difference between each probe and the spacecraft outer surface, and measures the resulting current flow as electrons from the plasma are attracted to the probes. In practice, the electrical potential is swept in such a way that both electron temperature and electron density can be derived. The duty cycle will be kept to less than 5 % in order to avoid spacecraft charging. A certain amount of on-board data processing will be performed prior to sending the data back to Earth. Given the high inclination of the orbit, the SLP instrument will allow a global monitoring of the ionosphere. Therefore, PICASSO will enable the study of space weather phenomena such as ionosphere-plasmasphere coupling, auroral structure, and ionospheric dynamics.

The Visible Spectral Imager for Occultation and Nightglow (VISION) is a hyper-spectral camera that will observe solar occultations by the Earth. This instrument integrates a variant of the VTT camera used in Aalto-1, but the instrument electronics and control software will be developed in-house. Given the 2.5° field of view of the camera, the spacecraft must possess accurate attitude control. VISION will be able to obtain vertical profiles of the composition of the upper atmosphere (incl. ozone) by observing the Earth's atmospheric limb during orbital sunset and sunrise. A secondary objective is to measure the deformation of the solar disk by atmospheric refraction, from which stratospheric and mesospheric temperature profiles can be retrieved. Finally, occasional full spectral observations of airglow and of polar auroras are also foreseen.

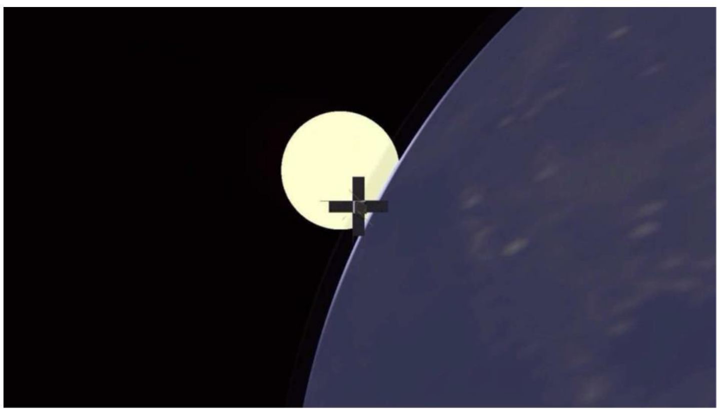

Figure 35: Impression of PICASSO observing a solar occultation.

Finally, the micro - bolometer sensors of the µBOS instrument (micro Bolometric Oscillation Sensor) measure the radiative flux integrated over their field of view as seen from each side of the CubeSat. In low Earth orbit, such instruments respond to both short wave solar radiation (incident from the Sun and reflected from Earth) and the Earth's long wave emitted infrared. Understanding the radiative balance between these contributions is an essential input to the study of Earth's climate. The spectral difference between the total solar irradiance and the Earth's infrared emission allows separating both contributions. The instrument has heritage from the Picard and Proba2 bolometers. Monitoring spatial and temporal variations in the outgoing and incoming radiative fluxes of the Earth can help to quantify the differences between fluxes over land and oceans, and variations in albedo due to varying ground cover and clouds.

The PICASSO mission is still in its infancy, with the full funding picture not clear yet. In 2013, the spacecraft bus will be acquired using Lotto funding. At present, the participating STCE teams are working hard to design the instruments. The next step will be the construction of prototypes. This is a story to be continued …

Development of new solar instrumentation

Future missions for space astronomy and solar research require the development of critical optical components for improved UV solar observations. For the future space missions planned to study the Sun (e.g., ESIO, PICASSO; see Figure 36), new technologies capable of operating at high temperatures and in harsh environments are developed and investigated. Since industry progress in these fields is clearly insufficient, it has been a successful tradition in solar-terrestrial physics to trigger and perform specific technological developments. At ROB/STCE, we have identified and developed a specific expertise in the development of UV detectors based on wide band gap material (WBGM).

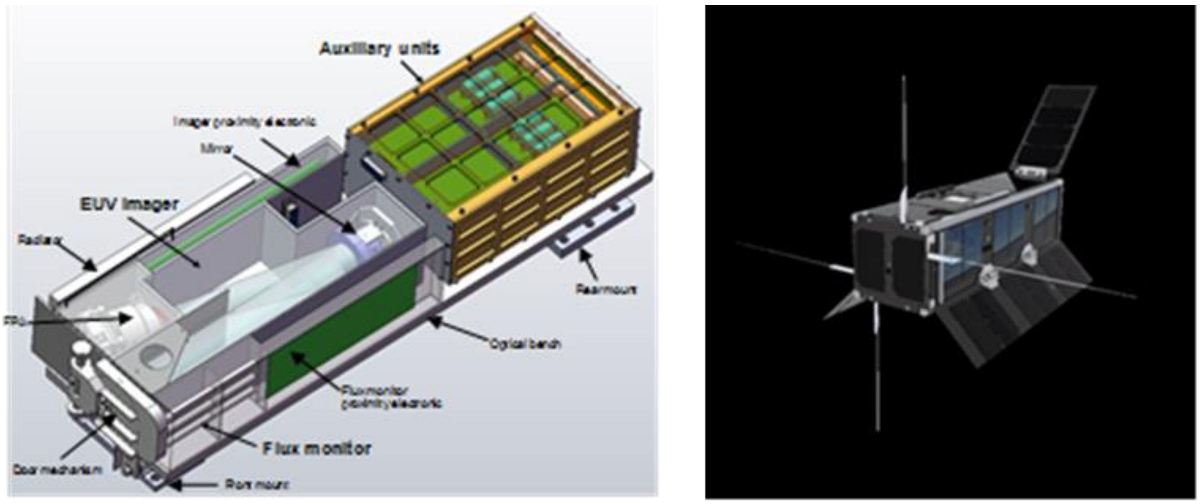

Figure 36: Schematic representation of (left) the EUV Solar Imager for Observations (ESIO) prototype and (right) Pico-satellite for Atmospheric and Space Science Observations (PICASSO) onboard a CubeSat (QB-50) to be launched in 2015.

In 2012, the STCE/ROB team "Advanced technology for Solar Observations", together with our partners, meets the challenge of building a new generation of ultraviolet detectors.

- **UV detectors developments (single pixel)**

Knowing the harsh space environment, the radiation effect at the detector level is anticipated with the use of WBGM-based photodetectors which are promising alternatives to the commonly used silicon photodetectors. By their nature, WBGM have very low sensitivity to visible light, a thermally-induced dark current much lower than other semiconductors, and a high level of radiation-hardness. For those reasons, WBGM-based photodetectors could significantly enhance the stability of the radiometric calibration of solar UV radiometers.

Figure 37: Photographs of the AlN MSM photodiodes mounted on ceramic packaging. The MSM surface area (from left to right) are 4, 3, 2 and 1 mm diameter with 2 µm interdigitated finger width and 5 µm spacing between two electrodes.

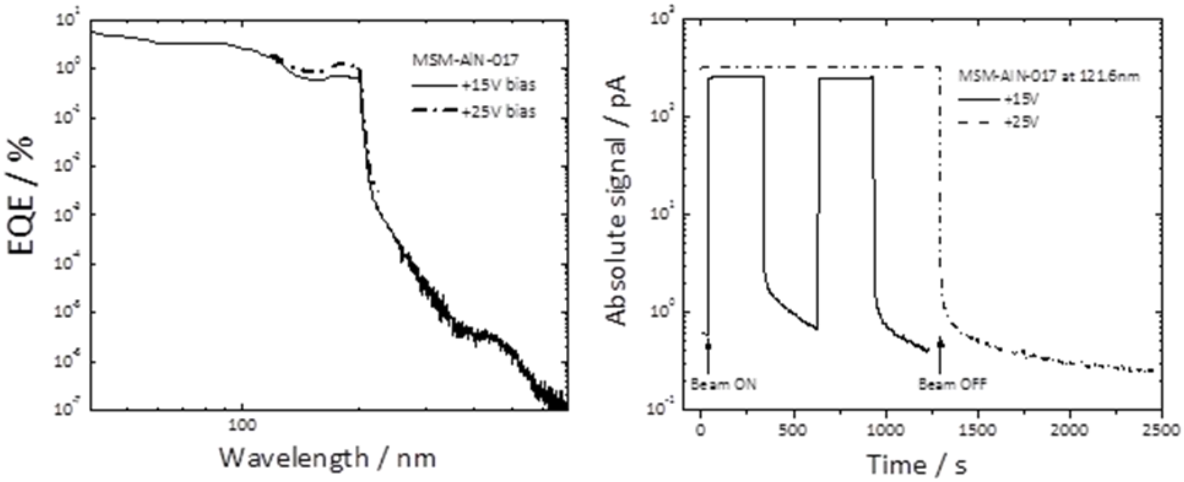

Figure 38: Left: Absolute external quantum efficiency of the MSM-AlN-017 photodetector (3 mm diameter) in the range between 40–700 nm at +15 V and +25 V. Right: Signal stability test (at room temperature) under +15 V and +25 V bias at power level ~ 0.17 µW at 121.6 nm wavelength.

After a first optimization step, innovative metal-semiconductor-metal (MSM) photodetectors based on aluminum nitride (AlN) were developed and characterized at DeMeLab (STCE/ROB) as shown in Figure 37. In the wavelength range of interest (here the 10-200 nm range), MSM-AlN is reasonably sensitive and stable under brief illumination with a negligible low dark current as shown in Figure 38.

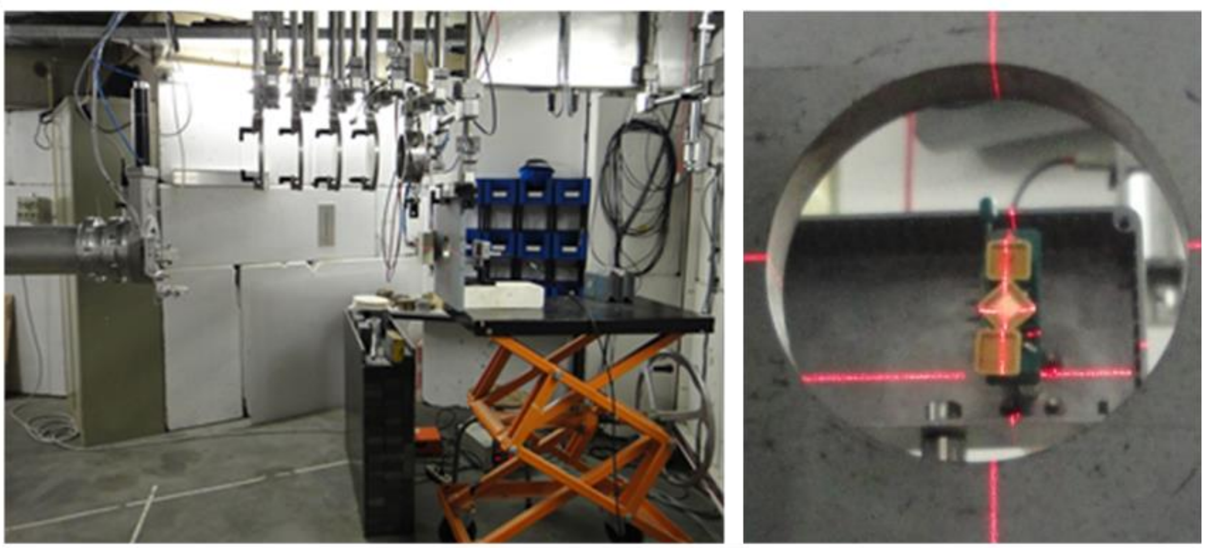

Figure 39: Photograph of the proton test facility at LIF-CRC in Louvain-La-Neuve, Belgium (left) and the irradiated detectors (right).

Radiation hardness against protons is a primary concern for upcoming solar missions in space during long-period interplanetary orbits or when flying in low-Earth orbit and exposed to inner belt protons especially because of the South Atlantic Anomaly (SAA). Both ionization and atomic displacement damage effects are often the main cause of space-based instrument degradation. To assess their impact effects on our detectors, irradiation tests using a beam of 14.4 MeV protons were performed at LIF-CRC (Belgium) (see Figure 39). No significant degradation of the detector performance has been observed which demonstrates a good radiation tolerance for proton fluence up to $1{\times}10^{11}$ /cm^2.

Solar Orbiter Workshop

Solar Orbiter is the next ESA flagship for studying our closest star, the Sun. It is currently scheduled for launch in 2017. By approaching as close as 0.28 AU (astronomical unit; 1AU is nearly 150 million km), Solar Orbiter will view the Sun with high spatial resolution and combine this with in-situ measurements of the surrounding heliosphere. Thanks to its unique orbit, Solar Orbiter will deliver images and data of the unexplored Sun's polar regions and the side of the Sun not visible from Earth.

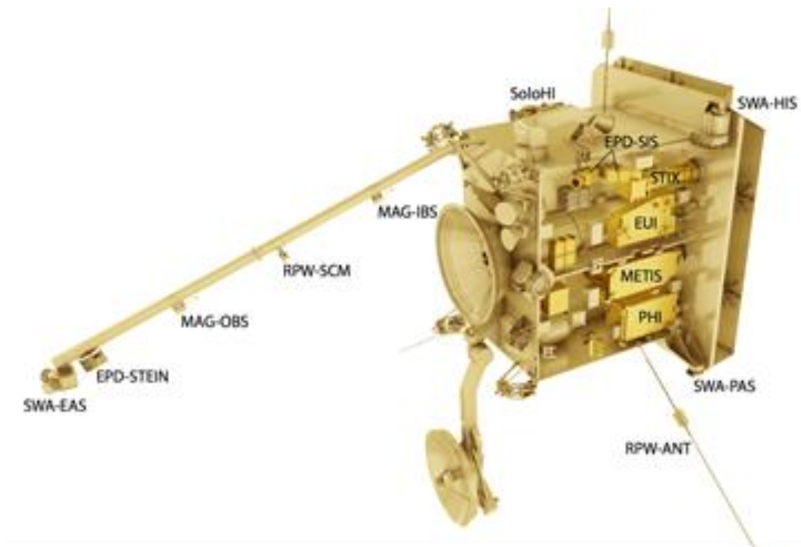

Figure 41: Solar Orbiter and its suite of remote sensing and in-situ instruments. Note in particular the heat shield in the back, the deployable high gain antenna at the bottom and the in-situ boom on the left. Belgium is a leading partner in the international consortium that is building the EUI instrument (EUI= Extreme Ultraviolet Imagers; Principal Investigator (PI): Pierre Rochus, CSL).

Figure 40: The conference poster was designed by Wim Vanderputten (Planetarium, Heizel). The poster includes the logos of the sponsors of the conference: ESA, BELSPO, STCE and CSL.

From 10 till 14 September, the scientific community behind Solar Orbiter assembled its "5th Solar Orbiter Workshop" (SO5) in the historical center of Bruges. 180 scientists attended and discussed how science can best profit from the unique opportunities offered by Solar Orbiter, which is a partnership between ESA and NASA. The scientific synergy of Solar Orbiter with Solar Probe Plus and other missions was also highlighted.

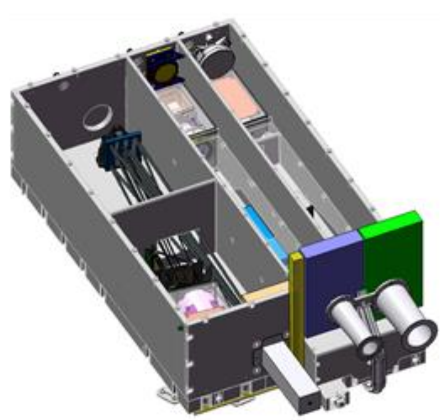

Figure 42: The EUI instrument will consist of 3 telescopes: 1 full sun imager (left) and two high resolution imagers (right). The latter two will image the solar corona in unprecedented resolution.

Solar physicists at STCE/ROB have a leading role in the EUI instrument onboard Solar Orbiter. The instrument concept was conceived at the Solar Physics group of ROB including the use of some of its key technologies (APS detectors, compression,…). EUI is now being built by an international consortium under the leadership of Pierre Rochus from the Centre Spatial de Liège (CSL). A group of about 10 researchers at STCE/ROB is actively supporting this development. In the operational phase of the mission (>2017), the EUI instrument will be operated from the EUI Data Center at STCE/ROB.

Figure 43: Many young, new researchers at the STCE took the opportunity of the Solar Orbiter Workshop being hosted in Belgium to get acquainted with this upcoming new mission.

The Scientific Organizing Committee (SOC), consisting of the principal investigators of all the instruments onboard Solar Orbiter, was co-chaired by Daniel Mueller (Project Scientist of Solar Orbiter, @ESA) and by Andrei Zhukov (Project Scientist of the EUI instrument onboard Solar Orbiter, @ROB).

Local Organization was taken care of by the well-trained STCE team including Anne Vandersyppe, Olivier Boulvin, Sarah Willems, Petra Vanlommel, Jan Janssens and Bram Bourgoignie. All details of the Solar Orbiter Workshop 5 can be found at http://www.stce.be/solarorbiter5/

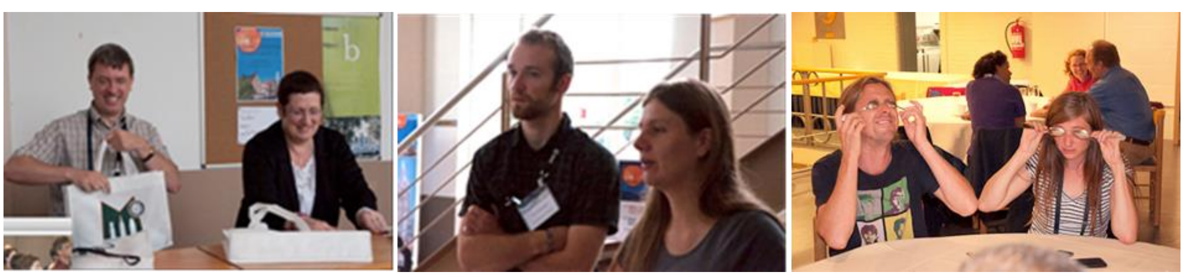

Figure 44: The Local Organizing Committee (LOC) at work: at the registration desk, the IT wizards, and keeping an eye on the pack during the conference dinner.

Integrated Water Vapor Observations: a techniques inter-comparison

Water vapor plays a dominant role in the climate change debate, as it is the most important greenhouse gas and provides the strongest positive feedback mechanism for the surface warming. However, observing water vapor over a climatological time period in a consistent and homogeneous manner is challenging, because water vapor is highly variable both in space and time. The three institutes from the Space Pole (ROB, RMI and BISA) formed a working group in the framework of the STCE to bring together their specific knowledge in the domain and to tackle this challenge thanks to their complementarity. In particular, we concentrate on the total amount of water vapor in a column extending from the surface to the top of the atmosphere, also called the “precipitable water vapor amount” or Integrated Water Vapor (IWV). This variable should increase in close association with climate warming, as dictated by a physical law which states that the water holding capacity of the atmosphere goes up at about 7% per degree Celsius increase in temperature.

To check this law with world-wide observations, we first have to assess which instruments and datasets are good candidates to retrieve homogenous, consistent and long-term IWV measurements. Therefore, we set up a world-wide techniques inter-comparison consisting of seven different devices: two ground-based (GPS and sun photometer), one in-situ (radiosondes, attached to weather balloons) and four satellite-based (measuring in the visible wavelength range, GOME/SCIAMACHY/GOME-2, and in the thermal infrared, AIRS). The map showing the 28 stations used in this study is presented in Figure 45.

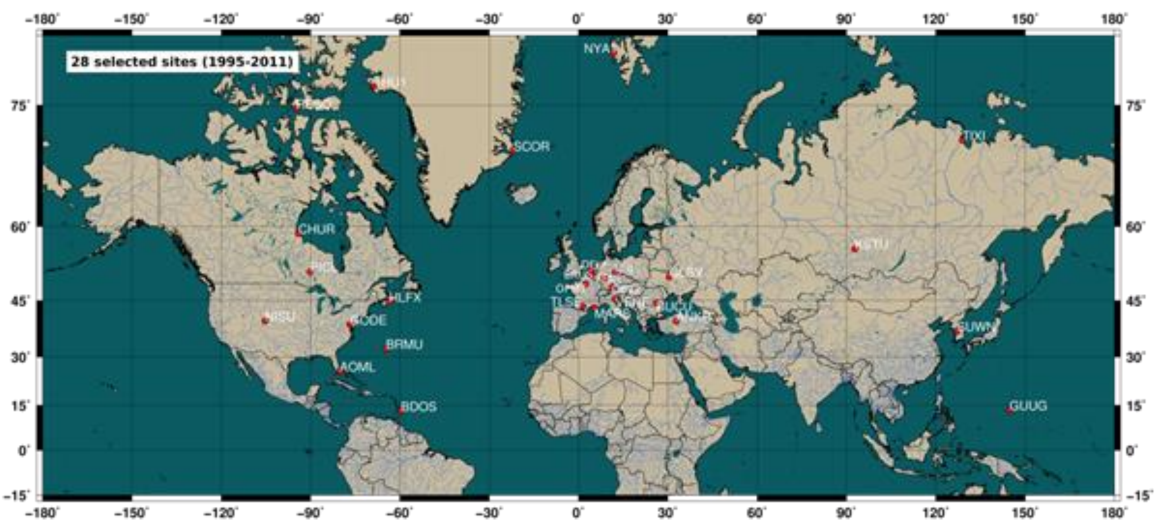

Figure 45: Map of the 28 sites that host at least two of the considered instruments.

We choose one reference IWV dataset, against which coincident and co-located measurements of the other instruments are evaluated (by means of so-called “scatter plots”). The best candidate reference dataset consists of the GPS observations from the International Global Navigation Satellite System Service (IGS), as the GPS-based IWV are provided by a homogeneous reprocessing and are available at high time frequency (every 5 minutes) and under all weather conditions. Figure 46 shows the summary of the statistical properties of the comparison of the IWV measurements of each instrument, against the co-located GPS IWV retrievals.

- First, it can be noted that the mean biases of the different techniques w.r.t. the GPS estimates vary only between -0.3 to 0.5 mm of IWV, but with a large variability around those mean values, especially for the satellite instruments.

- Secondly, we can conclude that the best correlations with the GPS technique (correlation coefficients r^2 closest to one) are obtained for the other ground-based technique (CIMEL sun photometer) and the in-situ instrument (radiosondes).

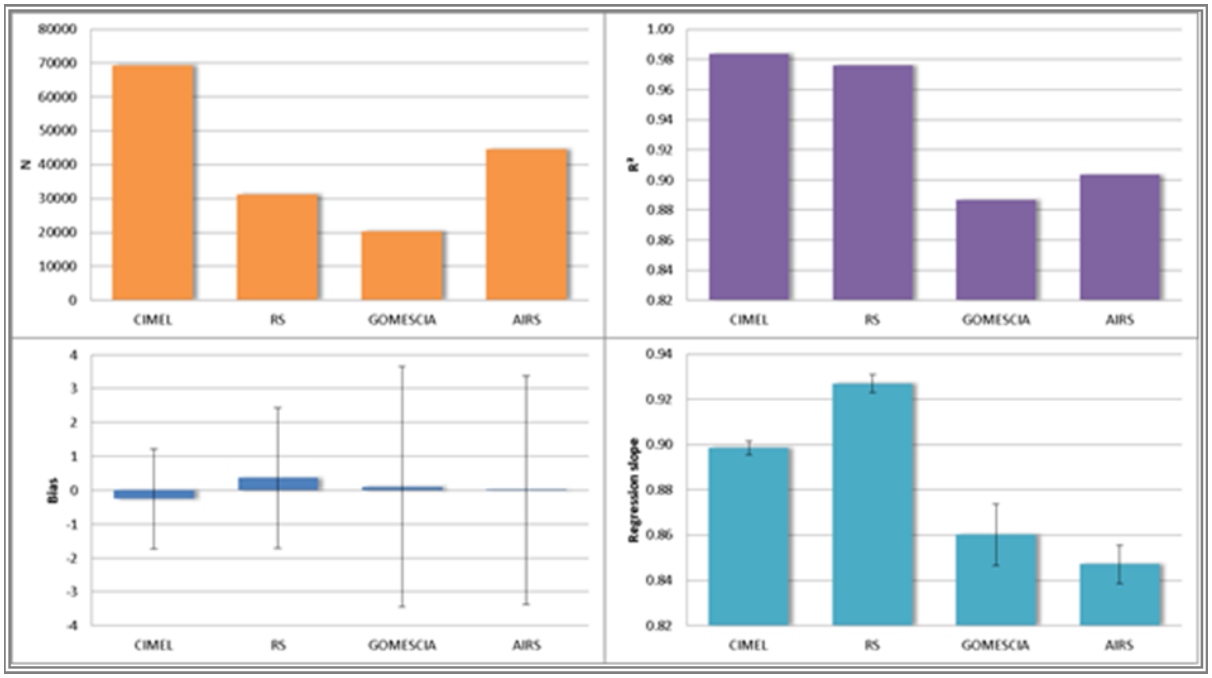

Figure 46: Column bar plots of scatter plot properties (number of couples N, bias, correlation coefficient r^2 and regression slope) of the different instruments versus GPS (averaged over all stations included in the techniques intercomparison). The error bars represent the Root Mean Square (bias) and the standard deviation (regression slope). CIMEL is a sun photometer, RS stands for radiosondes and the acronym GOMESCIA denotes the combination of GOME, SCIAMACHY and GOME-2 measurements.

A last consideration to make from Figure 46 is that the two all-weather devices (radiosondes and GPS) have the highest slope coefficient for their linear regression. A value of one means that the IWV measured by one of the techniques will change by the same quantity as the GPS IWV does. The fact that this value is significantly lower than one for the sun photometer and the satellite devices is related to the observation bias of those techniques: Measuring with these instruments is possible for low cloud fractions only. As a matter of fact, we found that the clearer the sky, the closer the regression slope w.r.t. GPS approaches one for especially the CIMEL and GOMESCIA IWV measurements. As a result, for high IWV values, when clouds might contribute to this water vapor amount in the sky, the GPS technique always gives higher IWV retrievals than the other techniques. On the other hand, for very small IWV values, the GPS technique seems less sensitive to the IWV than the other techniques and therefore gives rise to lower IWV values. Both effects are responsible for regression slopes w.r.t. GPS below 1.

This finding that GPS instruments seem to have different sensitivities to IWV at the IWV extremes than the other instruments, in part because of the observation bias of the other instruments, also leads to a seasonal and geographical dependency of the biases (and Root Mean Squares RMS) w.r.t. the GPS! Indeed, for larger IWV values, which are more frequent in northern hemisphere summer season and at lower latitude stations, the GPS retrieval technique leads to higher IWV values than the other instruments, so that the IWV bias w.r.t. GPS (instrument minus GPS) will be smaller (or negative). The reverse reasoning can then be done for the lower end IWV values. On the other hand, the RMS w.r.t.

GPS is minimal in winter and maximal in summer and decreases with increasing latitude (decreasing mean IWV).

Also, if one looks at the spatial pattern of the comparisons between IWV measurements obtained by a satellite device and those obtained with the GPS technique, one notices a large variability with latitude or longitude in the comparisons (e.g. mean IWV differences). This geographical variability is larger for satellite devices than for the comparison of the other techniques (one ground-based, one in-situ) with GPS. This is possibly due to the large pixel size of some of the satellite instruments compared to the GPS device. Because the IWV is highly variable in (horizontal) space, the pixel measured by the satellite instruments might contain contributions from clouds (that of course increase the IWV), whereas the GPS device might not! These differences can be more important for sites with a larger integrated water vapor content (tropical sites for instance), than for others (high-latitude sites). A follow-up study will now concentrate on the resulting IWV trends from the different datasets.

One of the main conclusions of this research is that CIMEL sun photometers and GPS are very valuable techniques to measure IWV and the most promising to build up long time series for climate applications, as long as the data homogeneity can be guaranteed.

Absolute spectrophotometry of the Sun

The Sun is a variable star. The variability of its electromagnetic spectrum presents a wide range of periodicities, varying from minutes to decades. The overall 11-year modulation of the solar energy flux comes from the magnetic activity of the Sun. The amplitude of this variability is also strongly wavelength dependent, being more pronounced for radio waves and from UV to X-rays.

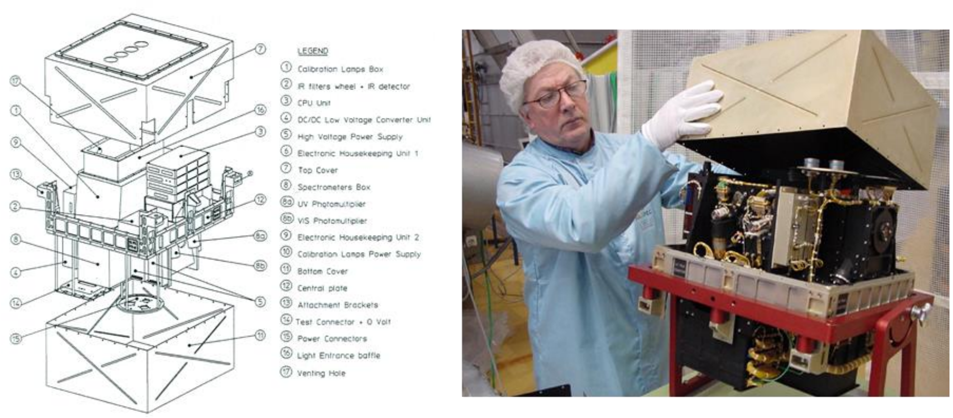

Figure 47: The new SOLAR version of SOLSPEC, as designed (on the left) and after its integration at IASB (right).

Radiometry, applied to the measurement of the energy flux of the Sun, studies this spectral distribution and its variability. This can be done using space qualified instruments (such as SOLSPEC, for SOLar SPECtrum, to which the present work was dedicated) that are designed for measuring the full solar spectrum above the atmosphere in absolute radiometric units (the spectral irradiance in $mW/m^2/nm$) normalized at 1 AU (Astronomical Unit). These measurements have to be performed from space to avoid the diffusion and absorption by the atmosphere.

The accurate determination of the solar spectral irradiance above the atmosphere is a main issue for the following research areas:

- In solar physics, this is required for studying the composition of the solar atmosphere, the atomic elements and internal physical processes at the origin of the emission. Modeling efforts compile these processes in order to reproduce the solar spectrum and its variability. The solar spectrum measurements are required for the validation of such semi-empirical modeling.
- Knowledge of the solar irradiance is also a prerequisite for the study of the photochemistry of the Earth's atmosphere and for climate modeling. The composition, the thermal structure, and the dynamics of the atmosphere are dependent on the incoming solar flux, its spectral distribution and variability. The measurements are of prime importance for the validation of radiative transfer and climate models.

Moreover, as each solar cycle presents a different behavior, there is a need for continuous measurements above the atmosphere, performed if possible by more than one instrument for redundancy. This has been done since 35 years by means of space qualified spectroradiometers. The SOLSPEC instrument brought a major contribution in this respect by participating to 5 space flights in the 80's and 90's. The project was initiated by the CNRS (France, actually the LATMOS-CNRS) and supervised by the CNES (France), with major collaborations from BIRA-IASB and the Heidelberg Observatory (Germany).

SOLSPEC is equipped with 3 coupled spectrometers using concave gratings, covering simultaneously the UV-VIS and IR spectral ranges. The detectors are photo multiplier tubes (PMTs) in photon counting mode for the UV-VIS and one photodiode for the IR. The first generation of SOLSPEC has been built to carry out the solar spectral irradiance from 200 to 2400 nm with an accuracy of 5 % in the UV and 3 % above.

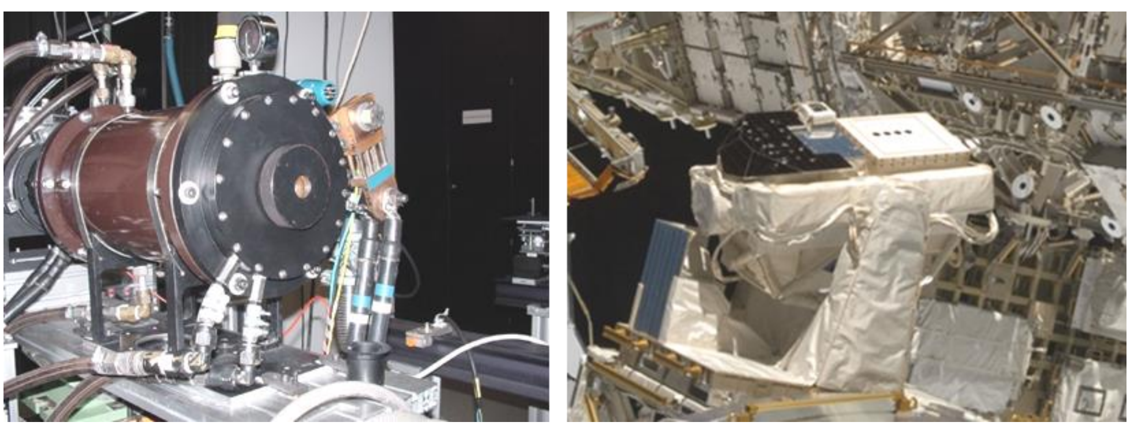

Figure 48: On the left: The black-body primary standard of spectral irradiance of the PTB (Physikalisch-Technische Bundesanstalt, Germany) used for the absolute calibration of SOLAR/SOLSPEC. On the right: The SOLAR payload after its stowage on the COLUMBUS European module on ISS (February 2008).

D. Bolsée completed his PhD thesis on absolute photometry of the Sun with SOLSPEC and presented it at the Faculty of Engineering Sciences (ULB, Brussels) on 8 May 2012. This PhD work was devoted to the refurbishment of SOLSPEC and its exploitation for the new long-term SOLAR mission, lasting 9 years, on board of the International Space Station (ISS) after its selection by ESA in 1997.

First, under the auspices of the Belgian Science Policy Office (BELSPO) and by the excellence of BIRA-IASB in space applications, major efforts were made by the SOLSPEC team for the software, the design and the realization of the new mechanical interface and the electronics. The work packages of the PhD were focused on the radiometry and metrology with the following results:

- The optical realignment of the spectrometers, the improvement of the spectral resolution and the extension of the spectral ranges covered by the instrument (166 nm to 3088 nm, containing more than 96 % of the total solar energy flux). SOLAR/SOLSPEC is now the only instrument in orbit measuring the solar irradiance up to 3 µm.
- The complete radiometric characterization of the instrument, for example, by the determination of the linearity, the wavelength scales, the diffuse light.
- The absolute calibration of the instrument, which is the relation between the radiometric absolute scales and the electronic signal, using the primary standard of spectral irradiance (black-body radiation) of the PTB (Physikalisch-Technische Bundesanstalt, Germany).
- The development of a new internal lamp unit for relative calibration using deuterium, tungsten and hollow cathode lamps integrated in the instrument. Indeed, the degradation of the responsivity and the spectral characteristics of the spectrometers due to the harsh space environment must be checked during the mission and the lamps must be used for the conservation of the built-in absolute radiometric scale.
- The development of a passive solar sensor for monitoring the alignment of the Sun during the solar measurements.
- The evaluation of the standard uncertainties, using the mathematical methodology applied in metrology. The results showed an uncertainty limited to 1 % between 500 and 1900 nm, 2 % from 370 to 2350 nm and around 4 % elsewhere, except for the end of the IR channel.

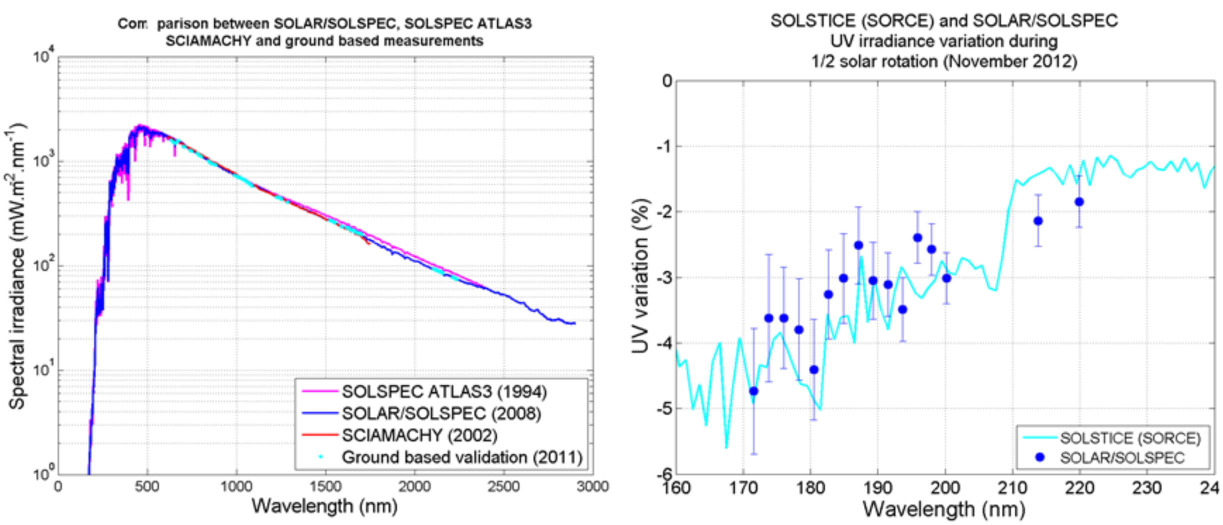

Figure 49: On the left: Comparison between the SOLSPEC ATLAS3, SCIAMACHY, SOLAR/SOLSPEC and the ground-based validation campaign. On the right: Variation of the solar UV irradiance as observed by SOLSTICE on SORCE and SOLAR/SOLSPEC during one half solar rotation (November 2012).

The data processing of the first results after the launch (8 February 2008) demonstrated the stability of the radiometric performance in space. The solar spectrum above the atmosphere was determined and compared to results obtained from the previous SOLSPEC missions and the ongoing SORCE and SCIAMACHY missions.

Controversial results were obtained for the IR part of the spectrum. SOLAR/SOLSPEC provided similar irradiance levels as SCIAMACHY, but different than current semi-empirical models or the reference solar spectrum from SOLSPEC ATLAS3 (Figure 49, left). In the continuation of the PhD, a validation campaign was organized. The objective was to use an instrument similar to SOLSPEC (a 'ground based version') calibrated against the same primary standard of spectral irradiance at the PTB. Using a high altitude measurement site and a technique to retrieve the TOA (Top Of Atmosphere) solar irradiance in the IR through atmospheric windows (Bouguer-Langley analysis) that is able to remove the effects of diffusion by molecules and aerosols, we obtained data points leading to a confirmation of the SOLAR/SOLSPEC results. After additional analysis we could answer the question: "is our full SOLAR/SOLSPEC spectrum compatible (after wavelength integration) with the accepted value of the solar constant, even if we measured a lower IR irradiance level?" affirmatively.

For the detection of the solar irradiance variability in the UV, arising with the new SC24, actual post thesis works are devoted to the analysis of the proxy of solar activity as the MgII index correlated to the solar UV variability observed during one solar rotation (27 days), leading to the determination of the scaling factors (which are the % of UV change, for 1 % of MgII index change). These results (Figure 49, right) are also compared to the ones obtained by the instrument SOLSTICE on SORCE (USA).

In conclusion, based on the experience gained during this PhD and the 30 before, we have become a very active player in the international effort for measuring the TOA spectral irradiance of the Sun, a key input for the solar and Earth sciences.

What is the value of the solar constant?

The Total Solar Irradiance (TSI) is an Essential Climate Variable (ECV) that describes how much energy the Earth is receiving from the Sun, and that is driving the climate on Earth. The RMIB is making space instruments for the measurement of the TSI with 11 space flights since 1983 – now exactly 30 years ago - and currently has two active instruments in space (see Figure 50). Diarad/Virgo has been measuring the TSI for a record time period of 17 years since 1996, and Sova-Picard is measuring since 2010. The RMIB space instrument team is

Mission	Instrument	Launch	Status
Spacelab 1	Solcon 1	1983	Short-term
Atlas 1	Solcon 2	1992	Returned to ground
Eureca	Sova 1	1992	10 months data, returned to ground
Atlas 2	Solcon 2	1993	Returned to ground
Atlas 3	Solcon 2	1994	Returned to ground
SOHO	**Diarad/Virgo**	**1995**	**Ongoing**
Hitchhiker TAS	Sova 1	1997	Returned to ground
Hitchhiker IEH-3	Solcon 2	1998	Returned to ground
Freestar	Solcon 2	2003	Instrument lost during return
Columbus/ISS	Diarad/Sovim	2008	1 year data, failure of power supply
Picard	**Sova-P**	**2010**	**Ongoing**

Figure 50: RMIB space instrument missions for the measurement of the Total Solar Irradiance. The currently active instruments in space are highlighted in green.

maintained thanks to the STCE.

The long term international measurements of the TSI started with ERB on Nimbus 7 in 1978. The RMIB contributions are Sova1, Diarad/Virgo, Diarad/Sovim and Sova-Picard (Sova-P). All instruments show similar variations of the TSI but have differences in absolute level. In the past, the American ACRIM, the Swiss PMOD and the Belgian RMIB groups agreed on a value of the solar constant around 1366 W/m^2 within +/- 1 W/m^2. The new American TIM/SORCE instrument, which was launched in 2003, measured at that time about 5 W/m^2 lower than the other instruments yielding a value of the solar constant of only 1361 W/m^2, with claimed accuracy better than 1 W/m^2!

In order to solve this discrepancy, the four international TSI teams were invited to review their individual instruments. In doing so, on the RMIB side we identified a systematic error in our TSI determination linked to the so-called non-equivalence between electrical and optical power. In our revised evaluation, we found a solar minimum TSI value around 1363 W/m^2 for our most accurate instrument – DIARAD/SOVIM on the ISS.

Figure 51: A member of the RMIB SOVA-P team checking the results of instrument testing.

The TIM team at LASP built the ground based TIM Radiometer Facility (TRF) allowing the comparison of a radiometer with a reference cryogenic radiometer. A ground witness of the space TIM radiometer agreed with the reference cryogenic radiometer both in power and irradiance comparison mode. Later, the PMOD and ACRIM teams made comparisons with the cryogenic radiometer at the TRF. They found a good agreement with the cryo for power comparisons, but they measured higher values for irradiance comparisons than the cryo. They accepted the explanation that their higher value was due to a higher than accounted for amount of scattered light in the view limiting baffle in front of their precision aperture. Hence, they recalibrated themselves against the TRF cryo radiometer, and found recalibrated TSI values in space close to the TIM/SORCE values.

The RMIB group went to the TRF as the last team. Our test radiometer was Sovar, the Refurbished Sova1 radiometer that flew in space in 1992, and was brought back to Earth by the Space Shuttle. By carefully comparing Sovar with the TRF cryo in different illumination modes, we assessed:

- There is a good comparison between Sovar and the cryo in power comparison mode. This result validates our revision of the non-equivalence determination.
- The TRF suffers from a diffuse light problem originating in the optical elements (lenses) that shape the TRF laser beam, which can be mistaken for scattered light within the radiometer. This result suggests that the TRF comparisons with the PMOD and ACRIM radiometers need to be re-examined for a possible confusion of diffuse – originating in the TRF optical elements - and scattered – originating in a radiometer - light.

- The diffraction and scattering of Sovar can be measured experimentally with the TRF and is in reasonable agreement with the theoretical correction used in the Sovar data reduction. This validates the Sovar diffraction and scattering correction.
- Sovar measures a higher power than the cryo in irradiance comparison mode. This can only be due to the underestimation of the diffraction and scattering around the cryo precision aperture. Hence, Sovar is not measuring too high, but rather the cryo is measuring too low! As the geometry of the TRF cryo is comparable to the geometry of TIM/SORCE, a similar error could occur for TIM/SORCE in space, explaining why it would measure too low.

As a result of our non-equivalence revision, and of our TRF comparison, we now have good confidence that we can announce a new value of the solar constant around 1363 W/m^2 at the solar minimum. Figure 52 shows our composite TSI measurements (in red) and a regression model (in green) based on Mount Wilson magnetograms for the previous solar cycle 23 and the current solar cycle 24. The good agreement within +/- 0.2 W/m^2 between the measurements and the magnetic regression model indicates that only changes in the magnetic field on the surface of the sun are responsible for TSI variations. The current solar cycle 24 is significantly lower than the previous solar cycle. This is in agreement with the sunspot measurements which show that the current solar cycle is the lowest one since 1906. A continuation of the TSI measurements gives us a unique opportunity to quantify the long term variation of the TSI, and hence the influence of the Sun on Earth's climate change.

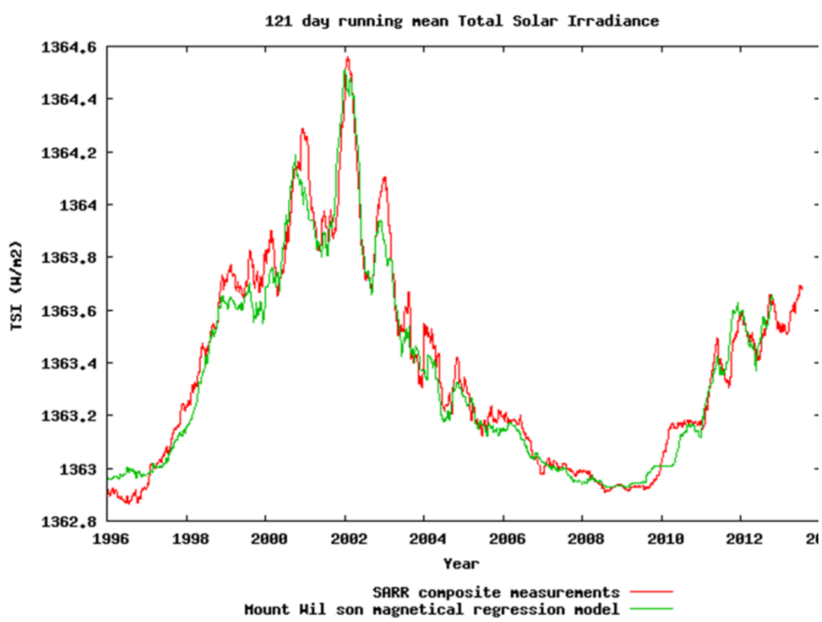

Figure 52: The composite TSI measurements (in red) and a regression model (in green) based on Mount Wilson magnetograms. The good correspondence indicates that only changes in the magnetic field on the surface of the Sun are responsible for TSI variations.

SIMBA the nanosatellite: measuring the Earth Radiation Imbalance

The Earth Radiation Imbalance is the small difference -about 0.5 W/m²- between the incoming solar radiation to the Earth -about 340.5 W/m²- and the outgoing terrestrial radiation -about 340 W/m²-, which is composed of reflected solar radiation (+/- 100 W/m²) and emitted thermal radiation (+/- 240 W/m²).

Within the current technological limitations, the incoming solar radiation is measured using cavity radiometers with a narrow opening angle, having an accuracy of the order of 0.1 % or 0.34 W/m². The outgoing terrestrial radiation is measured by higher resolution broadband radiometers like CERES and GERB with accuracies of the order of 1% or 1 W/m² for the reflected solar radiation and 0.5 % or 1.2 W/m² for the emitted thermal radiation. Clearly, the small signal of the earth radiation imbalance is overwhelmed by the sum of the calibration errors of the different instruments on the large and nearly equal quantities of incoming solar radiation and outgoing terrestrial radiation of which it is the difference.

Yet, the measurement of the Earth Radiation Imbalance is of fundamental importance, since it is the cause of climate change.

The Sun-earth IMBAlance (SIMBA) radiometer is an innovative concept for the Earth Radiation Imbalance developed within the STCE. The novel concept is to measure the incoming solar and the outgoing terrestrial radiation not with two separate instruments, but with one single instrument. SIMBA is a cavity radiometer similar to the ones used for measuring the incoming solar radiation, with an adapted wide field of view such that it can also measure the outgoing terrestrial radiation.

SIMBA is also technologically innovative. The cavity radiometer will be embarked on a so-called 3 Unit cubesat of 30 cm x 10 cm x 10 cm. Cubesats are miniaturized satellites originally developed for educational purposes, which are now rapidly gaining interest for scientific applications.

SIMBA was accepted for flight with the QB50 precursor flight. QB50 is a European project managed by the Von Karman Institute with the goal to launch 50 cubesats simultaneously. The funding for SIMBA is granted by the Belgian Science Policy Office (BELSPO) through the European Space Agency ESA. A SIMBA ESA GSTP project has started with a target launch date of August 2015. The SIMBA project is carried out by the Royal Meteorological Institute of Belgium (RMIB), in collaboration with the Katholieke Universiteit Leuven (KUL), the Vrije Universiteit Brussel (VUB), the French Latmos research laboratory, and the Royal Observatory of Belgium (ROB).

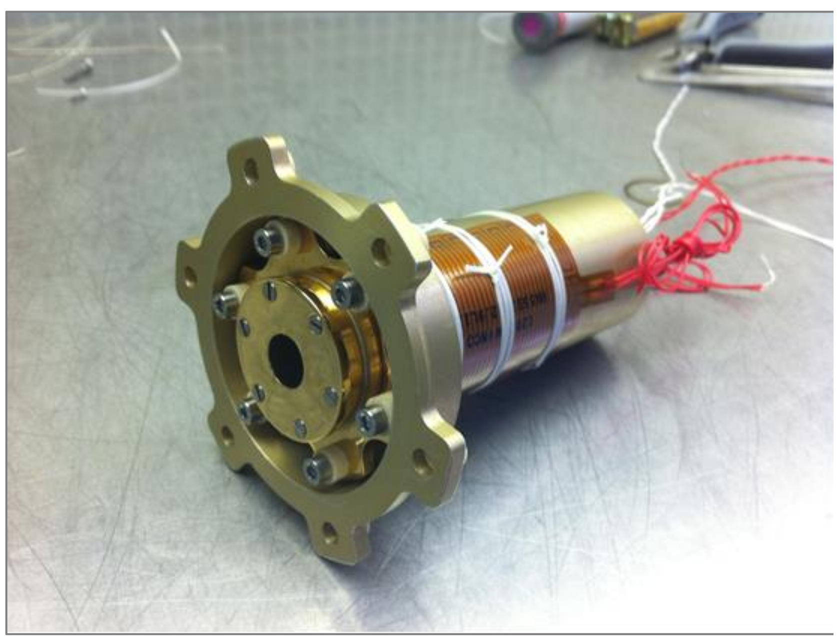

Figure 53: Prototype of the SIMBA main cavity detector.

Figure 53 shows the prototype of the SIMBA main cavity detector. It consists of a cylindrical cavity painted black on the inside, and mounted thermally isolated in an outer metallic housing. Radiation to be measured falls into the circular black opening to the left into the cavity and is absorbed there. The cavity is also heated through an electrical heating resistor. The power in the electrical heating resistor is regulated such that a constant temperature difference is maintained between the cavity and the housing. When radiative power falls into the cavity less electrical power is needed to maintain the constant temperature difference. The known regulated electrical power is a measurement of the unknown radiative power.

The goal of the first Simba satellite is to provide a technological demonstration of its concept. Our longer term goal is to obtain a constellation of Simba satellites which can measure the annual mean earth radiation with good spatial and temporal sampling.

Applications and Modeling

STAFF – Solar timeline viewer

At ROB, a new tool called STAFF (Solar Timelines viewer for AFFECTS) was developed. It is a brand-new, easy-to-use web tool (http://www.staff.oma.be) for viewing solar activity and space weather timeline data. It combines enormous datasets from different sources into one huge database and allows for comparing those on different time scales ranging from seconds to years.

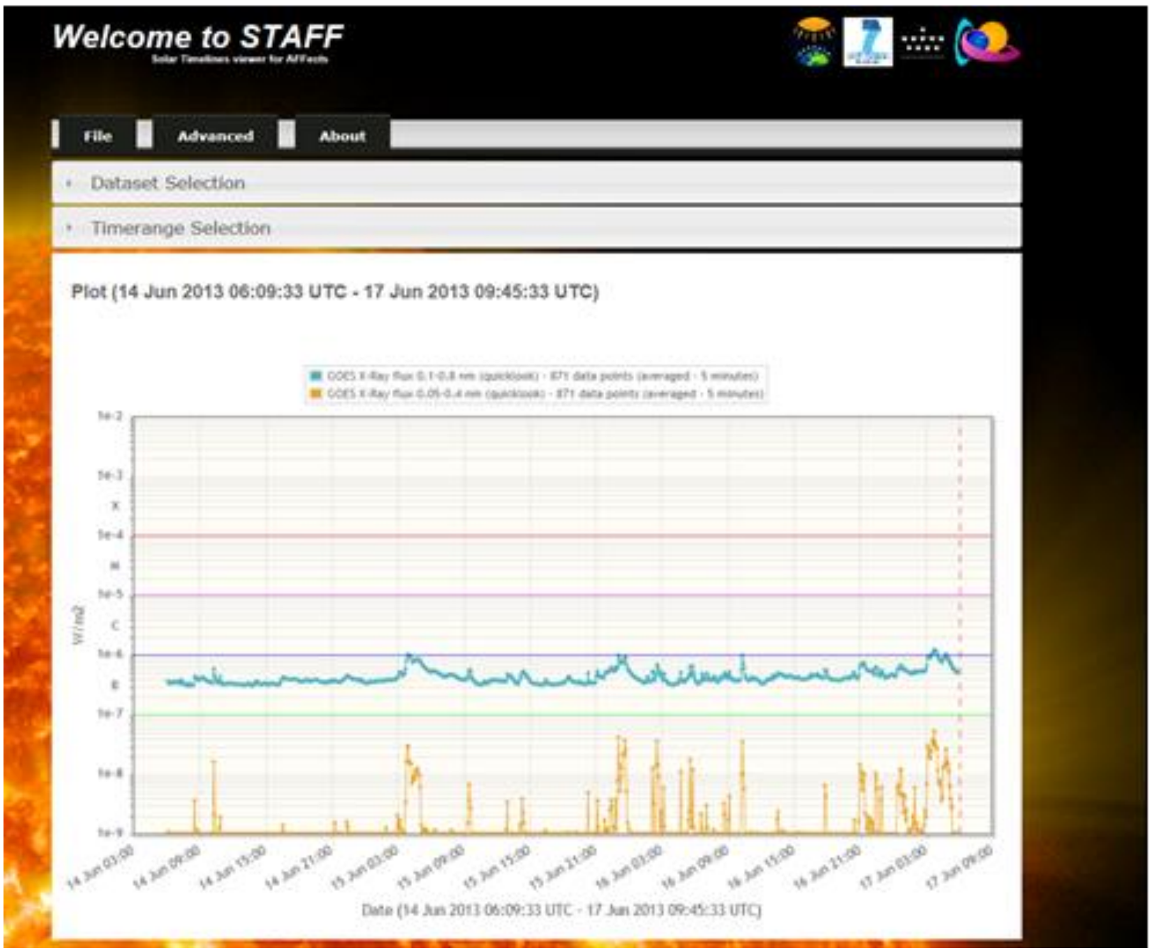

Figure 54: The STAFF web page, showing the x-ray flux from the GOES satellite for the last three days. Every peak in the curve corresponds to a solar eruption called "a solar flare".

STAFF has the ability to:

- Combine any dataset over any timeframe;
- Show data in near-real time;
- Export data as txt, csv or xls file;
- Export data as image;

- View the same dataset over previous solar rotations;
- The StaffBox allows any user to insert the power of STAFF into their own website.

These features make STAFF an ideal tool for space weather forecasting and research as well as for generating timeline plots to be used in presentations or publications.

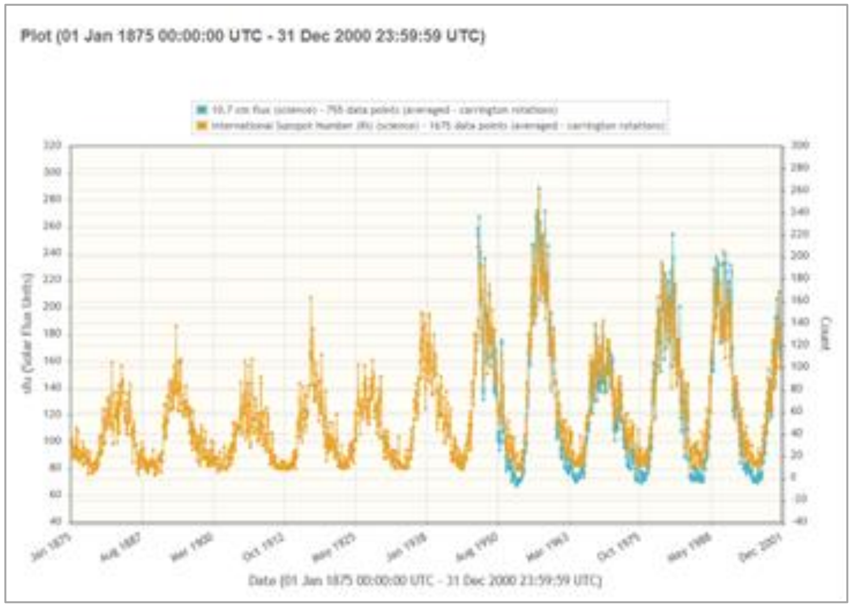

Figure 55: The International Sunspot Number and 10.7 cm radio flux are shown. Both provide an estimate of solar activity on long timescales.

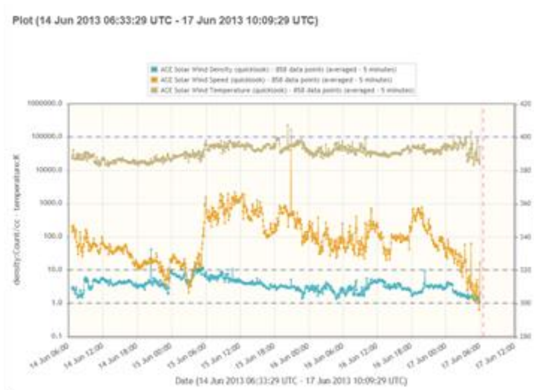

Figure 57: Near real-time plot of solar wind data from the ACE satellite.

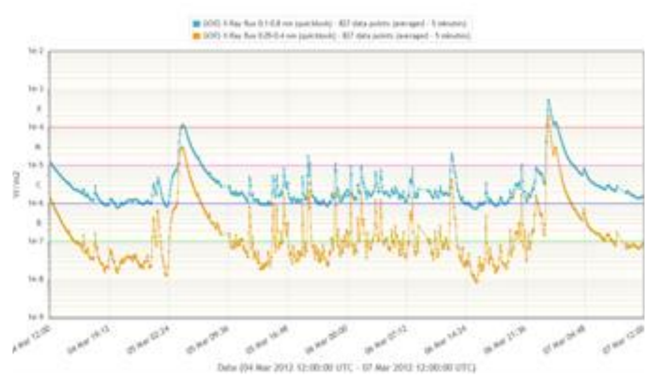

Figure 56: GOES x-ray data featuring two X-class flares, which are giant eruptions on the Sun.

STAFF was designed around the concept of combining timeline data, but with 4 constraints:

- Lots of data
- Speed
- Accessibility
- Usability

Taking on these 4 constraints proved quite a challenge, but after a thorough design phase, researchers found a workable solution.

Today, STAFF has over 30 datasets (and still growing) which you can combine over a timespan ranging over 150 years in just a few mouse clicks, resulting in a plot in less than 1 second. In order to use STAFF, the user only needs to visit the STAFF web page and can start right away.

ESA's SSA Program: SN-I SWE Precursor Services project

In order to protect Europe's space and ground-based infrastructure from space hazards and to inform the people about the condition of the space environment, ESA initiated the Space Situational Awareness (SSA) Program. It operates at two specific areas: the first one is the surveillance of objects orbiting the Earth in various orbits by detecting, tracking and imaging these objects; the second one concerns space weather that addresses primarily the effect of solar activity on manned space missions, satellites and ground infrastructure such as power grids and communication networks. As a first step in the development of a European SSA system, ESA launched the SSA Preparatory Program that focusses on the architecture of the future system, the specification of requirements and the provision of a set of precursor services covering the most urgent needs and based on existing assets.

In this framework, BIRA and ROB participated in the study "Space Weather Segment Precursor Services - Part-1: Definition and Service Consolidation" as experts in resp. space radiation and solar weather.

Figure 58 shows an overview of the architecture for SSA space weather element (SWE). The SWE service provision centers around the SWE Data Center at ESA's Redu station, and the SSA Space Weather Coordination Center (SSCC) located at the Space Pole in Belgium. The SSCC provides the first European Space Weather Helpdesk, with operators available to answer questions about the SWE service network or space weather conditions in general. BIRA initiated the SSCC. The provision of the user services is federated over a number of Expert Service Centers (ESCs) which are consortiums of expert groups with scientific and operating expertise in a particular service or a group of services. BIRA has been assigned as the coordinator of the ESC for Space Radiation and ROB for Solar Weather.

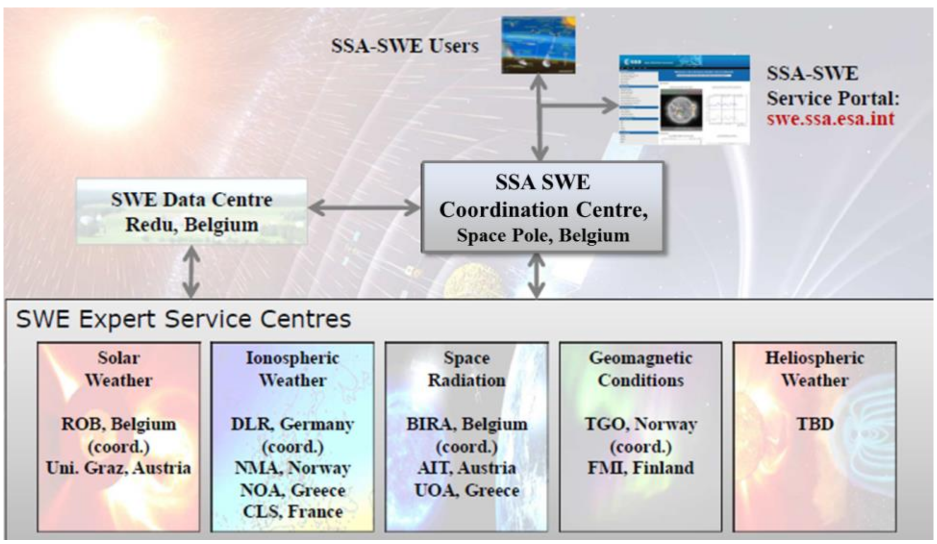

Figure 58: Space Weather Precursor Services Topology (© ESA)

The main goal of the SN-I project (Space weather and Near-Earth objects) was to define the SWE services and to consolidate them with potential users in the loop. As a first task led by ROB, a catalog was created with more than 500 SWE assets that have been identified in and outside Europe and includes high-quality scientific observations, results and models as well as a number of SWE products to local customers. Figure 59 gives the asset distribution according to type and SWE domain. All assets were investigated for their suitability to provide SSA SWE services and gaps were identified.

Considering all these assets as possible building blocks, roadmaps have been written for the development and implementation of the following services: Spacecraft Design (SCD) - Spacecraft Operation (SCO) - Human Space Flight (HSF) - Launch Operations (LAU) - Transionospheric Link (TIO) - Space Surveillance and Tracking (SST) - Non Space Systems Operations (NSO) - General Data Service (GEN). ROB was in charge of GEN and BIRA was responsible for the SCD, HSF and NSO services.

In order to meet the customer requirements, these services and their goals were assessed with some test-users in the loop. To achieve this, a SN-I workshop was held at the ROB to collect all the feedback from potential end-users for the various services.

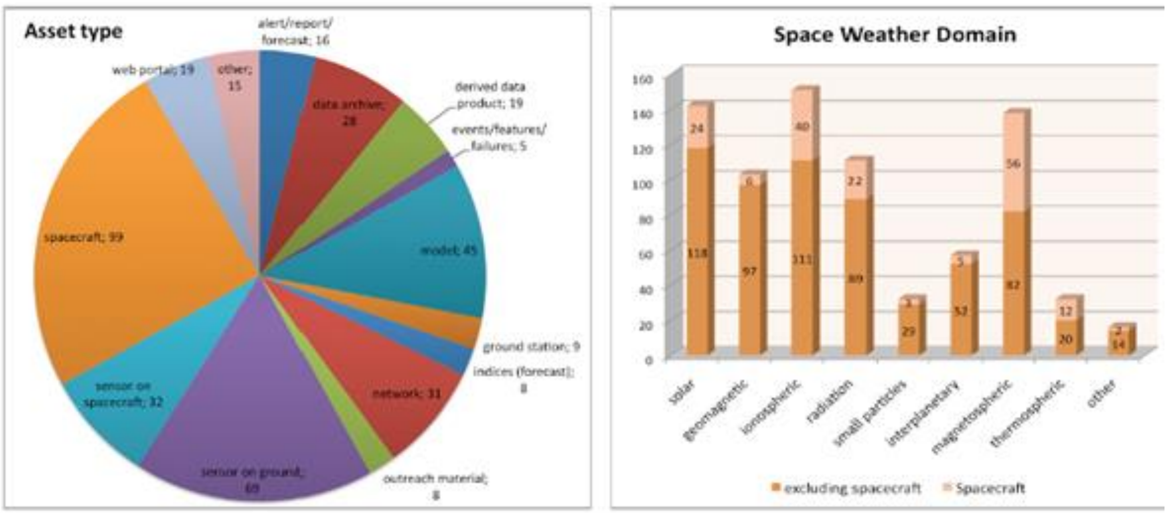

Figure 59: The different types of SWE assets (left panel) and their distribution according to the SWE domain (right panel).

During the project, six ESA owned SWE applications or precursor services have been deployed at Redu. They are accessible via the SSA SWE portal (see Figure 60).

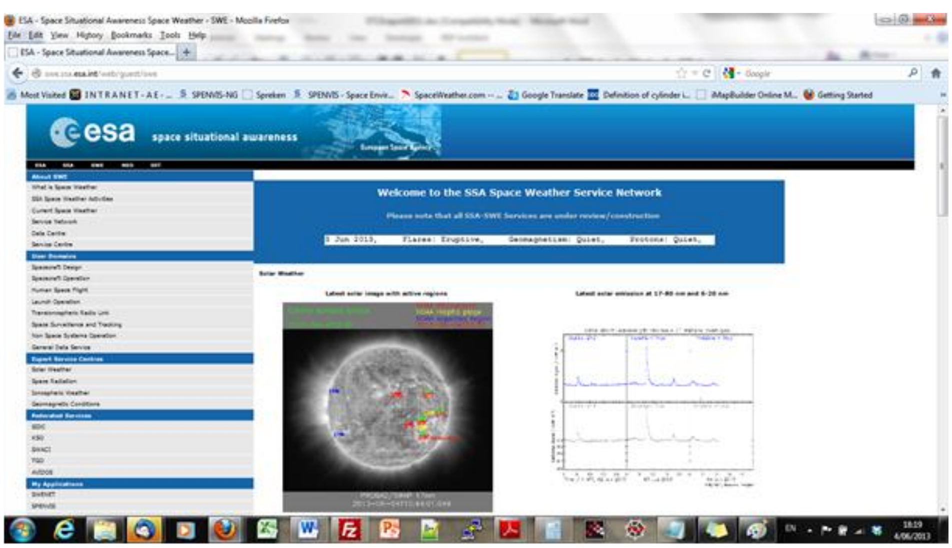

Figure 60: Screenshot of SSA Space Weather Service Network at ***http://swe.ssa.esa.int/web/guest/swe***

Improving the plasma density specification in the topside ionosphere

The ionosphere is the upper part of the atmosphere. It received this name because it is ionized by the Sun's ultra-violet light, and thus consists of a shell of free electrons, electrically charged atoms and molecules surrounding the Earth. As most of the space weather starts at the Sun, also the Earth's ionosphere is undergoing the effects of space weather.

Ground-based ionosondes have been successfully used to obtain the detailed distribution of electron density near the bottom of the ionosphere, i.e. below the density peak. However, they are not able to provide this distribution in the topside ionosphere. And, although it is possible to obtain the total electron content (TEC) of the ionosphere from GNSS data, additional information is required in order to reconstruct the electron density profile in the topside ionosphere.

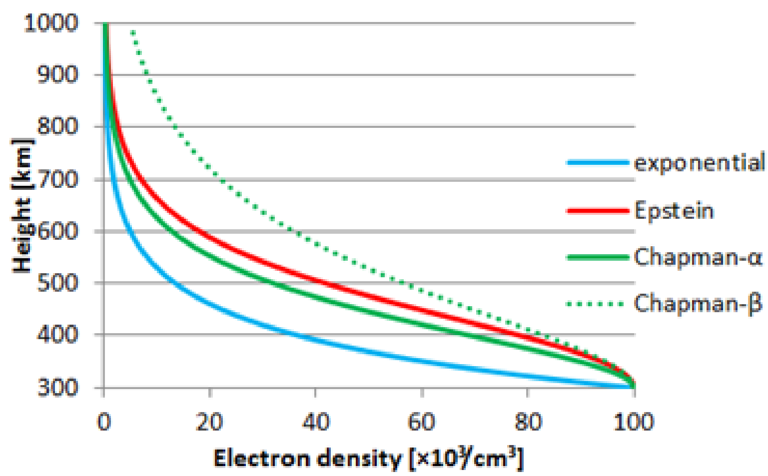

Figure 61: The four profilers often used to model the electron density distribution in the topside ionosphere. In order to illustrate the qualitative differences between their shapes, all profilers are shown here with the same peak (at 300 km), and with identical scale heights of 100 km.

One of the main problems is the selection of an appropriate theoretical model to help the reconstruction of the topside electron profile with information about the upper ion transition level (UTL) and the TEC measurements. In the literature, several such "profilers" have been used for a long time, with Exponential, Epstein, Chapman-α and Chapman-β being the most popular. Those four profilers are shown in the Figure 61. It can be seen that, all else being equal, they mainly differ in the way they model the ionosphere close to the peak density. The exponential profiler (blue line) results in a much sharper peak, while the others produce more broadened peaks. At higher altitudes, all four profilers "approach" the exponential one.

The important question is which of these profilers describes best the true shape of the electron density profile. In fact, it can be expected that the most appropriate profiler will not be the same in all circumstances. Rather, many different factors influence the shape of the ionosphere, and will thereby affect the most appropriate choice of the topside profiler. Among those external influences are solar and magnetic activity, magnetic latitude and longitude, local time and season.

In order to determine the influences of the different external drivers on the optimal topside profiler, a database of topside ionograms, obtained from ionosondes onboard satellites, was analyzed. This database is made available by the National Space Science Data Center (NSSDC) of the US, and can be found online on the ftp site of the NSSDC (ftp://nssdcftp.gsfc.nasa.gov/). This database contains electron density profiles for the topside ionosphere, which were calculated from the measurements of downward sounding ionosondes carried on four different spacecraft: Alouette-1 & -2 and ISIS-1 & -2 (Figure 62). These satellites flew during different time periods so that, by combining their data, a total of eighteen consecutive years of data coverage is available. This provides a unique opportunity to study the effect of the solar cycles.

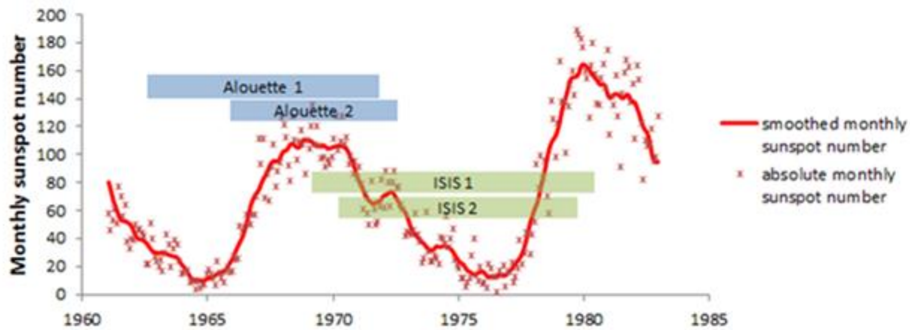

Figure 62: Overview of the coverage of different levels of solar activity – indicated by the monthly sunspot numbers – provided in the NSSDC database on topside soundings. There is continuous coverage for eighteen years, corresponding to almost two solar cycles. Cycle 20 is completely covered, as well as about half of both cycles 19 and 21.

One challenge was to mitigate the biases resulting from the different orbits of the four satellites. Since this study requires that each of the aforementioned profilers can be fitted to a measured profile from the peak height all the way up to the transition height, it was also necessary to select only those profiles that cover the entire topside ionosphere. About thirty thousand profiles remained available for our study after the necessary data selections were done, out of more than one hundred seventy thousand included in the database.

Nevertheless, there is enough data available to perform an analysis of the influences that the earlier mentioned factors have on the shape of the topside electron density profile. One example, of the correlation between the solar activity index F10.7 (measuring the flux of solar radiation with a wavelength of 10.7cm), and the shape which provides the best fit, can be seen in Figure 63. A trend can be discerned from this: low solar activity results in a larger fraction of the profiles having an exponential shape. Similar results are obtained when studying the effects of the other physical drivers on the ionosphere: All factors mentioned above do indeed have an influence on the shape of the topside ionosphere.

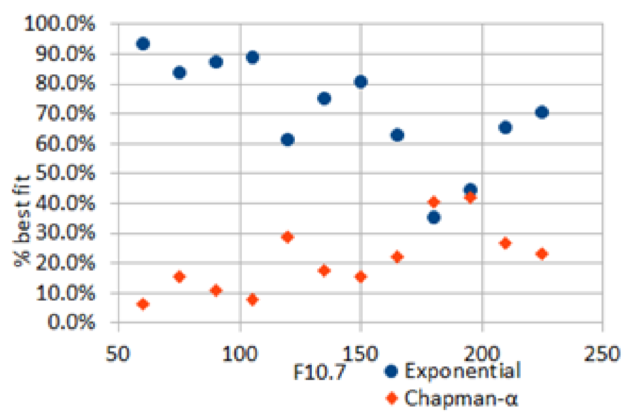

Figure 63: Percentages of profiles best fitted by the exponential and Chapman-α profilers (which provide the best fit most often), in relation to the solar activity index F10.7. Only profiles measured during daytime are included here.

However, those trends, on their own or combined, are not sufficiently indicative to serve as the basis for the choice of the most appropriate topside profiler under all conditions. There are several explanations for this.

First, the severe reduction of data, as well as the irregular distribution of the original data set, results in insufficient data for some combinations of time and magnetic coordinates. As no new topside soundings are currently underway, this problem is at the moment unsolvable.

A second problem lies with the indices for solar and magnetic activity: F10.7 for the solar activity, and the Kp and Dst indices to track the geomagnetic conditions. Those indices are calculated on a planetary scale and at hourly or daily time intervals. Therefore, they are not really suitable to predict the local and instantaneous variations of the ionosphere. Other recent work has shown similar results, and projects are underway to develop local, real-time indices which can be used instead. The correlations of such more advanced indices to the shape of the profile will undoubtedly be more pronounced, and therefore more useful as a basis for applications.

To allow for the prediction of the shape of the topside electron density distribution -and chose the appropriate profiler to model this distribution- without relying on any external indices, a study was also made of the correlations between this shape and several other characteristics of the ionosphere, which can be measured directly. The idea is that it is better to choose a topside profiler based on measurements that are done locally and with a good time resolution, rather than the global indices. These correlations were indeed found to be much clearer; two of them are illustrated in Figure 64.

Especially useful are the correlations to the height and density of the F2 peak, since these characteristics are provided by ground-based ionosondes. Currently we are working on implementing these results in our own models for the ionosphere, as well as looking into possible applications for other models, such as the International Reference Ionosphere (IRI) model.

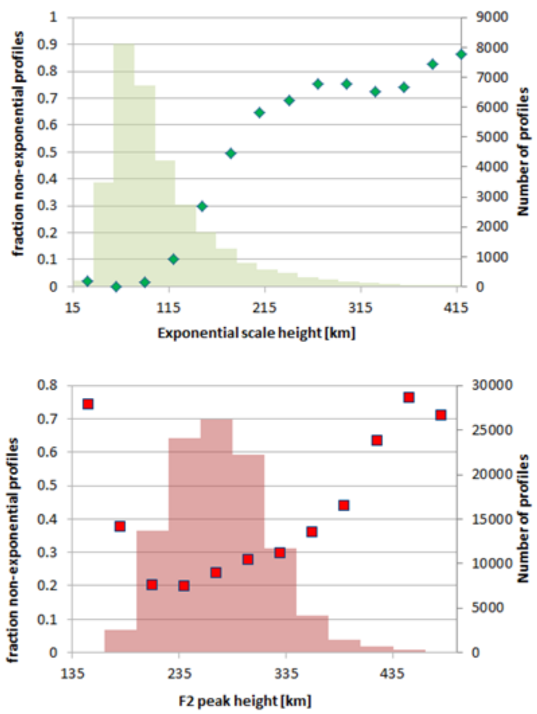

Figure 64: Correlation of the fraction of profiles not best fitted by the exponential profiler, in relation to the scale height (top, calculated using an exponential profile) and the height of the F2 density peak (bottom). The total number of profiles for each bin is displayed too, as a histogram.

Empirical model of the ionospheric TEC and disturbances during geomagnetic storms

The ionizing action of the Sun's extreme ultraviolet (EUV) radiation on the Earth's upper atmosphere produces free electrons. Above about 60 km, the number of these free electrons is sufficient to affect the propagation of electromagnetic waves. This “ionized” region of the atmosphere is a plasma and is referred to as the ionosphere. An increasing demand on a better modeling and understanding of the behavior of the ionospheric Total Electron Content (TEC) is required by the scientific community which uses electromagnetic wave signals passing through this layer of the Earth’s atmosphere. This is particularly the case for GNSS (Global Navigation Satellite Systems, e.g. GPS, GLONASS, GALILEO) for which the TEC between the ground receivers and the satellites is one of the main error sources for positioning applications, especially for single frequency users. Consequently, one of the future challenges of the space weather community is to predict the Earth's ionospheric state in response to variations of the solar activity and geomagnetic storm events.

The 23rd solar cycle (1996-2008) is the first full solar cycle ever having both GNSS-based TEC measurements as well as observed solar parameters. We used the 15 years of global GNSS-based TEC information and the daily solar index F10.7P (i.e. the new proxy used to retrieve the solar EUV fluxes):

1) to develop an empirical ionospheric climatological model to predict the Latitudinal Daily Mean TEC (LDM-TEC, i.e. the mean value of the TEC over a day at a given latitude) taking solar parameters as input;
2) to analyze the variation of the LDM-TEC during identified geomagnetic storm events.

- **Climatological empirical model**

Several solar parameters (e.g. daily Sunspot Number, F10.7 flux and derived F10.7P) were tested as input and different parameterizations were considered to estimate (i.e. to model) the LDM-TEC for a given day at a given latitude. The residuals between the modeled and the observed LDM-TEC are minimized by a least-squares adjustment.

The best model (Figure 65) is obtained using

1) a combination of linear, annual and semi-annual terms between the LDM-TEC and F10.7P;
2) a discretization with respect to the phases of the solar cycle.

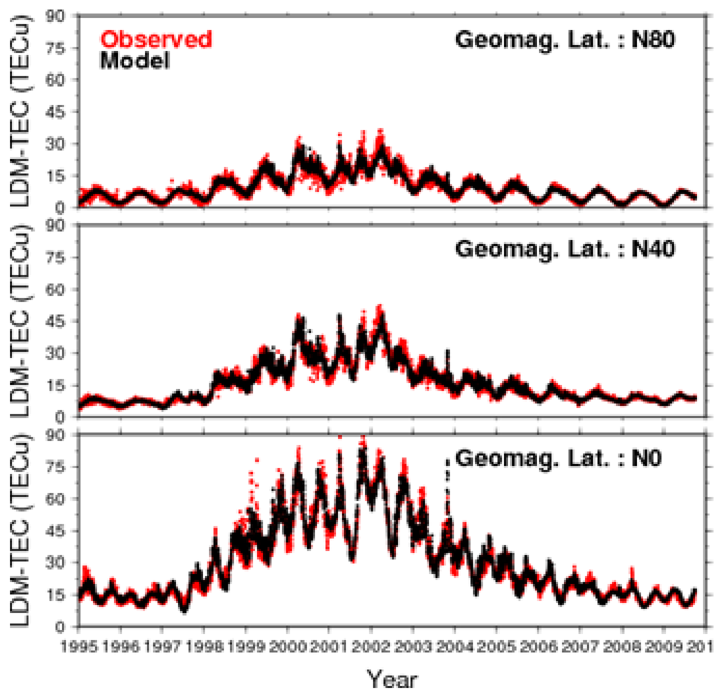

Figure 65: Estimated LDM-TEC (=model in black) and observed (in red) for different geomagnetic latitudes. Bottom: geomagnetic equator. Middle: mid-latitude region. Top: polar region.

Our best ionospheric climatological model has been tested in terms of yearly median absolute error (1.9 ± 0.9 TECu) and median relative error (7.3 ± 2.0 %). The relative error remains constant during the entire 23rd solar cycle which comforts us in the robustness of our climatological model with no degradation during the different phases of the solar activity.

Our empirical model of LMD-TEC reconstructed from F10.7P reflects the general variations of the ionospheric TEC, i.e. predominance of:

1) a linear correlation between F10.7P and LMD-TEC;
2) an annual term at high latitudes due to the solar zenith angle variation; and
3) a semi-annual term at low latitudes where the change of the ratio $[O]/[N_2]$ plays an important role.

The standard deviation (1σ) is 2.4±0.4 TECu and is lower than when we do not consider different solar activity phases (2.9±0.6 TECu). This confirms previous studies where different patterns of the global TEC are observed with respect to the solar activity phases.

- **Effect of geomagnetic storms on the ionosphere**

We investigated the major differences between the observed and modeled LDM-TEC. The differences greater than 15 TECu are concordant with 69 intense geomagnetic storm events that occurred during the period 1998-2005. The geomagnetic storms affect significantly the ionospheric LDM-TEC mainly in the polar regions, with a loss of ionization with respect to our climatological model and a peak one day after the onset (Figure 66). The mean difference between the observed and modeled LDM-TEC at the peak is -3.2 ± 1.5 TECu and becomes negligible 3-4 days after the onset.

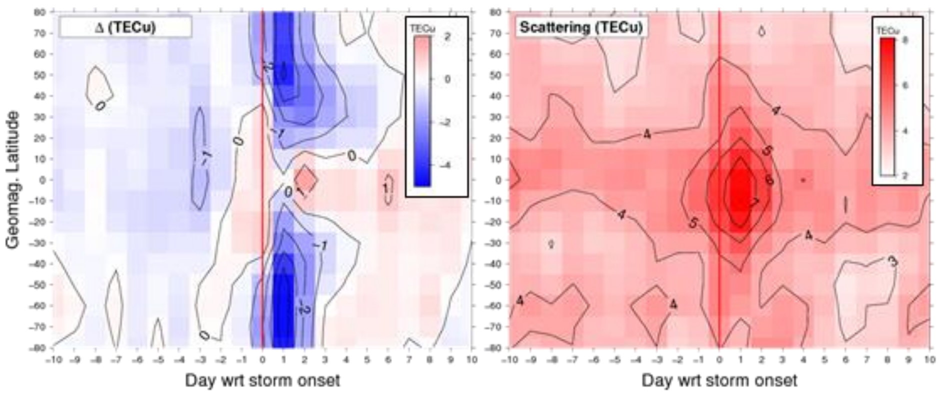

Figure 66: Mean differences between the LDM-TEC extracted from GNSS and the modeled LDM-TEC using our climatological model. These grids represent the stacking for the 69 intense geomagnetic storm events between 1998 and 2005 with respect to (wrt) the latitude, for 20 days around the onset. Red vertical line: day of the onset of the storms. Left: mean differences in TECu; Right: standard deviation of the mean differences.

This long term depletion in the TEC after geomagnetic storms can be explained by the contraction of the plasmasphere (a region of "cold" (low-energetic) particles that extends from about 1600 km to over 30,000 km above Earth's surface and is an extension of the ionosphere). Its contraction implies disturbances in the thermospheric circulation and a chemical loss in the ionosphere and, consequently, a decrease of TEC. To determine the best scenario and provide a physical/chemical explanation of our observations, an accurate knowledge of the plasmasphere-ionosphere system is now of prime importance, especially during geomagnetic storms.

LIDAR activities

- Introduction

In May 2011, RMI installed a LIDAR ceilometer (LIght Detection And Ranging) at Uccle that offers the opportunity to monitor the vertical profile of aerosols and the mixing layer height (MLH) on a continuous temporal scale. This LIDAR ceilometer is a Vaisala ceilometer CL51 equipped with pulsed near-infrared diode lasers (910±10 nm). In its normal full-range operation, the LIDAR sampling frequency provides a spatial resolution of 10 meters from ground level up to 15,000 meters every 6 seconds.

LIDAR ceilometers were primarily designed for cloud base height detection (for air traffic safety and weather forecasting). They greatly improved over the last years and now offer the opportunity to monitor the vertical profile of aerosols and the mixing layer height (MLH) on a continuous temporal scale. The knowledge of MLH can improve the forecasting of the dispersion of trace gases and aerosols in the lowest layers of the atmosphere and can also improve the accuracy of the greenhouse gas concentration budgets highly depending on MLH.

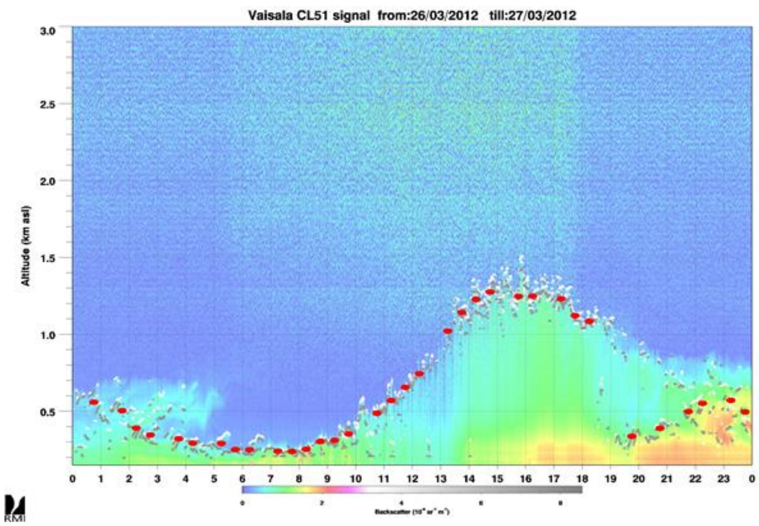

Figure 67: Example of one day of backscatter measurements at Uccle between 120 and 3000 m. The white points correspond to the level of the MLH detected by the gradient algorithm and the brown points correspond to the level of the MLH detected by the variance method. The red points correspond to the average of the MLH at which in a 30 minutes time frame, the maximum number of white and brown point is located, within a bandwidth of 165m.

- **MLH algorithm**

RMI developed an algorithm (illustrated in Figure 67) to retrieve the MLH from the LIDAR ceilometer measurements (backscatter profiles). This algorithm is based on two MLH detection methods frequently used in MLH estimation studies. The first method is the gradient method that is based on the detection of the significant vertical gradient in the backscatter profiles. The second method is the variance method that is based on the detection of the maximum temporal variance in the backscatter profiles. In the RMI's algorithm, the MLH is determined as the level at which in a 30 minutes time frame, the maximum number of levels is detected by the gradient method and by the variance method, within a bandwidth of 165m.

It is not possible to retrieve the MLH under precipitation, ground-based fog and strong convective conditions, and when aerosol concentrations are too low. The algorithm has been validated by comparing the MLH retrieved by LIDAR-ceilometer measurements with the MLH retrieved by radio-sounding (Uccle) and the boundary layer height (BLH) directly computed by other models.

The comparison was made at daily and monthly temporal scale on the data set of Uccle from May 2011 to January 2013. Under specific atmospheric conditions, the algorithm fails to retrieve a similar MLH than other remote sensing retrieval techniques. Therefore, we developed several MLH quality control flags based on the ceilometer measurements only to detect automatically the failure of the MLH retrieval algorithms without the support of additional measurements. The development of these quality flags is necessary for the future LIDAR-ceilometers that will be located in places where no other remote sensing measurements will be available to assess the accuracy of the MLH retrieved by the algorithm. The quality criteria on the MLH observations are crucial for the future use of the MLH in near real-time to forecast episodes of poor air quality.

The LIDAR ceilometer at Uccle and the MLH algorithm is fully automated. Its measurements are now accessible in real-time for its weather forecast office, and for other interested people (e.g. monitoring the air quality in Belgium and people responsible for the air traffic safety). Major interruptions in the LIDAR measurements have been very limited in 2012 (Figure 68).

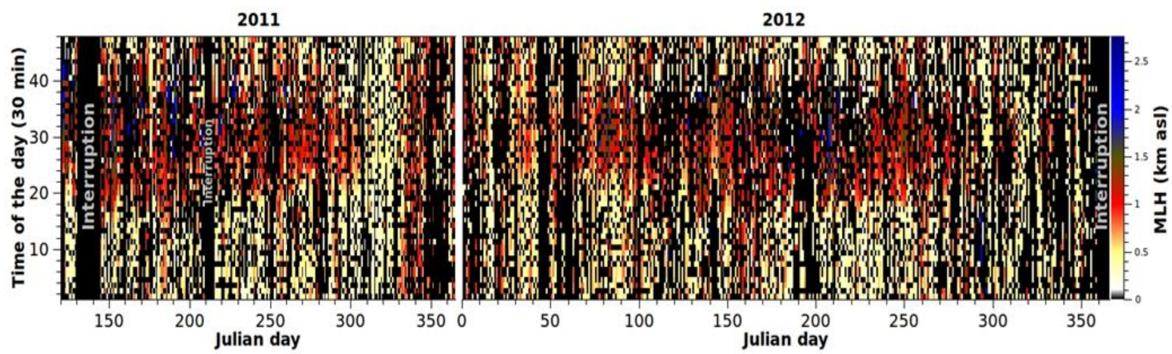

Figure 68: Retrieval of the MLH (colored scale) by the RMI's algorithm in function of the Julian day (between May 2011 and December 2012) and in function of the time of the day (per 30 minutes, vertical axis). Black color represents the periods in which the algorithm was unable to retrieve the MLH and the interruption periods in the LIDAR measurements.

- **Evolution of the MLH**

The monthly mean diurnal evolution of the MLH measurements for 2011 and 2012 is shown in Figure 69. The daily evolution of the MLH was asymmetric, one or two hours after sunrise, the MLH increased slowly and reached a maximum one or two hour after the noon before to decrease abruptly one or two hour after sundown. This daily cycle was observed only between March and October, and the highest maximum daily peaks (up to 2,000 meters) of the MLH occurred during the May-through-September period.

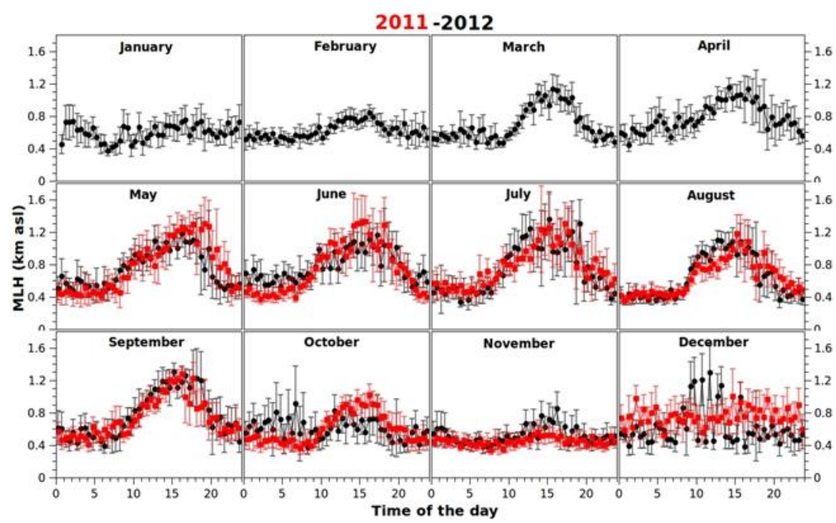

Figure 69: Monthly mean diurnal evolution of the MLH retrieved by the RMI's algorithm for 2011 and 2012. Error bars represent the confidence intervals (95%) of the mean of MLH.

- **Retrieval of the aerosol optical properties**

The aerosol optical properties can be obtained by the collocation of the sun photometer data with the LIDAR data under clear sky conditions, when the diurnal atmospheric boundary layer is homogeneously mixed and assuming the absence of stratospheric aerosols.

The backscatter LIDAR equation is undetermined due to its dependence on the two unknowns, backscatter and extinction coefficient. Both parameters characterize the aerosol optical properties and can be determined by inverting the equation. The backscatter-to-extinction ratio (BER) is widely used to permit the inversion of the LIDAR equation. The determination of a constant BER is possible with an iterative inversion approach and with sun photometer measurements to constrain the LIDAR inversion.

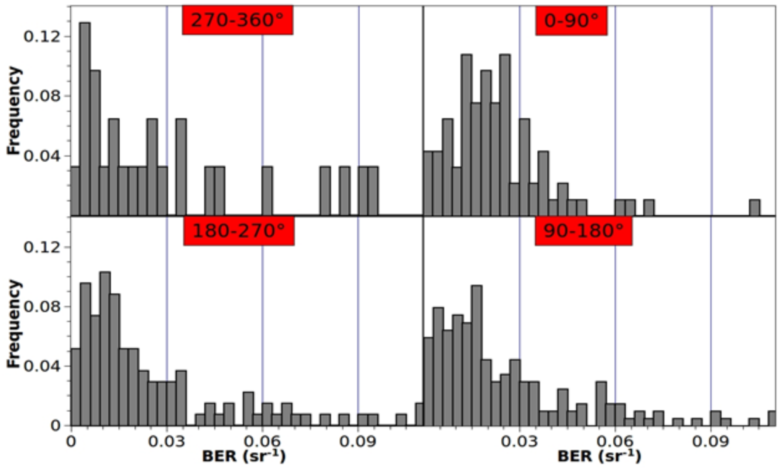

Figure 70: Frequency distribution of the retrieval of the BER for four wind sectors between May 2011 and January 2012.

At Uccle, sun photometer measurements are performed by BISA with an automatic sun tracking photometer installed on the top of their building. We have applied this method on our and their data set (sun photometer + LIDAR) between May 2011 and January 2012. The frequency distribution of the retrieval of the BER was computed for four wind sectors (Figure 70). No great differences were observed between the distributions except for winds with a supposed continental origin (0-90°) for which the BERs were frequently higher than in other wind sectors. The impact of continental aerosols on the LIDAR ratio, however, was probably not the only parameter affecting the BER. Indeed, the dependence of the BER to the humidity seems also to be a playing factor. Indeed, the laser beam emitted by the CL51 is absorbed by the water vapor and the LIDAR signal must be corrected for water absorption.

Publications

This list of publications consists only of the peer-reviewed articles and the presentations and posters at conferences. It does not include non-refereed articles, press releases, the daily, weekly and monthly bulletins that are part of our public services, the public outreach texts,… These data are available at the STCE-website http://stce.be/index.php or upon request.

Authors belonging to the STCE have been highlighted in the list of peer reviewed articles.

Peer reviewed articles

1. A. Bemporad, F.P. Zuccarello, C. Jacobs, **M. Mierla**, S. Poedts
Study of multiple coronal mass ejections at solar minimum conditions
Solar Physics, 281, pp.223-236

2. J. Birn, A.V. Artemyev, D.N. Baker, **M. Echim**, M. Hoshino, L.M. Zelenyi
Particle Acceleration in the Magnetotail and Aurora
Space Science Reviews, Volume 173, Issue 1-4, pp.49-102, 2012

3. K. Bonte, **D. Berghmans, A. De Groof**, K. Steed, S. Poedts
SoFAST: Automated Flare Detection with the PROBA2/SWAP EUV Imager
Solar Physics, Online First, DOI: 10.1007/s11207-012-0165-8

4. **C. Bruyninx**, Z. Altamimi, M. Becker, M. Craymer, L. Combrinck, A. Combrink, J. Dawson, R. Dietrich, R. Fernandes, R. Govind, T. Herring, A. Kenyeres, R. King, C. Kreemer, D. Lavallée, **J. Legrand**, L. Sánchez, A. Santamaria-Gomez, G. Sella, Z. Shen
A Dense Global Velocity Field based on GNSS Observations: Preliminary Results
Geodesy for Planet Earth, IAG Symposia Series, Vol 136, pp.19-26, DOI: 10.1007/978-3-642-20338-1_3

5. **C. Bruyninx**, H. Habrich, W. Söhne, A. Kenyeres, G. Stangl, C. Völksen
Enhancement of the EUREF Permanent Network Services and Products
Geodesy for Planet Earth, IAG Symposia Series, Vol 136, pp.27-35, DOI: 10.1007/978-3-642-20338-1_4

6. G. Cessateur, J. Lilensten, T. Dudok de Wit**, A. BenMoussa,** M. Kretzschmar
New observation strategies for the solar UV spectral irradiance
Journal of Space Weather Space Climate, 2, 2012, A16

7. K. Chandrashekhar, S.K. Prasad, D. Bannerjee, **D.B. Seaton**
Dynamics of Coronal Bright Points as seen by SWAP, AIA, and HMI
Solar Physics Online First, DOI: 10.1007/s11207-012-0046-1

8. I. Chifu, B. Inhester, **M. Mierla**, V. Chifu, T. Wiegelmann
First 4D reconstruction of an eruptive prominence using simultaneously three view directions
Solar Physics, 281, pp.121-135

9. C. Cid, H. Cremades, A. Aran, C.H. Mandrini, B. Sanahuja,B. Schmieder, M. Menvielle, **L. Rodriguez**, E. Saiz, Y. Cerrato, S. Dasso, C. Jacobs, C. Lathuillere, **A.N. Zhukov**
Can a Halo CME from the limb be geoeffective?
Journal of Geophysical research, 117, pp.A11102, DOI: 10.1029/2012JA017536

10. F. Clette, L. Lefèvre
Are the Sunspots really vanishing? Anomalies in solar cycle 23 and implications for long-term models and proxies
Journal of Space Weather and Space Climate, 2, pp.A06, DOI: 10.1051/swsc/2012007 (2012)

11. N.B. Crosby
Effects and Benefits of Space Exploration: Past, Present and Future
International Journal of Space Technology Management and Innovation, 2(1), 49-62, January-June 2012

12. **N.B. Crosby**, I. Van den Bergh, R. Bollen, J. Brabants, J. Cops, Y. Dillen, C. Doomen, J. Lambrechts, T. Stulens, T. Aäron, L. Vanlaer, S. Vinkesteijn
Five Centuries of Exploration: From Distant Shores to Distant Planets
AGU Space Weather Journal, 10, 2012, S03007, DOI: 10.1029/2011SW000658

13. **N.B. Crosby**, A.M. Veronig, **E. Robbrecht,** B. Vrsnak, S. Vennerstrom, O. Malandraki, S. Dalla, **L. Rodriguez**, N. Srivastava, M. Hesse, D. Odstrcil
Forecasting the Space Weather Impact: the COMESEP Project
AIP Conf. Proc., 1500, pp.159

14. **A.W. Delcloo**, A. Deckmyn, R. Hamdi, H. Van Langenhove, G. Foret, **H. De Backer**
Coupling of the CTM CHIMERE to the High Resolution LAM ALADIN for Belgium
Air Pollution Modeling and its Application XXI, NATO Science tor Peace and Security Series C: Environmental Security, 2012, Volume 4, Part 2, pp.315-319, DOI: 10.1007/978-94-007 -1359-8_54

15. **S. Dewitte, N. Clerbaux, A. Ipe, A. Velazquez, E. Baudrez, S. Nevens, I. Decoster**
Climate monitoring with Earth Radiation Budget measurements
AIP Conf. Proc. 1531, pp.612-615, 2012, DOI: http://dx.doi.org/10.1063/1.4804844

16. **S. Dewitte, E. Janssen, S. Mekaou**i
Science results from the Sova-Picard Total Solar Irradiance instrument
AIP Conf. Proc. 1531, pp.688-691, 2012, DOI: http://dx.doi.org/10.163/1.4804863

17. **L. Dolla, C. Marqué, D.B. Seaton,** T. Van Doorsseleare, **M. Dominique, D. Berghmans**, C. Cabanas, **A. De Groof,** W. Schmutz, **A. Verdini**, **M.J. West**, J. Zender, **A.N. Zhukov**
Time delays in quasi-periodic pulsations observed during the X2.2 solar flare on 2011 February 15
Astrophysical Journal, 749, pp.L16, DOI: 10.1088/2041-8205/749/1/L16

18. **M. Dominique, J.-F. Hochedez**, W. Schmutz, **I.E. Dammasch**, A.I. Shapiro, **M. Kretzschmar, A.N. Zhukov, D. Gillotay**, X. Stockman, **A. Ben Moussa**
The LYRA instrument onboard PROBA2: description and in-flight performance
Solar Physics, 283/1, 2012

19. D. Fussen, J. De Keyser, M. De Mazière, D. Pieroux, H. Lamy, S. Ranvier, E. Dekemper, A. Merlaud, E. Neefs, O. Karatekin, Z. Ping, V. Dehant, M. Van Ruymbeke, J.P. Noël
The PICASSO mission
In Proceedings of the ESA 4S Symposium, 2012

20. C. Guennou, F. Auchère, E. Soubrié, K. Bocchialini, **S. Parenti,** N. Barbey
On the Accuracy of the Differential Emission Measure Diagnostics of Solar Plasmas. Application to AIA / SDO. Part I: Isothermal plasmas.
The Astrophysical Journal Supplement Series, 203, pp.25

21. C. Guennou, F. Auchère, E. Soubrié, K. Bocchialini, **S. Parenti,** N. Barbey
On the Accuracy of the Differential Emission Measure Diagnostics of Solar Plasmas. Application to AIA / SDO. Part II: Multithermal plasmas.
The Astrophysical Journal Supplement Series, 203, pp.26

22. A.M. Gulisano, P. Demoulin, S. Dasso, **L. Rodriguez**
Expansion of magnetic clouds in the outer heliosphere
Astronomy and Astrophysics, 543, pp.A107

23. **H. Gunell**, H. Nilsson, G. Stenberg, M. Hamrin, T. Karlsson, **R. Maggiolo**, M. André, R. Lundin, I. Dandouras
Plasma penetration of the dayside magnetopause
Physics of Plasmas, Volume 19, Issue 7, 072906, 2012, DOI: 10.1063/1.4739446

24. J.P. Halain, **D. Berghmans**, **D.B. Seaton, B. Nicula, M. Mierla**, Alexandra Mazzoli, J.-M. Defise, P. Rochus
The SWAP EUV Imaging Telescope. Part II: In-flight Performance and Calibration
Solar Physics, Online First, DOI: 10.1007/s11207-012-0183-6

25. J.C. Jodogne, S.M. Stankov
Vertical transmission from catenaries
International Symposium on Antennas and Propagation (ISAP), Nagoya, Japan, ABS No.ISAP12-0147, pp.1067-1070

26. W. Keinreich, N. Muhr, A. M. Veronig, **A. De Groof**, M. Temmer, B. Vrsnak, **D.B. Seaton**
Solar TErrestrial Relations Observatory-A (STEREO-A) and PRoject for On-Board Autonomy 2 (PROBA2) Quadrature Observations of Reflections of Three EUV Waves from a Coronal Hole
Solar Physics, Online First, DOI: 10.1007/s11207-012-0023-8

27. E.K.J. Kilpua, **M. Mierla, L. Rodriguez, A.N. Zhukov, N.** Srivastava, **M.J. West**
Estimating travel times of coronal mass ejections to 1 AU using multi-spacecraft coronagraph data
Solar Physics Journal, 279, 477-496 (2012). DOI: 10.1007/s11207-012-0005-x

28. M. Kretzschmar, **I.E. Dammasch**, **M. Dominique**, J. Zender, G. Cessateur, **E. D'Huys**
Extreme Ultraviolet Solar Irradiance during the Rising Phase of Solar Cycle 24 Observed by PROBA2/LYRA
Journal of Space Weather and Space Climate, 2, pp.A14

29. M. Kretzschmar, **M. Dominique, I.E. Dammasch**
Sun-as-a-Star Observation of Flares in Lyman-alpha by the PROBA2/LYRA Radiometer
Solar Physics, Online First, DOI: 10.1007/s11207-012-0175-6

30. S.T. Kumara, R. Kariyappa, **M. Dominique**, **D. Berghmans**, L. Damé, J.-F. Hochedez, V.H. Doddamani, L.P. Chitta
Preliminary Results on Irradiance Measurements from Lyra and Swap
Advances in Astronomy, 2012, pp.1-5

31. M. Lazar, **V. Pierrard**, R. Schlickeiser, S. Poedts
Modeling space plasma dynamics with anisotropic Kappa distributions
ASS Proc., 33, 97-107, ISBN 978-3-642-30441-5, Ed. Manfred Leubner and Zoltan Voros, Springer-Verlag, Berlin Heidelberg, 2012.DOI: 10.1007/978-3-642-30442-2

32. L. Lefèvre, F. Clette
Survey and Merging of Sunspot Catalogs
Solar Physics, Online First, DOI: 10.1007/s11207-012-0184-5 (2012)

33. **J. Legrand, N. Bergeot, C. Bruyninx,** G. Wöppelmann, A. Santamaria-Gomez, M.-N. Bouin, Z. Altamimi
Comparison of Regional and Global GNSS Positions, Velocities and Residual Time Series
Geodesy for Planet Earth, IAG Symposia Series, Vol 136, pp.95-104, DOI: 10.1007/978-3-642-20338-1_12

34. J. Lilensten, G. Provan, S. Grimald, A. Brekke, E. Flückiger, **P. Vanlommel,** C. Simon Wedlund, M. Barthélémy, P. Garnier
The Planeterrella experiment: from individual initiative to networking
Journal of Space Weather and Space Climate, 3 (2013) A07

35. J. Logan, J. Stähelin, I.A. Megretskaia, J.-P. Cammas, V. Thouret, H. Claude, **H. De Backer**, M. Steinbacher, H.E. Scheel, R. Stübi, M. Fröhlich, R. Derwent
Changes in ozone over Europe since 1990: analysis of ozone measurements from sondes, regular aircraft (MOZAIC) and alpine surface sites
J. Geophys. Res., 117, D09301, DOI:10.1029/2011JD016952, 2012

36. **J. Magdalenić, C. Marqué, A.N. Zhukov,** B. Vršnak and A. Veronig
Flare-Generated Type II Burst without Associated Coronal Mass Ejection
Astrophysical Journal 746, pp.152-159, 2012

37. P.C.H. Martens, G.D.R. Attrill, A.R. Davey, A. J. Engell, S. Farid, P.C. Grigis, J.C. Kasper, K. Korreck, S.H. Saar, A. Savcheva, P. Testa, M. Wills-Davey, P.N. Bernasconi , N.E. Raouafi, **V. Delouille**, J.-F. Hochedez, J.W. Cirtain, C.E. DeForest, R.A. Angryk, I. De Moortel, T. Wiegelmann, M.K. Georgoulis, R.T.J. McAteer
Computer Vision for the Solar Dynamics Observatory
Solar Physics, 275, pp.79-113, 2012

38. **M. Mierla**, **D.B. Seaton, D. Berghmans**, I. Chifu, **A. De Groof**, B. Inhester, **L. Rodriguez**, G. Stenborg, **A.N. Zhukov**
Study of a Prominence Eruption using SWAP/PROBA2 and EUVI/STEREO Data
Solar Physics, DOI: 10.1007/s11207-012-9965-0

39. P.M. Miller, M.E. Koepke, **H. Gunell**
Laser-induced quasi-periodic mode hopping in competing ionization waves
Proceedings of the 39th EPS Conference on Plasma Physics and the 16th International Congress on Plasma Physics, Volume 36F, P4.179, ISBN 2-914771-79-7, Stockholm, Sweden, 2012

40. N.A. Murphy, M.P. Miralles, C.L. Pope, J.C. Raymond, H.D. Winter, K.K. Reeves, **D.B. Seaton**, A.A. van Ballegooijen, J. Lin
Asymmetric Magnetic Reconnection in Solar Flare and Corona Mass Ejection Current Sheets
Astrophysical Journal, 2012, Volume 752, p. 56

41. C.J. Owen, O. Amm, R. Bruno, **J. De Keyser**, M.W. Dunlop, J.P. Eastwood, A.N. Fazakerley, D. Fontaine, C. Forsyth, H. Hasegawa, P. Hellinger, D. Hercik, C. Jacquey, S. Milan, J. Raeder, D.G. Sibeck, S. Stverak, P. Travnicek, A.P. Walsh, J.A. Wild
IMPALAS: Investigation of MagnetoPause Activity using Longitudinally-Aligned Satellites-a mission concept proposed for the ESA M3 2020/2022 launch
Experimental Astronomy, 33(2-3), 365-401, 2012

42. **S. Parenti**, B. Schmieder, P. Heinzel, L. Golub
On the nature of prominence emission observed by SDO/AIA
Astrophysical Journal, 754, 1, id.66

43. D. Pérez-Suárez, S.A. Maloney, P. A. Higgins, D. S. Bloomfield, P. T. Gallagher, G. Pieratoni, X. Bonnin, B. Cecconi, V. Alberti, K. Bocchialini, **M. Dierckxsens**, A. Opitz, A. Le Blanc, J. Aboudarham, R. B. Bentley, J. Brooke, B. Coghlan, A. Csillaghy, C. Jacquey, B. Lavraud, M. Messerotti
Studying Sun-planet connections using the Heliophysics Integrated Observatory (HELIO)
Solar Physics, Volume 280, Issue 2, pp.603-621, 2012

44. H. Peter, L. Abbo, V. Andretta, F. Auchère, A. Bemporad, F. Berrilli, V. Bommier, A. Braukhane, R. Casini, W. Curdt, J. Davila, H. Dittus, S. Fineschi, A. Fludra, A. Gandorfer, D. Griffin, B. Inhester, A. Lagg, E. Landi Degl'Innocenti, V. Maiwald, R. Manso Sainz, V. Martinez Pillet, S. Matthews, D. Moses, **S. Parenti**, A. Pietarila, D. Quantius, N.-E. Raouafi, J. Raymond, P. Rochus, O. Romberg, M. Schlotterer, U. Schuehle, S. Solanki, D. Spadaro, L. Teriaca, S. Tomczyk, J. Trujillo Bueno, J.-C. Vial
Solar magnetism eXplorer (SolmeX)
Experimental Astronomy, 33, 271

45. V. Pierrard
Solar wind electron transport: interplanetary electric field and heat conduction
Space Science Review (solar wind), Issue 1, 172, 315-324, 2012, DOI: 10.1007/s11214-011-9743-6

46. V. Pierrard, K. Borremans
Fitting the AP8 spectra to determine the proton momentum distribution functions in space radiations
Radiation Measurements, 47, 401-405, 2012, DOI: 10.1016/j.radmeas.2012.04.002

47. V. Pierrard
Kinetic models for solar wind electrons, protons and ions
Chapter in “Exploring the solar wind”, 221-240, Intech, Edited by M. Lazar, ISBN 978-953-51-0339-4, 2012

48. V. Pierrard
Effects of suprathermal particles in space plasmas
ICNS Annual International Astrophysics Conference Proc., American Institute of Physics 1436, 61-66, 2012, DOI: 10.1063:1.4723591

49. V. Pierrard, K. Borremans
The ionosphere coupled to the plasmasphere and polar wind models
Numerical Modeling of Space Plasma Flows: Astronum-2011, ASP Conference series, vol. 459, N. V. Pogorelov, J. A. Font, E. Audit, and G. P. Zank, eds, 234-239, 2012

50. **V. Pierrard**, S. Benck
The dynamics of the terrestrial radiation belts and its links to the plasmasphere
AIP Conf. Proc., 1500, 216, DOI: 10.1063/1.4768769, 2012

51. **T. Podladchikova**, **R.A.M. Van der Linden**
Kalman Filter Technique for Improving Prediction of Smoothed Monthly Sunspot Numbers
Solar Physics, 277, pp.397-416

52. **O. Podladchikova**, A. Vuiets, P. Leontiev, **R.A.M. Van der Linden**
Recent Developments of NEMO: Detection of Solar Eruptions Characteristics
Solar Physics, 276, pp.479-490

53. P. Raulin, G.H. Trottet, M. Kretzschmar, E.L. Macotela, A.A. Pacini, F.C.P. Bertoni, **I.E. Dammasch**
Response of the low ionosphere to X-ray and Lyman-alpha solar flare emissions
Journal of Geophysical Research, 118, pp.570-575

54. **E. Robbrecht**, Y.M. Wang
Determining the North-South Displacement of the Heliospheric Current Sheet from Coronal Streamer Observations
Astrophysical Journal, 755 Issue 2, pp.135-144, 2012

55. S. Savage, G. Holman, K. Reeves, **D. Seaton,** & D. McKenzie
Low-Altitude Reconnection Inflow-Outflow Observations During the 2010 November 3 Eruption
Astrophysical Journal, 2012, Volume 754, p. 13

56. C. Scannell, D. Hurtmans, A. Boynard, J. Hadji-Lazaro, M. George, **A. Delcloo**, O. Tuinder, P.-F. Coheur, and C. Clerbaux
A review of the ozone hole from 2008 to 2010 as observed by IASI
Atmos. Meas. Tech., 5, 123-139, 2012

57. **D.B. Seaton**, **D. Berghmans**, **B. Nicula**, J.P. Halain, **A. De Groof**, T. Thibert, D.S. Bloomfield,
C.L.Raftery, P.T. Gallagher, F. Auchère, J.-M. Defise, **E. D'Huys**, J.H. Lecat, E. Mazy, P. Rochus, L. Rossi, U. Schuehle, V.A. Slemzin, M.S. Yalim, J. Zender
The SWAP EUV Imaging Telescope Part I: Instrument Overview and Pre-Flight Testing
Solar Physics, Online First, pp.217, DOI: 10.1007/s11207-012-0114-6

58. V.A. Slemzin, L. K. Harra, Alexander Urnov, S.V. Kuzin, Farid Goryaev, **D. Berghmans**
Signatures of Slow Solar Wind Streams from Active Regions in the Inner Corona
Solar Physics, Online First, DOI: 10.1007/s11207-012-0004-y

59. R. Soler, J.L. Ballester, **S. Parenti**
On the stability of thermal modes in cool prominence plasmas
Astronomy and Astrophysics, 2012, 540, pp.A7

60. **S. M. Stankov**, J.C. Jodogne, I. Kutiev, **K. Stegen**, R. Warnant
Evaluation of automatic ionogram scaling for use in real-time ionospheric density profile specification: Dourbes DGS-256/ARTIST-4 performance
Annals of Geophysics, Vol.55, No.2, pp.283-291, DOI: 10.4401/ag-4976

61. L. Teriaca, V. Andretta, F. Auchère, C. M. Brown, E. Buchlin, G. Cauzzi, J. L. Culhane, W. Curdt, J. M. Davila, G. Del Zanna, G. A. Doschek, S. Fineschi, A. Fludra, P. T. Gallagher, L. Green, L. K. Harra, S. Imada, D. Innes, B. Kliem, C. Korendyke, J. T. Mariska, V. Martínez-Pillet, **S. Parenti**, S. Patsourakos, H. Peter, L. Poletto, R. Rutten, U. Schühle, M. Siemer, T. Shimizu, H. Socas-Navarro, S. K. Solanki, D. Spadaro, J. Trujillo-Bueno, S. Tsuneta, S. Vargas Dominguez, J.-C. Vial, R. Walsh, H. P. Warren, T. Wiegelmann, B. Winter, P. Young
LEMUR: Large European Module for solar Ultraviolet Research
Experimental Astronomy, 2012, 34, 273

62. G. Thuillier, M. DeLand, A. Shapiro, W. Schultz, **D. Bolsée**, S.M.L. Melo
The Solar Irradiance as a Function of the Mg II Index for Atmosphere and Climate Modeling
Solar Physics, 277, Issue 2, 245-266, 2012, DOI: 10.1007/s11207-011-9912-5

63. A. Vaivads, G. Andersson, S.D. Bale, C.M. Cully, **J. De Keyser**, M. Fujimoto, S. Grahn, S. Haaland, H. Ji, Y.V. Khotyaintsev, A. Lazarian, B. Lavraud, I.R. Mann, R. Nakamura, T.K.M. Nakamura, Y. Narita, A. Retinò, F. Sahraoui, A. Schekochihin, S.J. Schwartz, I. Shinohara, L. Sorriso-Valvo
EIDOSCOPE: Particle acceleration at plasma boundaries
Experimental Astronomy, 33(2-3), 491-527, 2012

64. **A. Verdini**, R. Grappin, M. Velli
Coronal heating in coupled photosphere-chromosphere-coronal systems: turbulence and leakage
Astronomy and Astrophysics, 538, pp.A70 (2012)

65. **A. Verdini**, R. Grappin, R. Pinto, M. Velli
On the Origin of the 1/f Spectrum in the Solar Wind Magnetic Field
Astrophysical Journal Letters, 750, pp.L33

66. **A. Verdini**, R. Grappin
Transition from weak to strong cascade in MHD turbulence
Physical Review Letters, 109, pp.025004

67. G. Voitcu, **M. Echim**, R. Marchand
Comparative study of forward and backward test-kinetic simulation approaches
Computer Physics Communications, Volume 183, Issue 12, pp.2561-2569, 2012

68. G. Voitcu, **M. Echim**
Ring-shaped velocity distribution functions in energy-dispersed structures formed at the boundaries of a proton stream injected into a transverse magnetic field: Test-kinetic results
Physics of Plasmas, Volume 19, Issue 2, pp.022903-022903-13, 2012

69. Y.-M. Wang, R. Grappin, **E. Robbrecht**, and N.R. Sheeley, Jr
On the nature of the solar wind from coronal pseudostreamers
Astrophysical Journal, 749, pp.182-195(2012)

70. A.G. Yahnin, T.A. Yahnina, H. Frey, **V. Pierrard**
Sub-oval aurora spots: Mapping relatively to plasmapause
Journal of Atmospheric and Solar-Terrestrial Physics, vol. 99, 61-66, 2013, http://dx.doi.org/10.1016/j.jastp.2012.09

71. J. Zender, **D. Berghmans**, D.S. Bloomfield, **C. Cabanas Parada**, **I.E. Dammasch**, **A. De Groof**, **E. D'Huys**, **M. Dominique**, P.T. Gallagher, **B. Giordanengo**, P. Higgins**, J.-F. Hochedez**, **M.S. Yalim**, **B. Nicula**, **E. Pylyser**, L. Sanchez-Duarte, G. Schwehm, **D.B. Seaton**, **A. Stanger**, **K. Stegen**, **S. Willems**
The Projects for Onboard Autonomy (PROBA2) Science Centre: Sun Watcher Using APS Detectors and Image Processing (SWAP) and Large-Yield Radiometer (LYRA) Science Operations and Data Products
Solar Physics, Online First, DOI: 10.1007/s11207-012-0033-6 (2012)

72. F. P. Zuccarello , A. Bemporad, C. Jacobs, **M. Mierla**, S. Poedts, F. Zuccarello
The Role of Streamers in the Deflection of Coronal Mass Ejections: Comparison between STEREO Three-dimensional Reconstructions and Numerical Simulations
Astrophysical Journal, 744, pp.id. 66

Presentations and posters at conferences

1. W. Aerts, Q. Baire, C. Bruyninx, J. Legrand, E. Pottiaux
Towards better GNSS observations at the new IGS reference station BRUX: multipath mitigation and individual antenna calibration
AGU Fall Meeting, San Francisco, US, December 3-7, 2012 (invited)

2. Q. Baire, C. Bruyninx, E. Pottiaux, J. Legrand, W. Aerts
Differences between GPS receiver antenna calibration models and influence on geodetic positioning
AGU Fall Meeting, San Francisco, US, December 3-7, 2012

3. Q. Baire, E. Pottiaux, C. Bruyninx, P. Defraigne, W. Aerts, J. Legrand, N. Bergeot, J.-M. Chevalier
Impact of Individual GNSS Antenna Calibrations Used in the EPN on Positioning
EUREF 2012 Symposium, Saint Mandé, France, June 6-8, 2012

4. Q. Baire, E. Pottiaux, C. Bruyninx, P. Defraigne, W. Aerts, J. Legrand, N. Bergeot, J.-M. Chevalier
Impact of different individual GNSS receiver antenna calibration models on geodetic positioning
European Geosciences Union General Assembly 2012, Vienna, Austria, April 22-27, 2012

5. Q. Baire, E. Pottiaux, C. Bruyninx, P. Defraigne, W. Aerts, J. Legrand, N. Bergeot, J.-M. Chevalier
Evaluation of Individual Antenna Calibrations Used in the EPN
IGS Workshop 2012, Olsztyn, Poland, July 23-27, 2012 (poster)

6. M. Barthélemy, H. Lamy, J. Lilensten, C. Simon Wedlund
A spectropolarimeter to study the auroral polarization spectrum
EGU General Assembly 2012, Vienna, Austria, April 22-27, 2012 (poster)

7. A. BenMoussa, B. Giordanengo, S. Gissot, I.E. Dammasch and M. Dominique
Degradation of LYRA after 3 years in orbit
ESWW9 – PROBA2 session, November 6, 2012, Brussels, Belgium (invited)

8. A. BenMoussa, A. Soltani, T. Saito, S. Averin, J-C Gerbedoen and J.C. De Jaeger
Developments and characterization of wide band gap photodetectors for EUV Solar Observations
IUMRS-ICEM2012, September 23-28, 2012, Yokoyama, Japan

9. B. Bentley, D. Berghmans, A. Csillaghy, G. Lapenta, C. Jacquey, M. Messeroti, J. Aboudarham
CASSIS – Considerations for Collaborative Environments (Poster)
9th European Space Weather Week, November 5-9, Brussels, Belgium

10. B. Bentley, D. Berghmans, A. Csillaghy
A Collaborative Research Environment for Heliophysics
EGU General Assembly 2012, April 22-27, 2012, Vienna, Austria

11. N. Bergeot, I. Tsagouri, C. Bruyninx, J. Legrand, J.-M. Chevalier, P. Defraigne, Q. Baire, E. Pottiaux
Effect of Space Weather on Ionospheric Total Electron Content Variation during the 23rd Solar Cycle
European Geosciences Union General Assembly 2012, Vienna, Austria, April 22-27, 2012 (poster)

12. N. Bergeot, J.-M. Chevalier, C. Bruyninx, E. Pottiaux, Q. Baire, J. Legrand, P. Defraigne, W. Aerts
New Near-Real Time Ionospheric Products Based on Real-time EPN Data
EUREF 2012 Symposium, Saint Mandé, France, June 6-8, 2012

13. N. Bergeot, I. Tsagouri, C. Bruyninx, J. Legrand, J.-M. Chevalier, P. Defraigne, Q. Baire, E. Pottiaux
Effect of Space Weather on Ionospheric Total Electron Content Variation during the 23rd Solar Cycle
EGU 2012, March 23-27, 2012, Vienna, Austria

14. N. Bergeot, J.-M. Chevalier, L. Benoit, C. Bruyninx, J. Legrand, E. Pottiaux, Q. Baire, P. Defraigne
Near Real Time Ionospheric Models from European Permanent Network GPS Data
EUREF 2012 Symposium, Saint Mandé, France, June 6-8, 2012

15. D. Berghmans, E. Robbrecht, R. Van der Linden
The SIDC, a European Space Weather Prediction Center
TIEMS Oslo Conference «Space Weather and Challenges for Modern Society», October 22-24, 2012, Oslo, Norway, (invited)

16. K. Bonte, I.E. Dammasch, F. Verstringe, D. Berghmans, A. De Groof, M. Dominique, M. Kretzschmar, B. Nicula, E. Pylyser, D. Seaton, K. Stegen
Space Situational Awareness services offered by PROBA2
9th European Space Weather Week, Brussels, Belgium (poster)

17. K. Borremans, V. Pierrard
The Dynamics of the Earth's Inner Magnetosphere
General Scientific Meeting 2012 of the Belgian Physics Society and the Vrije Universiteit Brussel, Brussels, Belgium, May 30, 2012 (poster)

18. K. Borremans, V. Pierrard
The Dynamics of the Earth's Inner Magnetosphere
European Summer School on Fundamental Processes in Space Weather, Spinetto, Italy, June 4-9, 2012 (poster)

19. K. Borremans, V. Pierrard
The dynamics of the Earth's inner magnetosphere
URSI Forum 2012, Academy Palace of Brussels, September 14, 2012 (poster)

20. H. Brenot, C. Champollion, A. Deckmyn, R. Van Malderen, N. Kumps, R. Warnant, M. De Mazière
Humidity 3D field comparisons between GNSS tomography, IASI satellite observations and ALARO model
EGU General Assembly 2012, Geophysical Research Abstracts, Vol. 14, EGU2012-4285, 2012

21. C. Bruyninx, W. Aerts, P. Defraigne, J. Legrand, F. De Doncker, D. Lafourte
BRUX: A New EPN and IGS Reference Station in Brussels
EUREF 2012 Symposium, Saint Mandé, France, June 6-8, 2012 (poster)

22. C. Bruyninx, W. Aerts, P. Defraigne, J. Legrand, Q. Baire, F. De Doncker, D. Lafourte
BRUX: A New EPN and IGS Reference Station in Brussels
IGS Workshop 2012, Olsztyn, Poland, July 23-27, 2012 (poster)

23. C. Bruyninx, J. Ihde, Z. Altamimi, E. Brockmann, A. Caporali, R. Dach, J. Dousa, R. Fernandes, H. Habrich, H. Hornik, A. Kenyeres, M. Lidberg, R. Pacione, M. Poutanen, M. Sacher, W. Söhne, G. Stangl, J.A. Torres, C. Völksen, G. Weber
EUREF's Efforts to Meet the Challenge of the Changing Geodetic Landscape
8th FIG Regional Conference 2012, Montevideo, Uruguay, November 26-29, 2012 (invited)

24. C. Bruyninx, H. Habrich, J. Ihde, W. Söhne, G. Weber
The Role of EUREF in a Changing GNSS Landscape
United Nations/Latvia Workshop on the Applications of Global Navigation Satellite Systems, Riga, Latvia, May 14-18, 2012

25. C. Bruyninx, Q. Baire, J. Legrand, F. Roosbeek
Recent Developments in the EUREF Permanent Network (EPN) and its Central Bureau
EUREF 2012 Symposium, Saint Mandé, France, June 6 - 8, 2012

26. S. Chabanski, M. Kruglanski et al.,
SSA Space Weather Coordination Center
9th European Space Weather Week, November 5-9, 2012, Brussels (poster)

27. J.-M. Chevalier, N. Bergeot, C. Bruyninx, E. Pottiaux, Q. Baire, J. Legrand, P. Defraigne, W. Aerts
GNSS-based Near-Real Time Ionospheric Monitoring over Europe Available On-Line
IGS Workshop 2012, Olsztyn, Poland, July 23-27, 2012 (poster)

28. J.-M. Chevalier, N. Bergeot, C. Bruyninx, E. Pottiaux, Q. Baire, J. Legrand, P. Defraigne, W. Aerts
New Near-Real Monitoring Time of the Ionosphere over Europe Available On-line
European Geosciences Union General Assembly 2012, Vienna, Austria, April 22-27, 2012 (poster)

29. N.B Crosby, A. Veronig, E. Robbrecht, B. Vrsnak, S. Vennerstrom, O. Malandraki, S. Dalla, L. Rodriguez, N. Srivastaba, M. Hesse, D. Odstrcil
COMESEP Project: Space Weather Impact forecasting
Solar and Heliospheric Influences on the Geospace, Bucharest, Romania, October 1-5, 2012 (poster)

30. N.B. Crosby, A. Veronig, E. Robbrecht, B. Vrsnak, S. Vennerstrom, O. Malandraki, S. Dalla, L. Rodriguez, N. Srivastaba, M. Hesse, D. Odstrcil
Forecasting Geomagnetic Storms and Solar Energetic Particle Events: the COMESEP Project
XXVI Scientific Meeting of the Argentine Association of Geophysics, Tucumán, Argentina, November 5-9, 2012 (poster)

31. N.B. Crosby, A. Veronig, E. Robbrecht, B. Vrsnak, S. Vennerstrom, O. Malandraki, S. Dalla, L. Rodriguez, N. Srivastaba, M. Hesse, D. Odstrcil
Forecasting the Space Weather Impact: the COMESEP Project
International Symposium on Solar-Terrestrial Physics, Pune, India, November 6-9, 2012 (poster)

32. N.B. Crosby, M.J. Rycroft
Space Weather: Hazard Assessment, Mitigation and Forecasting
16th ISU Annual International Symposium, International Space University (ISU) Campus, Strasbourg, France, February 21-23, 2012

33. N.B. Crosby
COMESEP: the SEP side of the Project
Splinter - Solar Storms: Solar Energetic Particle (SEP) events, 9th European Space Weather Week, Brussels, Belgium, November 5-9, 2012

34. N.B. Crosby, A. Veronig, E. Robbrecht, B. Vrsnak, S. Vennerstrøm, O. Malandraki, S. Dalla, N. Srivastava, M. Hesse, D. Odstrcil
Forecasting Geomagnetic Storms and Solar Energetic Particle Events: the COMESEP Project
European Geosciences Union General Assembly 2012, Vienna, Austria, April 22-27, 2012 (poster)

35. N.B. Crosby, A. Veronig, E. Robbrecht, B. Vrsnak, S. Vennerstrøm, O. Malandraki, S. Dalla, N. Srivastava, M. Hesse, D. Odstrcil
Forecasting Geomagnetic Storms and Solar Energetic Particle Events: COMESEP
Space Weather Effects on Humans in Space and on Earth International Conference, Space Research Institute, Moscow, Russia, June 4-8, 2012 (poster)

36. N.B. Crosby
Power-Law Distributions: from the Sun to the Earth
Thunderstorms and Elementary Particle Acceleration 2012 conference (TEPA 2012), Moscow, Russia, July 9-11, 2012 (poster)

37. L. Dame, M. Kretzschmar, I.E. Dammasch, S.T. Kumara, R. Kariyappa, M. Dominique, S. Ueno, S. Khaled
Solar Activity Monitoring of flares and CMEs precursors: the importance of Lyman-alpha
COSPAR 39th Scientific Assembly, Mysore, India

38. I.E. Dammasch, M. Dominique, M.Kretzschmar, P.C. Chamberlin
Thermal evolution of flares observed by PROBA2/LYRA
COSPAR 39th Scientific Assembly, 9th TIGER Symposium, Mysore, India

39. I.E. Dammasch, M. Dominique, M.Kretzschmar
Two years of solar observation with PROBA2/LYRA: An overview
12th Hvar Astrophysical Colloquium, Hvar, Croatia

40. I.E. Dammasch
Flares observed by LYRA on PROBA2
Solar and Heliospheric Influences on the Geospace, Bucharest, Romania (invited)

41. I.E. Dammasch, L. Lefevre
Correlation between sunspot numbers and EUV irradiance as observed by LYRA on PROBA2
9th European Space Weather Week, Brussels, Belgium (poster)

42. I.E. Dammasch
Space weather data and services at ROB/SIDC
Solar and Heliospheric Influences on the Geospace, Bucharest, Romania (invited)

43. F. Darrouzet, S. Ranvier, H. Lamy, J. De Keyser, J. Lichtenberger
Whistlers detected by the Belgian VLF antenna of Humain
5th VERSIM Workshop, Sao Paulo, Brazil, September 3-6, 2012

44. F. Darrouzet, S. Ranvier, J. De Keyser, H. Lamy, J. Lichtenberger
Whistlers Detected by a Belgian VLF Measurement System
22nd URSI Benelux Forum, Brussels, Belgium, September 14, 2012 (poster)

45. F. Darrouzet, S. Ranvier, J. De Keyser, H. Lamy, J. Lichtenberger
Detection of Whistlers by the Belgian VLF Antenna: Statistical Analysis and Comparison with Cluster Data
Joint Cluster-THEMIS meeting (including ARTEMIS), LASP, Boulder, Colorado, USA, October 1-5, 2012 (invited)

46. F. Darrouzet, S. Ranvier, J. De Keyser, H. Lamy, J. Lichtenberger
Whistlers detected by the Belgian VLF antenna of Humain
9th European Space Weather Week, Brussels, Belgium, November 5-9, 2012 (poster)

47. V. De Bock, H. De Backer, R. Van Malderen
Analysis of an extensive time series of UV irradiation and AOD measurements in the UV-B region at Uccle, Belgium
International Radiation Symposium 2012, Berlin, Germany, August 6-10, 2012

48. P. Defraigne, G. Cerretto, F. Lahaye, Q. Baire, D. Rovera
Near real-time comparison of UTC(k)'s through a Precise Point Positioning approach
EFTF, Goteborg, April 2012.

49. P. Defraigne, Q. Baire, E. Pottiaux
Using IGS products for near real-time comparison of UTC(k)'s
IGS Workshop, Olsztyn, July 2012.

50. J. De Keyser, F. Darrouzet
On the role of systematic errors in multi-spacecraft gradient computation
Geophysical Research Abstracts, Vol. 14, EGU General Assembly, Vienna, Austria, April 22-27, 2012 (poster)

51. J. De Keyser
Gradients and systematic errors
Joint Cluster-THEMIS meeting (including ARTEMIS), LASP, Boulder, Colorado, USA, October 1-5, 2012 (poster)

52. J. De Keyser, M. Echim, H. Lamy, C. Simon Wedlund, H. Gunell, I. Mann, A. Tjulin, J. I. Moen, T.A. Bekkeng

Auroral plasma research with cubesat - EISCAT coordinated observations
4th European CubeSat Symposium, Brussels, Belgium, January 30 – February 1, 2012

53. J. De Keyser
Comets and Space Weather
European Space Weather Week 2012, Brussels, Belgium, November 5-9, 2012 (invited)

54. J. De Keyser, S. Ranvier, D. Pieroux, D. Fussen, O. Karatekin
The PICASSO mission: A Belgian cubesat for the study of the upper atmosphere, the ionosphere, and the magnetosphere of the Earth
General Meeting of the Belgian Physical Society, Brussels, Belgium, May 30, 2012

55. V. Delouille
Exploring Heterogeneous Solar Data
5th Solar Orbiter Workshop, Bruges, Belgium, September 10-14, 2012 (invited)

56. V. Delouille, B. Mampaey, C. Verbeeck, R. De Visscher
Coronal Hole detection on SDO images
6th Solar Image Processing Workshop, Bozeman, MT, USA, August 13-16, 2012 (poster)

57. V. Delouille, B. Mampaey, C. Verbeeck, R. De Visscher
Coronal Hole Detection on SDO images
5th Solar Orbiter Workshop, Bruges, Belgium, September 10-14, 2012 (poster)

58. A. Devos, S. Chabanski, M. Kruglanski, and the SN-IV Consortium
ESA SSA Space weather service Coordination Centre and Portal to the SSA-SWE precursor service network
9th European Space Weather Week (ISWW9) meeting, Brussels, Belgium, November 5-9, 2012 (demo at fair)

59. A. Devos, M. Dumbovic, L. Rodriguez, E. Robbrecht, B. Vrsnak, S. Davor, R. Domagoj, M. Dierckxsens, V. Astrid, M. Temmer, S. Vennerstrom, K. Leer
Statistical models relating geomagnetic activity to Coronal Mass Ejections (CMEs)
9th European Space Weather Week, Brussels, Belgium, November 5-9, 2012 (poster)

60. A. Devos, C. Verbeeck, E. Robbrecht, P. Vanlommel
Statistical evaluation of space weather forecasting at the Regional Warning Center in Belgium
9th European Space Weather Week (ESWW9) meeting, Brussels, Belgium, November 5-9, 2012 (poster)

61. E. D'Huys, D. Seaton, C. Jacobs, A. De Groof, S. Poedts
Multi-spacecraft Analysis and modeling of a solar eruption on August 14, 2010
First European school on Fundamental processes in space weather: a challenge in numerical modeling, SWIFF network, June 4-9, Spineto, Italy (poster)

62. E. D'Huys, D. Seaton, C. Jacobs, A. De Groof, S. Poedts
Multi-spacecraft Analysis and modeling of a solar eruption on August 14, 2010
5th Solar Orbiter Workshop, September 10-14, Bruges, Belgium (poster)

63. E. D'Huys, D. Seaton, K. Bonte, D. Berghmans, S. Poedts
Initiation Mechanisms for CMEs Without Distinct Coronal Signatures
9th European Space Weather Week, November 5-9, 2012, Brussels, Belgium (poster)

64. M. Dierckxsens, G. Dorrian, I. Patsou, K. Tziotziou, M. Marsh, N. Lygeros, N.B. Crosby, S. Dalla, O. Malandraki
Statistical Analysis of solar energetic particles Events and related solar Activity
9th European Space Weather Week, Brussels, Belgium, November 5-9, 2012 (poster)

65. L. Dolla, C. Marqué, D. Seaton, T. Van Doorsselaere, M. Dominique, D. Berghmans, C. Cabanas, A. De Groof, W. Schmutz, A. Verdini, M. J. West, J. Zender and A. N. Zhukov
Could Solar Orbiter observe Quasi-Periodic Pulsations during flares?
5th Solar Orbiter Workshop, Bruges, Belgium (poster)

66. L. Dolla, C. Marqué, D. Berghmans, C. Cabanas, M. Dominique, A. De Groof, D. Seaton, T. Van Doorsselaere, A. Verdini, M. West, J. Zender, A. Zhukov
Could Solar Orbiter observe Quasi-Periodic Pulsations during flares?
5th Solar Orbiter Workshop, September 10-14, 2012, Bruges, Belgium (poster)

67. M. Dominique, L. Dolla, T. Van Doorsselaere, C. Marqué, A. Zhukov
Quasi-periodic pulsations in solar flares
2012 SDO EVE Science Conference, October 30-November 1, 2012, Yosemite Lodge, USA

68. M. Dominique, D. Seaton, I.E. Dammasch, A. BenMoussa, K. Stegen, E. Pylyser
Status of degradation onboard PROBA2
9th European Space Weather Week, Brussels, Belgium (poster)

69. M. Dominique, I Dammasch, M. Kretzschmar
LYRA on-board PROBA2: instrument performances and latest results
COSPAR 39th Scientific Assembly, Mysore, India (invited)

70. M. Dominique
LYRA status and inter-instrument comparison
2012 SDO EVE Science Conference, California (USA)

71. M. Dominique, I. Dammasch
LYRA status update
9th European Space Weather Week, PROBA2 splinter, Brussels, Belgium

72. R. De Visscher
An overview of tools and techniques for parallel computation in solar image processing
6th Solar Information Processing Workshop, Bozeman, MT, USA, August 13-16, 2012

73. S. Dewitte, A. Chevalier
Simba: the Sun-earth IMBAlance radiometer
QB50 symposium, Brussels, February 2012

74. S. Dewitte, A. Chevalier
Simba: the Sun-earth IMBAlance radiometer
Ceres science team meeting, Princeton, USA, October 2012

75. S. Dewitte
Climate monitoring with Earth Radiation Budget measurements
Eumetsat conference, Sopot, Poland, September 2012

76. S. Dewitte
Climate monitoring with Earth Radiation Budget measurements
Ceres science team meeting, Princeton, USA, October 2012

77. M. Dumbovic, B. Vrsnak, S. Davor, R. Domagoj, A. Devos, L. Rodriguez, E. Robbrecht, M. Dierckxsens, M. Temmer, S. Vennerstrom, K. Leer
Forecasting of geomagnetic activity caused by Coronal Mass Ejections (CMEs)
12th Hvar Astrophysical Colloquium "The Sun and Heliosphere", Hvar, Croatia, September 3-7, 2012

78. M. Echim, J. De Keyser, R. Maggiolo
Quasi-stationary magnetosphere-ionosphere coupling and auroral acceleration from satellite observations and kinetic models
International Substorm Conference 2012, Lüneburg, Germany, September 2-7, 2012

79. M. Echim
Kinetic effects for entry and transport of plasmoids
Session ST24, AOGS - AGU (WPGM) Joint Assembly, Singapore, August 13-17, 2012 (invited)

80. M. Echim
Quasi-stationary magnetosphere-ionosphere coupling and auroral acceleration from satellite observations and kinetic models
11th International Conference on Substorms, Lüneburg, Germany September 2-7, 2012 (invited)

81. M. Echim, T. Zhang, C. Munteanu, R. Lundin, S. Barabash
Comparative kinetic investigation of the magnetopause of Venus and the Earth
Session ST03, AOGS - AGU (WPGM) Joint Assembly, Singapore, August 13-17, 2012

82. R. Fernandes, L. Bastos, C. Bruyninx, N. D'Agostino, J. Dousa, A. Ganas, M. Lidberg, J.-M. Nocquet, and the WG4 Member Team
The Contribution of the Geodetic Community (WG4) to EPOS
European Geosciences Union General Assembly 2012, Vienna, Austria, April 22-27, 2012

83. D. Fussen, J. De Keyser, M. De Mazière, D. Pieroux, H. Lamy, S. Ranvier, E. Dekemper, A. Merlaud, O. Karatekin, V. Dehant, M. Mitrovic, M. Van Ruymbeke, J.-P. Noel, Z. Ping
Picasso: A triple cubesat mission for atmospheric and space science
4th European CubeSat Symposium, Brussels, Belgium, January 30-February 1, 2012

84. A.M. Gulisano, P. Démoulin, S. Dasso, L. Rodriguez
Features of the Expansion of flux ropes in the outer heliosphere
55th annual meeting of the Argentinean Astronomy Association, Buenos Aires, September 17-21, 2012

85. H. Gunell, I. Mann, J. De Keyser, L. Andersson
Vlasov simulations of electron trapping on auroral field lines
Geophysical Research Abstracts, Vol. 14, EGU General Assembly, Vienna, Austria, April 22-27, 2012 (poster)

86. H. Gunell, G. Stenberg, R. Maggiolo, H. Nilsson, M. Hamrin, T. Karlsson
Cluster observations of plasmoids interacting with the magnetopause
3rd Cluster Themis Workshop, Boulder, Colorado, USA, October 1-5, 2012 (poster)

87. M. Haberreiter, V. Delouille, I. Ermolli, C. Verbeeck, R. Qahwaji
Physics-based Modeling of the Variations of the solar EUV Spectrum
9th European Space Weather Week, November 5-9, 2012, Brussels, Belgium

88. M. Haberreiter, M. Dasi Espuig, V. Delouille, G. Del Zanna, T. Dudok de Wit, I. Ermolli, M. Kretzschmar, N. Krivova, H. Mason, R. Qahwaji, W. Schmutz, S. Solanki, G. Thuillier, K. Tourpali, Y. Unruh, C. Verbeeck, M. Weber, T. Woods
A Collaborative FP7 Effort towards the First European Comprehensive SOLar Irradiance Data Exploitation (SOLID)
9th European Space Weather Week, November 5-9, 2012, Brussels, Belgium (poster)

89. J. Ihde, Z. Altamimi, E. Brockmann, C. Bruyninx, A. Caporali, J. Dousa, R. Fernandes, H. Habrich, H. Hornik, A. Kenyeres, M. Lidberg, J. Mäkinen, M. Poutanen, M. Sacher, W. Söhne, G. Stangl, J.A. Torres, C. Völksen, G. Weber
EUREF's Infrastructure Galileo Ready
7th Meeting of the International Committee on Global Navigation Satellite Systems (ICG), Beijing, China, November 5-9, 2012

90. E. Janssen, S. Dewitte
Calculation of the efficiency of the cavity in an adiabatic case
ISSI meeting, Bern, March 2012

91. J. Jones, G. Guerova, J. Dousa, O. Bock, G. Elgered, H. Vedel, E. Pottiaux, S. De Haan, R. Pacione, G. Dick, J. Wang, S.I. Gutman, J. Wickert, K. Rannat, G. Liu, J. J. Braun, Y. Shoji
International Collaboration in the field of GNSS-Meteorology and Climate Monitoring
AGU Fall Meeting, San Francisco, US, December 3-7, 2012 (poster)

92. J. Jones, E. Pottiaux, G. Guerova, J. Dousa, G. Dick, O. Bock, R. Pacione, G. Elgered, H. Vedel, S. De Haan
Advanced GNSS Tropospheric Products for the Monitoring of Severe Weather Events and Climate (GNSS4SWEC)
IGS Workshop 2012, Olsztyn, Poland, July 23-27, 2012 (poster)

93. S. Kochenova, C. Lerot, M. De Mazière, V. Letocart
Importance of polarization for remote sensing of the Earth's atmosphere
EGU General Assembly, Vienna, Austria, April 22-27, 2012 (poster)

94. S. Kochenova, M. De Mazière, N. Kumps, A.C. Vandaele, S. Vandenbussche, T. Kerzenmacher, and V. Letocart
Retrieval of volcanic ash and ice cloud physical properties together with gas concentration from IASI measurements with the help of the AVL model
International Radiation Symposium, Dahlem Cube, Berlin, Germany, August 6-10, 2012 (poster)

95. E. Kraaikamp, C. Verbeeck, O. Podlachikova, P. Lisnichenko
NEMO: Near real-time dimming and EIT wave detection on SDO/AIA
European Space Weather Week 9, Brussels, Belgium, November 5-9, 2012 (poster)

96. E. Kraaikamp, C. Verbeeck, O. Podlachikova, P. Lisnichenko
Dimming and EIT wave detection on SDO/AIA first results by NEMO
SIPWork VI, Montana State University, USA, August 13-16, 2012 (poster)

97. E. Kraaikamp
Lucky Imaging with AutoStakkert!
European Space Weather Week 9, Brussels, Belgium, November 5-9, 2012 (tutorial and fair)

98. M. Kretzschmar, I.E. Dammasch, M. Dominique
Variations of solar extreme ultraviolet irradiance in the rising phase of solar cycle 24 as observed by PROBA2/LYRA
COSPAR 39th Scientific Assembly, Mysore, India

99. D. Lacatus, A. Paraschiv, M. Mierla, L. Rodriguez, E. Kilpua
Studies of CMEs causing Geomagnetic Storms in the Period 2007-2011
Solar and Heliospheric Influences on the Geospace, Bucharest, Romania, October 1-5, 2012 (poster)

100. Q. Laffineur, H. Debacker, O. Brasseur
Retrieval and validation of mixing layer height with LIDAR-ceilometer
Meteoclim 2012, ULg, Liège, Belgium, June 1, 2012

101. H. Lamy, S. Ranvier, M. Anciaux, D. Calders, J. De Keyser, E. Gamby
Radio polarization measurements of meteor trail echoes with BRAMS
Geophysical Research Abstracts, Vol. 14, EGU General Assembly, Vienna, Austria, April 22-27, 2012 (poster)

102. H. Lamy, C. Simon Wedlund, J. De Keyser, H. Gunell, M. Barthélemy, J. Lilensten
Eiscat-related activities at the Belgian Institute for Space Aeronomy
EISCAT 3D SWG Meeting, Rome, Italy, January 12, 2012

103. H. Lamy
BRAMS, the Belgian RAdio Meteor Stations: latest developments
IMC 2012, La Palma, Spain, September 20-23, 2012

104. H. Lamy
BRAMS: a Belgian Am-Pro collaboration to detect and characterize meteors with radio techniques
European Planetary Science Congress 2012, Madrid, Spain, September 23-28, 2012 (invited)

105. H. Lamy, S. Ranvier, M. Anciaux
Radio polarization measurements of meteor trail echoes with BRAMS
European Planetary Science Congress 2012, Madrid, Spain, September 23-28, 2012 (poster)

106. H. Lamy, M. Barthélemy, J. Lilensten, C. Simon Wedlund, V. Bommier
Polarization of auroral emission lines in the Earth's upper atmosphere: a review
AOGS-AGU Joint Meeting, Singapore, August 14, 2012

107. G. Lechat, H. Lamy, V. Pierrard, N. Meyer-Vernet, K. Issautier, I. Zouganelis
New developments in exospheric theory of the solar wind
Solar Wind 13, Hawaii USA, June 25-30, 2012

108. K. Leer, S. Vennerstrom, A. Veronig, L. Rodriguez, B. Vrsnak
Statistical study of false alarms of geomagnetic storms
9th European Space Weather Week, Brussels, Belgium, November 5-9, 2012 (poster)

109. L. Lefèvre, F. Clette
Are the sunspots vanishing?
2nd Sunspot Workshop, May 21-25, 2012, Brussels

110. L. Lefèvre
What are small sunspots?
Mini Sunspot workshop, September 2012, Sunspot, NM, USA

111. L. Lefèvre, F. Clette, S. Vennerstrom
Historical Sunspot Data Analysis in the context of the COMESEP project
ESWW9, November 5-9, 2012, Brussels (poster)

112. J. Legrand, C. Bruyninx, E. Saria, J. Griffiths, M.R. Craymer, J.H. Dawson, A. Kenyeres, A. Santamaría-Gómez, L. Sanchez, Z. Altamimi
Densification of the ITRF through the weekly combination of regional and global GNSS solutions
AGU Fall Meeting, San Francisco, US, December 3-7, 2012 (poster)

113. J. Legrand, C. Bruyninx, J. Griffiths, M.R. Craymer, J.H. Dawson, A. Kenyeres, A. Santamaría-Gómez, L. Sanchez, Z. Altamimi
Evaluation of GNSS Solutions submitted to IAG WG "Integration of Dense Velocity Fields in the ITRF"
EUREF 2012 Symposium, Saint Mandé, France, June 6-8, 2012

114. J. Legrand, C. Bruyninx, E. Saria, J. Griffiths, M.R. Craymer, J.H. Dawson, A. Kenyeres, A. Santamaría-Gómez, L. Sanchez, Z. Altamimi
First Combination of GNSS Solutions Submitted to IAG WG "Integration of Dense Velocity Fields in the ITRF"
IGS Workshop 2012, Olsztyn, Poland, July 23-27, 2012 (poster)

115. C. Lerot, M. Van Roozendael, R. Spurr, S. Kochenova, D. Loyola, V. Natraj, J. van Gent, J.C. Lambert, D. Balis, M. Koukouli, C. Zehner
Towards an improved total ozone climate data record from GOME, SCIAMACHY and GOME-2 as part of the ESA climate change initiative
ATMOS-2012 (Advances in Atmospheric Science and Applications), Bruges, Belgium, June 18-22, 2012 (poster)

116. J. Lilensten, M. Barthélemy, P.O. Amblard, J. Moen, H. Rothkaehl, C. Simon Wedlund, H. Lamy
Calibrated polarization parameters of the auroral red line in Hornsund
EGU General Assembly 2012, Vienna, Austria, April 22-27, 2012 (poster)

117. J. Magdalenić, C. Marqué, A. N. Zhukov, L. Rodriguez, M. Mierla, V. Krupar, B. Cecconi, M. Maksimović
Tracking the CME-driven shock wave
XII Hvar Astrophysical Colloquium, September 3-7, 2012, Hvar, Croatia

118. J. Magdalenić, C. Marqué, A. N. Zhukov, L. Rodriguez, M. Mierla, V. Krupar, B. Cecconi, M. Maksimović
Tracking the CME-driven shock wave on 05 March 2012
9th European Space Weather Week, November 5-9, 2012, Brussels, Belgium

119. J. Magdalenić, C. Marqué, A. N. Zhukov, L. Rodriguez, M. Mierla, V. Krupar, B. Cecconi, M. Maksimović
Tracking the CME-driven shock wave on 05 March 2012
AOGS – AGU (WPGM) Joint Assembly, August 13-17, 2012, Singapore

120. V. Malisse, C. Verbeeck
STAFF demo
European Space Weather Week 9, Brussels, Belgium, November 5-9, 2012

121. C. Marqué
Service de Surveillance Radio-Solaire
Forum Météorologie de l'Espace, Paris, France, November 23, 2012

122. C. Marqué
Activités en météorologie de l'espace en Belgique
Forum Météorologie de l'Espace, Paris, France, November 23, 2012

123. C. Marqué, N. Bergeot, W. Aerts, J.-M. Chevalier, J. Magdalenic, B. Nicula
Impact of a solar radio Burst on the EPN GNSS Network
9th European Space Weather Week, Brussels, Belgium, November 5-9, 2012 (poster)

124. M.C. Martinez-Belda, P. Defraigne
First investigations on using Galileo E5AltBOC for time transfer
IGS Workshop 2012, Olsztyn, Poland, July 23-27, 2012 (poster)

125. M. Mierla, L. Feng, L. Rodriguez, I. Chifu, B. Inhester
3D reconstruction of coronal mass ejections: where are we?
Solar Information processing workshop VI, Bozeman, MT, USA, August 13-16, 2012 (invited)

126. M. Mierla, C. Oprea, N. Srivastava, L. Rodriguez, D. Besliu-Ionescu, O. Stere, G. Maris Muntean
Empirical model for predicting the occurrence of major geomagnetic storms during SC23
Solar and Heliospheric Influences on the Geospace, Bucharest, Romania, October 1-5, 2012

127. M. Mierla, H. Cremades, C. Mandrini, L. Rodriguez, L. Balmaceda
Study of 26 April 2008 Coronal Mass Ejection
The conference Rocks'n Stars, Goettingen, Germany, October 8-11, 2012

128. P.M. Miller, M.E. Koepke, H. Gunell
Laser-induced quasiperiodic mode hopping in competing ionization waves
The 39th EPS Conference on Plasma Physics and the 16th International Congress on Plasma Physics, Stockholm, Sweden, July 2-6, 2012 (poster)

129. C. Munteanu, S. Haaland, B. Mailyan, M. Echim, K. Mursula
Improving solar wind propagation delay estimation using wavelet denoising
9th European Space Weather Week, November 5-9, 2012, Brussels, Belgium (poster)

130. S. Parenti
Observational properties of the hot component of active regions: a review
39th COSPAR Scientific Assembly, Mysore, India, July 14-July 22, 2012 (poster)

131. S. Parenti, B. Schmieder, P. Heinzel, and L. Golub
Prominences observations with SDO/AIA
Spectroscopy of the dynamic Sun, London, April 18, 2012

132. S. Parenti, B. Schmieder, P. Heinzel, and L. Golub
Prominences observations with SDO/AIA
39th COSPAR Scientific Assembly, Mysore, India. July 14-July 22, 2012

133. S. Parenti
Elements abundance studies with LEMUR
Solar-C science meeting, Tokyo, January 30-February 3, 2012

134. V. Pierrard, S. Benck, F. Darrouzet, K. Borremans
Dynamics of the space radiation belts
ICNS International Astrophysics Conference, Space weather: The Space Radiation Environment, Palm Springs, USA, March 19-23, 2012 (invited)

135. V. Pierrard, K. Borremans
Space weather models of the inner magnetosphere: the ionosphere-plasmasphere coupled system, the polar wind and the radiation belts
EGU, Vienna (Austria), April 23-27, 2012 (poster)

136. V. Pierrard
Quand le Soleil crée les aurores
Université du Luxembourg, Campus Kirchberg, May 10, 2012 (invited)

137. V. Pierrard, H. Lamy, Y. Voitenko, J. Lemaire
Non-thermal velocity distribution functions in space plasmas
Annual scientific meeting of the Belgian Physical Society, VUB, Brussels, May 30, 2012 (poster)

138. V. Pierrard
Coupling at the Earth
Lecture for the First European School on: Fundamental processes in Space Weather: a challenge in numerical modeling, June 4-9, 2012, Spineto, Tuscany, Italy (invited teacher)

139. S. Poedts, G. Lapenta, A. Lani, H. Deconinck, B. Fontaine, J. Depauw, N. Mihalache, D. Heyndrickx, J. De Keyser, N.B. Crosby, L. Rodriguez, R. Van der Linden
The ESA Virtual Space Weather Modeling Centre Phase 1
9th European Space Weather Week 2012, Brussels, Belgium, November 5-9, 2012 (poster)

140. E. Pottiaux, G. Bennit, C. Bruyninx, W. Aerts, Q. Baire, N. Bergeot, J.-M. Chevalier, P. Defraigne, J. Legrand, F. Meeuws
GNSS Research and Services at ROB to Support Meteorology and Nowcasting Applications
IGS Workshop 2012, Olsztyn, Poland, July 23-27, 2012 (poster)

141. E. Pottiaux, J.-M. Chevalier, N. Bergeot, T. Coupin, W. Aerts, C. Bruyninx, Q. Baire, P. Defraigne, J. Legrand
Using Real-Time GNSS Data for Atmospheric Monitoring
PPP-RTK & Open Standards Symposium, Frankfurt am Main, Germany, March 12-13, 2012 (poster)

142. E. Pottiaux, R. Van Malderen, H. Brenot, S. Beirle, C. Bruyninx, H. De Backer, M. De Mazière, C. Hermans, K. Mies, T. Wagner
On the Use of the IGS REPRO1 Product for Climate Change Analysis: An IWV Inter-technique Comparison Study
IGS Workshop 2012, Olsztyn, Poland, July 23-27, 2012 (poster)

143. E. Prouteau, M. Gravelle, M. Guichard, D. Mesmaker, Q. Baire, C. Bruyninx, G. Wöppelmann
TIGA Network Coordination: Monitoring Data Fluxes and Providing Metadata
IGS Workshop 2012, Olsztyn, Poland, July 23-27, 2012 (poster)

144. S. Ranvier, D. Pieroux, J. De Keyser, M. Echim, C. Simon Wedlund, H. Lamy, H. Gunell, I. Mann, A. Tjulin, J. Moen
Space weather investigation with PICASSO
European Space Weather Week 2012, Brussels, Belgium, November 5-9, 2012 (poster)

145. S. Ranvier, H. Lamy, M. Anciaux, J. De Keyser, S. Calders, E. Gamby
Radio polarization measurements of meteor trail echoes with BRAMS
URSI Forum 2012, Brussels, Belgium, September 14, 2012

146. L. Rodriguez, A. N. Zhukov, M. Mierla, E. Kilpua, S. Dasso, M. J. West
Internal characteristics of magnetic clouds at 1 AU
13th International Solar Wind Conference, Hawaii, USA, June 18-22, 2012 (poster)

147. L. Rodriguez, A. N. Zhukov, M. Mierla, D. Lacatus, A. Paraschiv, E. Kilpua, S. Dasso, M. J. West
Internal characteristics of magnetic clouds at 1 AU
5th Solar Orbiter Workshop, Bruges, Belgium, September 10-14, 2012 (poster)

148. L. Rodriguez, A. N. Zhukov, M. Mierla, D. Lacatus, A. Paraschiv, E. Kilpua, S. Dasso, M. J. West
Internal characteristics of magnetic clouds at 1 AU
Solar and Heliospheric Influences on the Geospace, Bucharest, Romania, October 1-5, 2012 (poster)

149. L. Rodriguez
Space Weather, from theory and observations to operational forecasting
XXVI Scientific Meeting of the Argentine Associatio0n of Geophysics, Tucumán, Argentina, November 5-9, 2012

150. D. Sapundjiev, M. Nemry, S. M. Stankov, S. Spassov, J.C. Jodogne
Cosmic ray intensity measurements at the RMI Geophysical Centre of Dourbes
European Space Weather Week ESWW-2012, November 5-9, 2012, Brussels, Belgium (poster)

151. D. Seaton, J. De Keyser
Space weather effects on PROBA2
9th European Space Weather Week 2012, Brussels, Belgium, November 5-9, 2012 (poster)

152. D. Seaton, M. Dominique, D. Berghmans, B. Nicula, E. Pylyser, K. Stegen, J. De Keyser
Space Weather and Particle Effects on the Orbital Environment of PROBA2
ESWW9, November 5-9, 2012 Brussels, Belgium (poster)

153. C.L. Simon Wedlund, H. Lamy, B. Gustavsson, T. Sergienko, U. Brandström, J. De Keyser
Auroral electron fluxes and characteristic energy of precipitating electrons inferred by ALIS and EISCAT
Geophysical Research Abstracts, Vol. 14, EGU General Assembly, Vienna, Austria, April 22-27, 2012 (poster)

154. C.L. Simon Wedlund, H. Lamy, B. Gustavsson, T. Sergienko, U. Brandstrom, J. De Keyser
On auroral arc formation: Study of volume emission rates and electron precipitation with ALIS and EISCAT
AOGS - AGU (WPGM) Joint Assembly 2012, Singapore, August 13-17, 2012

155. S.M. Stankov, T. Verhulst, K. Stegen
Evaluation of theoretical ionospheric profilers using topside sounding data
COSPAR Scientific Assembly, July 14-22, 2012, Mysore, India, ABS No. COSPAR12-C11-0107-12

156. S.M. Stankov, K. Stegen, I. Kutiev
Empirical model of the TEC storm-time response in Europe for use in regional ionospheric specification and forecast
COSPAR Scientific Assembly, July 14-22, 2012, Mysore, India, ABS No. COSPAR12-C11-0100-12

157. S.M. Stankov, P. Marinov, I. Kutiev
Reconstruction of the vertical ionospheric electron density distribution from multi-instrument observation data
COSPAR Scientific Assembly, July 14-22, 2012, Mysore, India, ABS No. COSPAR12-C02-0016-12

158. B.J. Thompson, M.L. Mays, M.J. West
EUV Dimmings: Formation Mechanisms and Associated Phenomena, SH44A-03
AGU Fall Meeting, San Francisco, USA, December 2012 (invited)

159. S. Valdes, I. Omar, G. Lawrence, J. Watermann, E. de Donder, M. Kruglanski, D. Berghmans, M. Danielides
Roadmaps for Future Operational Space Weather Services
Talk at ESWW9, November 5-9, 2012, Brussels, Belgium

160. S. Vandenbussche, S. Kochenova, A.C. Vandaele, N. Kumps, M. De Mazière
Retrieval of Saharan desert dust optical depth from thermal infrared measurements by IASI
EGU General Assembly, Vienna, Austria, April 22-27, 2012

161. S. Vandenbussche, S. Kochenova, A.C. Vandaele, N. Kumps, M. De Mazière
Retrieval of Saharan desert dust properties from hyperspectral thermal infrared measurements by IASI
ATMOS-2012 (Advances in Atmospheric Science and Applications), Bruges, Belgium, June 18-22, 2012

162. P. Vanlommel
COST Action ES0803, Final report WG3: 'Exploitation, dissemination, education and outreach'
ESWW9, November 9, Brussels, Belgium

163. P. Vanlommel
Where communication meets space weather
Solar and Heliospheric influences on the geospace, October 1, Bucharest, Romania

164. R. Van Malderen, M. Allaart, A. Delcloo, H. De Backer
The detection of ozone anomaly events and inhomogeneities in the ozonesonde time series of Uccle, Belgium, by comparison with the nearby station of De Bilt (Netherlands)
Quadrennial Ozone Symposium 2012, Toronto, Canada, August 26-31, 2012

165. R. Van Malderen, E. Pottiaux, H. Brenot, S. Beirle, K. Mies, C. Hermans, M. De Mazière, T. Wagner, H. De Backer, C. Bruyninx
Evaluating the potential of ground-based instruments to validate the quality of integrated water vapor data measured by satellite-based observing techniques
GEWEX Water Vapor Assessment Workshop 2012, Offenbach, Germany, September 26-28, 2012

166. R. Van Malderen, H. Brenot, E. Pottiaux, T. Wagner, C. Hermans, M. De Mazière, H. De Backer, C. Bruyninx
Inter-technique comparison of integrated water vapor measurements for climate change analysis
European Geosciences Union General Assembly 2012, Vienna, Austria, April 22-27, 2012 (poster)

167. R. Van Malderen, E. Pottiaux, H. Brenot, K. Mies, S. Beirle, T. Wagner, C. Hermans, M. De Mazière, H. De Backer, C. Bruyninx
Inter-technique comparison of integrated water vapor measurements for climate change analysis
MeteoClim 2012, Liège, Belgium, June 1, 2012

168. R. Van Malderen, E. Pottiaux, H. Brenot, S. Beirle
Evaluating the potential of Integrated Water Vapor data from ground-based, in-situ and satellite-based observing techniques
WMO Technical Conference on Meteorological and Environmental Instruments and Methods of Observation (TECO) 2012, Brussels, Belgium, October 16-18, 2012

169. C. Verbeeck, V. Malisse, B. Bourgoignie, B. Mampaey, V. Delouille, R. De Visscher and the AFFECTS team
The STAFF viewer: all space weather timelines brought together in one powerful web application
European Space Weather Week 9, Brussels, November 5-9, 2012 (poster)

170. A. Verdini, R. Grappin, M. Velli
On the Origin of the 1/f Spectrum in the Heliosphere
Heliocorona Meeting, Bonn, Germany, February 1, 2012

171. A. Verdini, R. Grappin, M. Velli
The role of leakage in the turbulent heating of coronal loop
SW 13 meeting, Hawaii, USA, June 18, 2012

172. A. Verdini, R. Grappin, M. Velli
On the Origin of the 1/f Spectrum in the Heliosphere
COSPAR 39th assembly, Mysore, India, July 21, 2012

173. A. Verdini
A mechanism for the formation of 1/f spectrum in the Heliosphere
Workshop on turbulent cascade in the Solar Wind, Paris, France, September 20, 2012

174. A. Verdini
Building small scales in MHD turbulence
Workshop on Plasma Astrophysics, Firenze, Italy, November 7, 2012

175. A. Verdini, R. Grappin
Transition from weak to strong cascade in MHD turbulence
Poster contribution, SW 13 meeting, Hawaii, USA, June 18-22, 2012 (poster)

176. A. Verdini, R. Grappin, R. Pinto, M. Velli
On the origin of the 1/f spectrum in the solar wind magnetic field
SW 13 meeting, Hawaii, USA, June 18-22, 2012 (poster)

177. A. Verdini, R. Grappin, R. Pinto, M. Velli
On the origin of the 1/f spectrum in the solar wind magnetic field
Poster contribution, 5th Solar Orbiter Workshop, Bruges, Belgium, September 10-14, 2012 (poster)

178. G. Voitcu, M. Echim
Kinetic modeling and simulations of tangential discontinuities
9th European Space Weather Week, November 5-9, 2012, Brussels, Belgium (poster)

179. Y. Voitenko, V. Pierrard, J. De Keyser
Linking turbulence and velocity distributions in the solar wind
Solar Orbiter meeting From the Heliosphere into the Sun, Bad Honnef, Germany, February 1-3, 2012

180. Y. Voitenko, J. De Keyser, V. Pierrard
MHD-kinetic transition in the solar wind turbulence
AOGS - AGU (WPGM) Joint Assembly, Resorts World Convention Centre, Singapore, August 13-17, 2012 (invited)

181. Y. Voitenko, J. De Keyser
Dispersive Alfvénic turbulence in solar-terrestrial relations
IAU XXVIII General Assembly, Special Session 10 Dynamics of the Star-Planet Relations, Beijing, China, August 27-31, 2012

182. M.J. West, S. Parenti
Comparing radiative signatures of cooling in coronal loops
39th COSPAR Scientific Assembly, Mysore, India, July 14-22 2012

183. M. J. West, A. N. Zhukov, L. Dolla, L. Rodriguez
Coronal seismology using EIT Waves: Estimation of the coronal magnetic field in the quiet Sun
Spectroscopy of the Dynamic Sun Workshop, London, UK, April 18-20 (poster)

184. P. Zhu, M. van Ruymbeke, O. Karatekin, V. Dehant
The bolometric oscillation sensor for the micro-, nano-, and pico-satellites, designed at Royal Observatory of Belgium,
5th QB50 symposium, January 30-February 1, 2012, Brussels, Belgium

185. P. Zhu, O. Karatekin, J-P. Noel, M. van Ruymbeke, V. Dehant
A high-dynamic and accurate electromagnetic radiation and thermal energy detector for planetary mission
EGU2012, April 22-27, Vienna, Austria

186. A.N. Zhukov
Large-scale coronal "waves"
39th COSPAR Scientific Assembly, Mysore, India, July 14-22, 2012 (invited)

187. A.N. Zhukov
Linking small-scale and large-scale physical processes in coronal mass ejections
39th COSPAR Scientific Assembly, Mysore, India, July 14-22, 2012 (invited)

188. A.N. Zhukov and the SIGMA consortium
The Solar Investigation using a Global coronal Magnetograph
5th Solar Orbiter Workshop, September 10-14, 2012, Bruges, Belgium (poster)

189. A.N. Zhukov, F. Auchère, S. Parenti, L. Abbo, V. Andretta, G. Aulanier, P. Barthol, L. Belluzzi, A. Bemporad, D. Berghmans, A. Berlicki, K. Bocchialini, V. Bommier, E. Buchlin, G. Cauzzi, W. Curdt, F. Delmotte, L. Dolla, S. Fineschi, M. Georgoulis, C. Gontikakis, L. Green, S. Gunar, M. Haberreiter, J.-P. Halain, L. Harra, P. Heinzel, B. Inhester, T. Katsiyannis, S. Krucker, J. Kuhn, E. Landi degl'Innocenti, F. Landini, H. Lin, D. Mackay, J. Magdalenić, S. Mancuso, R. Manso Sainz, C. Marqué, M. Mierla, D. Moses, B. Nicula, H. Peter, N.-E. Raouafi, E. Robbrecht, P. Rochus, L. Rodriguez, M. Romoli, U. Schühle, D. Seaton, D. Socker, S. Solanki, J. Štěpán, L. Teriaca, J. Trujillo Bueno, G. Tsiropoula, A. Verdini, J.-C. Vial, D. Williams, J. Woch, A. Yeates

SIGMA (Solar Investigation using a Global coronal Magnetograph): a new space mission to measure the magnetic field in the solar corona
XII Hvar Astrophysical Colloquium “The Sun and Heliosphere”, Hvar, Croatia, September 3-7, 2012 (poster)

190. A.N. Zhukov, F. Auchère, S. Parenti, L. Abbo, V. Andretta, G. Aulanier, P. Barthol, L. Belluzzi, A.Bemporad, D. Berghmans, A. Berlicki, K. Bocchialini, V. Bommier, E. Buchlin, G. Cauzzi, W. Curdt, F. Delmotte, L. Dolla, S. Fineschi, M. Georgoulis, C. Gontikakis, L. Green, S. Gunar, M. Haberreiter, J.-P. Halain, L. Harra, P. Heinzel, B. Inhester, T. Katsiyannis, S. Krucker, J. Kuhn, E. Landi degl’Innocenti, F. Landini, H. Lin, D. Mackay, J. Magdalenić, S. Mancuso, R. Manso Sainz, C. Marqué, M. Mierla, D. Moses, B. Nicula, H. Peter, N.-E. Raouafi, E. Robbrecht, P. Rochus, L. Rodriguez, M. Romoli, U. Schühle, D. Seaton, D. Socker, S. Solanki, J. Štěpán, L. Teriaca, J. Trujillo Bueno, G. Tsiropoula, A. Verdini, J.-C. Vial, D. Williams, J. Woch, A. Yeates
SIGMA, Solar Investigation using a Global coronal Magnetograph, A new space mission to measure the magnetic field in the solar corona
5th Solar Orbiter Workshop, Bruges, Belgium, September 10-14, 2012 (poster)

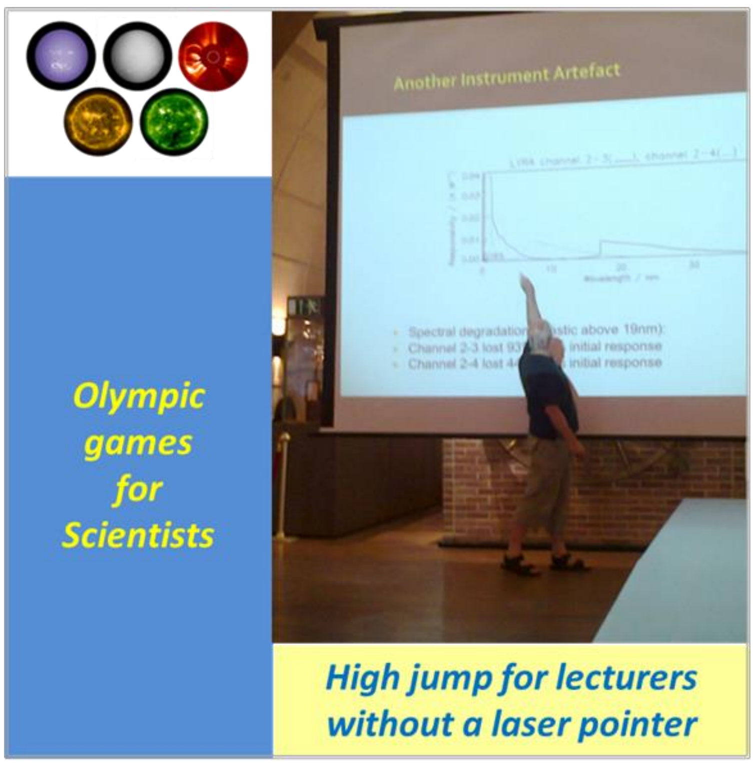

List of abbreviations

3D	Three dimensional
4D	Four dimensional
ACE	Advanced Composition Explorer
ACRIM	Active Cavity Radiometer Irradiance Monitor
AFFECTS	Advanced Forecast For Ensuring Communications Through Space
AGU	American Geophysical Union
AIA	Atmospheric Imaging Assembly (SDO)
AIP	American Institute of Physics
AIRS	Atmospheric Infra-Red Sounder
AIT	Austrian Institute of Technology
ALADIN	Air Limitée Adaptation Dynamique développement InterNational
ALARO	Aire Limitée Adaptation/Application de la Recherche à l'Opérationnel
ALIS	Auroral Large Imaging System
AlN	Aluminum Nitride
ALTIUS	Atmospheric Limb Tracker for Investigation of the Upcoming Stratosphere
AOD	Aerosol Optical Depth
AOGS	Asia Oceania Geosciences Society
APS	Active Pixel Sensor
ApJ	The Astrophysical Journal
ARTEMIS	Acceleration, Reconnection, Turbulence and Electrodynamics of the Moon's Interaction with the Sun
ASL	Above Sea Level
ATLAS	ATmospheric Laboratory for Applications and Science
ATMOS	Advances in Atmospheric Science and Applications
AU	Astronomical Unit; about 150 million km
AVL	ASIMUT-(V)LIDORT model (IASI)
BELSPO	Belgian Science Policy Office
BER	Backscatter-to-Extinction Ratio
BIRA	Belgisch Instituut voor Ruimte-Aëronomie
BISA	Belgian Institute for Space Aeronomy
BOS	Bolometric Oscillation Sensor
BRAMS	Belgian RAdio Meteor Stations
BUSOC	Belgian User Support and Operation Center
C/N_0	Carrier-to-noise ratio
CaII K	Singly ionized Calcium (K-line)
CACTus	Computer Aided CME Tracking software
CALLISTO	Compound Astronomical Low frequency Low cost Instrument for Spectroscopy and Transportable Observatory
CCD	Charge-Coupled Device
CERES	Clouds and Earth's Radiant Energy System (radiometer)
CESRA	Community of European Solar Radio Astronomers
CH	Coronal Hole
CHARM	Contemporary physical challenges in Heliospheric and AstRophysical Models
CME	Coronal Mass Ejection
CNES	Centre National d'Etudes Spatiales
CNRS	Centre National de la Recherche Scientifique
COMESEP	Coronal Mass Ejections and Solar Energetic Particles
COPUOS	COmmittee on the Peaceful Uses of Outer Space (UN)
COSPAR	COmmittee on SPAce Research
COST	(European) COoperation in Space & Technology
CRC	Cyclotron Research Centre (in Louvain-La-Neuve)
CSL	Centre Spatial de Liège
Cubesat	A small satellite measuring 10cm x 10cm x 10cm
dB	Decibel
DEM	Differential Emission Measure
DeMeLab	Detector Measurements Laboratory

DIARAD	DIfferential Absolute RADiometer
DLR	Deutsche Zentrum für Luft- und Raumfahrt
DOI	Digital Object Identifier
DOY	Day Of Year
DPD	Debrecen Photographic Data
Dst	Disturbance Storm index
E-GVAP	EUMETNET EIG GNSS water VApor Program
ECV	Essential Climate Variable
EDAS	EGNOS Data Access Service
EGNOS	European Geostationary Navigation Overlay Service
EGU	European Geosciences Union
eHEROES	Environment for Human Exploration and RObotic Experimentation in Space
EISCAT	European Incoherent SCATter scientific association
EIT	Extreme ultraviolet Imaging Telescope (SOHO)
EPN	EUREF Permanent Network
EPOS	European Plate Observing System
EPS	European Physical Society
EPT	Energetic Particle Telescope (PROBA-V)
EQE	External Quantum Efficiency
ERB(S)	Earth Radiation Budget (Satellite)
ESA	European Space Agency
ESC	Expert Service Centre
ESIO	EUV Solar Imager for Operations
ESTEC	European Space Research and Technology Centre
ESWP	European Space Weather Portal
ESWW	European Space Weather Week
EU	European Union
EUI	Extreme-Ultraviolet Imager (Solar Orbiter)
EUMETNET	European Meteorological services Network
EUMETSAT	European Organisation for the Exploitation of Meteorological Satellites
EUREF	EUropean Reference Frame
EUV	Extreme Ultraviolet
EUVI	Extreme Ultraviolet Imager (STEREO/SECCHI)
EVE	Extreme Ultraviolet Variability Experiment (SDO)
$F_{10.7\ cm}$	Solar radio flux at 10.7 cm wavelength
FeIX	8 times ionized iron
FIG	Fédération Internationale des Géometres (International Federation of Surveyors)
FMI	Finnish Meteorological Institute
FP7	Framework Program 7
Galileo	European GNSS
GEN	General Data Service (SN-I)
GERB	Geostationary Earth Radiation Budget (radiometer)
GLONASS	GLObal NAvigation Satellite System (Russia)
GNSS	Global Navigation Satellite System
GNSS4SWEC	Advanced GNSS tropospheric products for the monitoring of Severe Weather Events and Climate
GOES	Geostationary Operational Environmental Satellite
GOME	Global Ozone Monitoring Experiment
GOMESCIA	combination of GOME, SCIAMACHY and GOME-2 measurements
GPS	Global Positioning System (USA)
GSAC	GPS Seamless Archive Centers
GSTP	General Support Technology Programme (ESA)
H-alpha	A red visible spectral line created by Hydrogen
HMI	Heliospheric and Magnetic Imager (SDO)
HQ	Headquarters
HSF	Human Space Flight (SN-I)
IAG	International Association of Geomorphologists
IAS(B)	Institut d'Aéronomie Spatiale de Belgique
IASI	Infrared Atmospheric Sounding Interferometer
ICEM	International Conference on Electronic Materials

ICG	International Committee on GNSS
ICME	Interplanetary CME
ICNS	Integrated Communications Navigation and Surveillance (conference)
ICT	Information and Communication Technologies
IDL	Interactive Data Language
IEEE	Institute of Electrical and Electronics Engineers
IEH-3	International Extreme Ultraviolet Hitchhiker-03
IERS	International Earth Rotation Service
IGS	International GNSS Service
IMC	International Meteor Conference
IMPALAS	Investigation of MagnetoPause Activity using Longitudinally-Aligned Satellites
IR	Infrared
IRI	International Reference Ionosphere
ISES	International Space Environment Service
ISIS	International Satellites for Ionospheric Studies
ISS	International Space Station
ISSI	International Space Science Institute
ISU	International Space University
IT	Information Technology
ITRF	IERS Terrestrial Reference Frame
IUAP	Intra-University Attraction Pole network
IUMRS	International Union of Materials Research Societies
IWV	Integrated Water Vapor
JSWSC	Journal of Space Weather and Space Climate
Kp	A geomagnetic index, ranging from 0 (quiet) to 9 (extremely severe storm)
KUL	Katholieke Universiteit Leuven
LASCO	Large Angle Spectrometric Coronagraph (SOHO); small (C2) and wide (C3) field of view
LASP	Laboratory for Atmospheric and Space Physics
LATMOS	Laboratoire Atmosphères, Milieux, Observations Spatiales
LAU	LAUnch operations (SN-I)
LCS	Local Coronal Signature
LDM	Latitudinal Daily Mean
LEMUR	Large European Module for solar Ultraviolet Research
LIDAR	LIght Detection And Radar
LIF	Light Ion radiation Facility (in Louvain-La-Neuve)
LOC	Local Organizing Committee
LYRA	Lyman Alpha Radiometer (PROBA2)
μBOS	micro Bolometric Oscillation Sensor
μm	micrometer (10^{-6} meter)
M-flare	Medium x-ray flare
MCM	Management Committee Meeting
METIS	Multi Element Telescope for Imaging and Spectroscopy (Solar Orbiter)
MeV	Mega electronvolt (10^{6} . 1.6 . 10^{-19} Joule)
MHD	Magneto-Hydro-Dynamic
MHz	Megahertz (10^{6}/s)
MLH	Mixing Layer Height
MOZAIC	Measurement of Ozone and Water Vapor by Airbus In-Service Aircraft
MSM	Metal-Semiconductor-Metal
MSSL	Mullard Space Science Laboratory
mW	milliWatt (10^{-3} W)
N_2	Nitrogen (molecule)
NASA	National Aeronautics and Space Administration
NEMO	Novel EIT wave Machine Observing
NIR	Near InfraRed
nm	nanometer (10^{-9} meter)
NMA	Norwegian Mapping Authority
NOA	National Observatory of Athens
NOAA	National Oceanic and Atmospheric Administration (numbering of sunspots)
NRT	Near Real-Time

NSO	Non-Space systems Operations (SN-I)
NSSDC	National Space Science Data Center
NWP	Numerical Weather Prediction
O	Oxygen
PCA	Principal Component Analysis
PCO	Phase Center Offset
PCTR	Prominence-Corona Transition Region
PCV	Phase Center Variation
PhD	Doctor of Philosophy
PI	Principal Investigator
PICASSO	Pico-satellite for Atmospheric and Space Science Observations
PMOD	Physikalisch-Meteorologisches Observatorium Davos
PMT	Photo Multiplier Tube
ppm	parts per million
ppb	parts per billion
PROBA	PRoject for OnBoard Autonomy
PRODEX	PROgram for the Development of scientific Experiments
PTB	Physikalisch-Technische Bundesanstalt
QB50	A network of 50 cubesats to be launched simultaneously (FP7)
Ri	International sunspot number
RINEX	Receiver Independent Exchange Format
RMI(B)	Royal Meteorological Institute (of Belgium)
RMS	Root Mean Square
ROB	Royal Observatory of Belgium
RS	Radiosonde
RSTN	Radio Solar Telescope Network (USAF)
RWC	Regional Warning Centre
σ	Standard deviation
S/N	Signal-to-Noise
SAA	South Atlantic Anomaly
SARR	Space Absolute Radiometer Reference
SC24	Solar Cycle 24
SCD	Spacecraft Design (SN-I)
SCIAMACHY	SCanning Imaging Absorption spectroMeter for Atmospheric CHartographY (ENVISAT)
SCO	Spacecraft Operation (SN-I)
SDO	Solar Dynamics Observatory
SECCHI	Sun Earth Connection Coronal and Heliospheric Investigation (STEREO)
SEP	Solar Energetic Particle
SFU	Solar Flux Unit (10^{-22} W m^{-2} Hz^{-1})
SIDC	Solar Influences Data analysis Center
SIGMA	Solar Investigation using a Global coronal Magnetograph
SIMBA	Sun-earth IMBAlance radiometer
SIPWork	Solar Information Processing Workshop
SLP	Sweeping Langmuir Probe
SN	Space weather and Near-earth objects
SO5	Solar Orbiter Workshop 5
SOC	Scientific Organizing Committee
SOHO	SOlar & Heliospheric Observatory
SOLCON	SOLar CONstant radiometer
SOLID	SOLar Irradiance Data exploitation (FP7)
SOLMEX	SOLar Magnetism EXplorer
SolO	Solar Orbiter
SOLSPEC	SOLar SPECtrum
SOLSTICE	Solar Stellar Irradiance Comparison Experiment
SORCE	Solar Radiation and Climate Experiment
SOTERIA	SOlar-Terrestrial Investigations and Archives
SOVA	SOlar constant and VAriability
SOVAP	SOlar VAriability Picard
SOVAR	Refurbished SOVA1 radiometer
SOVIM	Solar Variations and Irradiance Monitor
SPENVIS	Space Environment Information System
SPICE	Spectral Imaging of the Coronal Environment (Solar Orbiter)
sr	steradian
SSA	Space Situational Awareness
SSCC	SSA Space Weather Coordination Centre
SSN	SunSpot Number

SST	Space Surveillance and Tracking (SN-I)
STAFF	Solar Timelines viewer for AFFECTS
STCE	Solar-Terrestrial Centre of Excellence
STEREO	Solar-TErrestrial RElations Observatory
SWAP	Sun Watcher using APS detector and image Processing (PROBA2)
SWE	Space WEather
SWENET	(European) Space WEather NETwork
SWG	Science Working Group
SWSC	Space Weather and Space Climate journal
SWT	Science Working Team
SWWT	(European) Space Weather Working Team
TAS	Technology Applications and Science
TEC	Total Electron Content
TECO	TEchnical Conference on meteorological and environmental instruments and methods of Observation (WMO)
TECU	Total Electron Content Unit
TEPA	Thunderstorms and Elementary Particle Acceleration
TGO	Tromsø Geophysical Observatory
THEMIS	Time History of Events and Macroscale Interactions during Substorms
TID	Travelling Ionospheric Disturbance
TIM	Total Irradiance Monitor
TIO	Trans-IOnospheric link (SN-I)
TOA	Top Of Atmosphere
TOSCA	Towards a more complete assessment of the impact of solar variability on the Earth's climate
TRF	TIM Radiometer Facility
TRL	Technology Readiness Level
TSI	Total Solar Irradiance
UK	United Kingdom
ULB	Université Libre de Bruxelles
ULg	Université de Liège
UOA	University Of Athens
USAF	United States Air Force
USET	Uccle Solar Equatorial Table
UT	Universal Time
UTL	Upper ion Transition Level
UV	Ultraviolet
V	Volt
VIRGO	Variability of solar IRradiance and Gravity Oscillations
VIS	VISual
VISION	Visible Spectral Imager for Occultation and Nightglow
VLF	Very Low Frequency
VTT	Technical research Centre of Finland
VUB	Vrije Universiteit Brussel
W	Watt
WBGM	Wide Band Gap Material
WDC	World Data Centre
WDS	World Data Service
WMO	World Meteorological Organization
WP	Work Package
WPGM	Western Pacific Geophysics Meeting
X-flare	Extreme x-ray flare
XUV	Extreme Ultraviolet
ZTD	Zenith Total Delay